ALMA MATER STUDIORUM - UNIVERSITÀ DI BOLOGNA

SCUOLA DI INGEGNERIA E ARCHITETTURA

DIPARTIMENTO DI INGEGNERIA INDUSTRIALE

CORSO DI LAUREA IN INGEGNERIA EDILE-ARCHITETTURA

TESI DI LAUREA

in

Acustica Applicata e Illuminotecnica

ENHANCEMENT OF ACOUSTIC CONDITIONS IN THE PERE PRUNA CIVIC CENTRE, BARCELONA: MEASUREMENTS, EVALUATION AND ACOUSTIC TREATMENT PROJECT

CANDIDATO
Giulio Quaranta

RELATORE:
Chiar.mo Prof. Massimo Garai

RELATORE ESTERO:
Prof. Josep Martí Roca

CORRELATORI:
Ing. Giulia Fratoni
Prof. Marc Arnela Coll

Anno Accademico 2022/23

Sessione II

Contents

List of figures

List of tables

Acknowledgements

First and foremost, I want to give a heartfelt thanks to Professor Massimo Garai and Engineer Giulia Fratoni for their unwavering support and the enthusiasm they've shared with me while delving into this subject over the past years.

I'd also like to express my gratitude to the members of the research team at the University of Barcelona I had the pleasure of working with: Marc Arnela Coll, Carmen Julia Martinez, Josep Martí Roca and Marcio Avelar. I truly appreciate their consideration and the invaluable confrontation and support they've provided.

I want to extend my thanks to all my family members and friends who've been with me throughout these years, understanding the efforts and sacrifices made to reach this milestone. A special shoutout goes to Marco, my course mate and partner in adventures since the beginning of our university journey. It would have been a tougher road without the mutual support and encouragement we've given each other.

Last but not least, I'd like to thank my dad, as well as my brothers, who have always believed in me. But most of all, I want to thank my mother, for the love and support she always gave me. She never questioned the dedication and determination I put into my studies.

This achievement marks a pivotal moment in my life. It coincides with the culmination of a seven-year journey, characterized not only by education and training but also, and most importantly, by immeasurable personal growth. It signifies the attainment of a long-cherished goal, opening doors to an ambitious and inspiring future.

Reaching this important achievement would not have been possible without all of you. Sincere thanks to everyone.

Giulio Quaranta, Bologna, October 2023

Sommario

Il progetto di trattamento acustico oggetto di questa tesi di laurea è stato condotto in collaborazione con due gruppi di ricerca: il gruppo di Fisica Tecnica Ambientale del Dipartimento di Ingegneria Industriale di Bologna (DIN) e il gruppo Human - Environment Research (HER) del Dipartimento di Acustica dell'Università Ramon Llull, a Barcellona.

Il nucleo della ricerca è incentrato su un caso studio specifico: il Centre Civic Pere Pruna, una struttura pubblica oggi adibita a centro culturale, situata nel quartiere di Sant Gervasi a Barcellona, in Spagna. Si tratta di una ex chiesa ristrutturata e convertita a spazio multifunzionale, con una programmazione culturale specializzata in musica e arte contemporanea. La sala offre numerose attività, tra cui concerti di musica da camera, esposizioni artistiche e conferenze. Tuttavia, le condizioni acustiche della sala allo stato attuale non sono assolutamente idonee ad ospitare questo tipo di eventi; lo spazio infatti, in seguito al suo rinnovamento e al cambio di funzione, non ha ricevuto nessun trattamento, mantenendo le proprietà acustiche tipiche di una chiesa.

Pertanto, con il presente studio si vuole proporre un progetto di intervento volto al miglioramento delle caratteristiche acustiche della sala. Gli stessi responsabili del centro culturale hanno manifestato un forte interesse per questo intervento dichiarando la necessità di una proposta accurata di trattamento acustico, rendendo questo progetto di ricerca ancora più utile ed interessante.

Per contestualizzare il lavoro svolto, è essenziale conoscere il contesto teorico e storico in cui questo studio si inserisce, in modo da fornire le basi per una migliore comprensione delle metodologie utilizzate. Il primo capitolo è dedicato a questo approfondimento, fornendo una panoramica dei principi fondamentali che costituiscono la base dello studio dell'Acustica delle Sale.

Innanzitutto, si esaminano i principi basilari dell'acustica fisica, fondamentali per comprendere come le onde sonore si propagano e si comportano all'interno di ambienti chiusi. Successivamente, si esplorano le linee guida stabilite dalla normativa ISO 3382, dedicata alle metodologie da seguire per le misurazioni acustiche – le stesse realizzate nella sala oggetto di studio – e alla definizione dei principali parametri acustici utilizzati per valutare oggettivamente la qualità acustica di uno spazio.

A seguire, vengono esposti i principali eventi storici che hanno giocato un ruolo cruciale nello sviluppo dell'Acustica Architettonica moderna come campo di esplorazione scientifica. Tale processo, come vedremo, è accompagnato da progressi tecnologici e computazionali che culminano nella creazione della risposta all'impulso come principale strumento di estrazione dei parametri acustici.

A conclusione di questo primo capitolo, si presenta un conciso inventario delle principali tipologie di sale da concerto oggi conosciute e utilizzate in tutto il mondo, seguendo l'evoluzione da geometrie di base a design moderni e sperimentali.

Una volta completata questa contestualizzazione preliminare, si entra nel cuore della tesi con l'introduzione del caso studio in questione, il Centre Civic Pere Pruna. La sua storia e l'evoluzione architettonica subita nel corso degli anni sono di grande importanza per comprendere appieno le motivazioni di certe scelte stabilite in fase progettuale. Questa cornice storica è completata da una succinta analisi geometrica e acustica dello stato attuale, grazie alla quale è stato possibile impostare le misurazioni acustiche.

Le misurazioni in situ rappresentano una fase cruciale del progetto, poiché consentono di valutare l'acustica attuale della sala in maniera precisa e organica. La loro esecuzione è accompagnata dalla redazione di un protocollo, in cui sono stati elencati gli strumenti utilizzati – provenienti dal laboratorio di acustica dell'università di Barcellona – nonché le procedure effettuate secondo normativa, garantendo risultati accurati e attendibili. Una volta ottenuti i dati dalle misurazioni, si procede con l'elaborazione dei dati stessi e l'analisi dei risultati, così da estrarre informazioni significative sullo stato dell'acustica nella sala, fornendo una base solida per le fasi successive.

A supporto delle misurazioni, vengono utilizzati due tra più rinomati e affidabili software di simulazione acustica: CATT-Acoustic e ODEON. Dopo una breve analisi comparativa degli algoritmi implementati nei due programmi, si prosegue con la calibrazione acustica: un modello numerico della sala importato nei due software he permesso di simulare lo stato di fatto della sala, come punto di partenza per la successiva fase di proposta progettuale. I dati estratti da ogni software vengono messi a confronto con quelli ottenuti dalle misurazioni effettuate in situ, per poi analizzarne le variazioni e stabilire alcune tendenze.

A questo punto, si procede con la fase di progettazione acustica. È importante sottolineare che l'intervento presenta numerose criticità. Il ricco patrimonio artistico e architettonico presente

nella sala impone alcune restrizioni e limita notevolmente la quantità di superfici potenzialmente soggette a trattamenti acustici. Inoltre, si deve assicurare che il progetto rispetti il carattere originale dell'ambiente, evitando qualsiasi intervento invasivo.

Il trattamento prevede l'utilizzo di una varietà di materiali fonoassorbenti in grado di assorbire le onde sonore a diverse bande di frequenza. Questi materiali sono selezionati in base alle esigenze specifiche e posizionati strategicamente all'interno della sala al fine di garantire un miglioramento acustico uniforme.

Per concludere, si effettua una nuova simulazione dello stato di progetto sia in CATT-Acoustic che in ODEON. Infine, si traggono le conclusioni: i risultati vengono estratti e analizzati, permettendo di valutare l'efficacia delle soluzioni proposte.

Abstract

The acoustic treatment project, subject of this thesis, has been developed in collaboration with the Environmental Technical Physics research group of the Department of Industrial Engineering in Bologna (DIN) and the Human-Environment Research (HER) research group of the Department of Acoustics at Ramon Llull University in Barcelona.

The core of the research is focused on a specific case study: the Centre Civic Pere Pruna, a public facility currently used as a cultural centre located in the Sant Gervasi neighbourhood of Barcelona, Spain. It is a former church that has been renovated and converted into a multipurpose space with a specialized cultural program in music and contemporary art. The hall hosts various activities, including chamber music concerts, art exhibitions, and conferences. However, the current acoustic conditions of the hall are not suitable for hosting these types of events. The space, following its renovation and change of function, has received no acoustic treatment, retaining the acoustic properties typical of a church.

Therefore, this study aims to present a project for improving the acoustic characteristics of the hall. The responsible parties of the cultural centre have expressed a strong interest in this intervention, stating the need for a thorough proposal for acoustic treatment, making this research project even more valuable and interesting.

To contextualize the work done, it is essential to understand the theoretical and historical context in which this study fits, providing the basis for a better understanding of the methodologies used. The first chapter is dedicated to this exploration, providing an overview of the fundamental principles that form the foundation of the field of Room Acoustics.

Firstly, the basic principles of physical acoustics are examined, fundamental for understanding how sound waves propagate and behave within enclosed environments. Subsequently, the guidelines established by ISO 3382 standards, dedicated to the methodologies for acoustic measurements – the same performed in the study's hall – and the definition of the main acoustic parameters used to objectively assess the acoustic quality of a space are explored.

Following that, the main historical events that have played a crucial role in the development of modern Architectural Acoustics as a field of scientific exploration are presented. This process, as we will see, is accompanied by technological and computational advancements that culminate in the creation of impulse response as the primary tool for extracting acoustic parameters.

To conclude this first chapter, a concise inventory of the main types of concert halls known and used worldwide today is presented, following the evolution from basic geometries to modern and experimental designs.

Once this preliminary contextualization is completed, we will delve into the heart of the thesis with the introduction of the case study at hand: the Centre Civic Pere Pruna. Its history and architectural evolution over the years are of great importance to fully understand the motivations behind certain design choices. This historical framework is complemented by a succinct geometric and acoustic analysis of the current state, which allowed for the setup of acoustic measurements.

In-situ measurements represent a crucial phase of the project, as they allow for a precise and organic evaluation of the hall's current acoustics. Their execution is accompanied by the drafting of a protocol, listing the tools used – provided from the acoustics laboratory at the University of Barcelona – as well as the procedures performed according to standards, ensuring accurate and reliable results. Once the data from the measurements are obtained, data processing and results analysis are carried out to extract meaningful information about the state of acoustics in the hall, providing a solid foundation for the subsequent phases.

To support the measurements, two of the most renowned and reliable acoustic simulation software tools are used: CATT-Acoustic and ODEON. After a brief comparative analysis of the algorithms implemented in both programs, acoustic calibration is performed: a numerical model of the hall imported into the two software tools simulates the actual state of the hall as a starting point for the subsequent design proposal phase. The data extracted from each software are compared to the results obtained from the in-situ measurements, and variations are analysed to establish certain trends.

At this point, it is possible to proceed to the acoustic treatment project phase. It is important to emphasize that the intervention presents several critical aspects. The rich artistic and architectural heritage present in the hall imposes certain restrictions and significantly limits the amount of surfaces potentially subject to acoustic treatment. Furthermore, it will be necessary to ensure that the project respects the original character of the environment, avoiding any invasive interventions.

The treatment involves the use of a variety of sound-absorbing materials capable of absorbing sound waves at different frequency bands. These materials are selected based on specific

requirements and strategically positioned inside the hall to ensure a uniform acoustic improvement.

To conclude, a new simulation of the project state is carried out in both CATT-Acoustic and ODEON. Finally, conclusions are drawn: the results are extracted and analysed, allowing for an evaluation of the effectiveness of the proposed solutions.

Introduction

The science of Acoustics plays a profound role in our lives, influencing our experiences, emotions, and perceptions in ways often unnoticed but deeply impactful. From the sublime harmony of a well-tuned concert hall to the quietude of a tranquil library, acoustics shape our environments and interactions in countless ways.

Throughout antiquity, acoustics has held fundamental significance in artistic expression and representation. From the Greeks to the Romans, spaces like theatres and auditoriums have always been characterized by careful acoustic analysis. However, until the last century, this analysis was purely qualitative. Today, thanks to the development of advanced technologies and in-depth mathematical studies, the science of Acoustics has evolved into a rigorous and precise scientific method, consisting of complex formulations and multiple considerations. These considerations now encompass various aspects, from physics to psychology, from architecture to engineering. It is within this multifaceted realm that this exploration and inquiry begin.

The investigation carried out in this work delves into the intricate field of Architectural Acoustics, where the design of spaces is intentionally tailored to enhance or manipulate the acoustic experience within them. It is a realm where science meets art, where mathematical precision converges with aesthetic sensibility, and where the tangible and the intangible merge to create spaces that resonate with human emotion.

While it has made significant progress over the years, the field of Architectural Acoustics remains a complex and evolving area of study. One of the reasons for this ongoing evolution is the inherent complexity of sound itself. Sound is a multi-dimensional phenomenon that interacts with various architectural elements such as walls, ceilings, and floors in intricate ways. Achieving precise control over these interactions to create optimal acoustic environments is a challenging task.

Moreover, the acoustic performance of a space is highly dependent on its purpose. A room designed for classical music concerts will have different acoustic requirements compared to one intended for speeches or rock concerts. This variability adds another layer of complexity to the field, as there is no one-size-fits-all solution. Additionally, the human perception of sound is influenced by subjective factors, including individual preferences and cultural differences.

These factors can introduce uncertainties into the design process, as what sounds pleasant to one person may not be the same for another.

Furthermore, advancements in materials and technologies continually introduce new possibilities and challenges. Innovative acoustic materials and digital simulation tools provide architects and acousticians with more options than ever before, but navigating this sea of choices can be daunting.

The principal purpose of this thesis project has been to introduce innovative methodologies for the measurement and acoustic modelling of multipurpose halls, particularly those possessing significant artistic and architectural value while exhibiting challenging acoustic characteristics. Throughout the research, several prestigious concert halls were scrutinized, including two halls within the Palau de la Musica Catalana, three halls within the Conservatorio Municipal de Barcelona, and lastly, the space within the Centre Civic Pere Pruna. It was determined that the latter presented the most intriguing and complex acoustic challenges.

Indeed, the subject of this thesis project epitomizes the complexity inherent in architectural acoustics. The Centre Civic Pere Pruna stands as a unique hybrid configuration, marrying elements of modernist and ecclesiastical architecture with a modernized hall that engages in a compelling dialogue with its historical past. Simultaneously, the chosen space presents considerable challenges in terms of acoustic conditions, as no acoustic treatment has been applied to the venue following its modernization. Therefore, the Pere Pruna facility poses a fascinating challenge for the objectives of this thesis. It represents an intriguing scenario in which the necessary acoustic interventions must harmonize with the artistic and architectural integrity, avoiding any form of invasive alterations.

This perspective helped to justify the selection of this particular space for the research. Additionally, this choice was further validated by the fact that some members of the Barcelona acoustic research group are directly involved in organizing activities promoted by the cultural centre. Professor Marc Arnela Coll, the coordinator of the HER research group, serves as the director of the choir established by the centre and has direct connections with the responsible individuals of the cultural association. This played a pivotal role in selecting the venue, as it facilitated direct communication with the stakeholders, enabling a comprehensive understanding of their needs, desires, and the true project requirements of the venue from the outset.

In this captivating context, it became imperative to undertake an in-depth research project. The Centre Civic Pere Pruna holds tremendous potential, and it is essential to ensure that this potential can be fully realized.

Figure 1. First inspection at the Centre Civic Pere Pruna

The HER (Human - Environment Research) research group at Ramon Llull University, Campus La Salle in Barcelona, is at the forefront of a fascinating research project. They are exploring a groundbreaking method for measuring and parameterizing iconic concert and multi-purpose halls, focusing on an ultrasonic speaker prototype known as the Omnidirectional Parametric Loudspeaker (OPL). This technology holds the potential to replace conventional dodecahedral loudspeakers, which have raised concerns about the reliability of acoustic measurements, especially in matter of the directionality at high frequencies.

This thesis project aligns seamlessly with the research initiative. It aims to develop an acoustic-architectural project characterized by a dual comparison. On one hand, the project evaluates the performance of both the conventional dodecahedral loudspeaker and the innovative OPL. On the other hand, it leverages two renowned simulation software tools for room acoustics, CATT-Acoustic and ODEON, to provide comprehensive insights into the complexity of acoustic parameters.

In relation to the first aspect being considered, a rigorous plan for acoustic measurements has been meticulously developed, forming the fundamental basis of this project. In addition to the aforementioned loudspeaker devices – served as sound sources – a variety of precise instruments for capturing and processing acoustic signals, including microphones, amplifiers, and advanced data processing software, have been employed. These measurements offer indispensable insights into the current acoustic characteristics of the hall, providing crucial guidance for the formulation of acoustic treatments. The significance of precise measurements cannot be overstated, as they underpin every aspect of the project, from the initial assessment to the final implementation.

In addition to acoustic measurements, advanced simulation tools play a pivotal role in the project's success. Two renowned Geometrical Acoustic (GA)-based software programs, CATT-Acoustic and ODEON, serve as valuable allies in understanding the hall's acoustic behaviour. They enable a comprehensive exploration of the myriad parameters at play, offering insights into limitations and uncertainties of the tools, but, most importantly, opportunities for the acoustic enhancement. These simulation tools provide the project with a virtual laboratory, allowing for extensive testing and refinement of acoustic interventions before implementation. Finally, the comparative analysis between the acoustic simulations and measurements will furnish a comprehensive understanding of the issue, forming the foundation for the proposal of acoustic treatments.

Integrating this innovative research approach into the context of Centre Civic Pere Pruna, a space of historical and architectural significance, poses a unique challenge.

The building's transformation over time reflects the evolving needs of the community it serves. The building suffered damage during the Spanish Civil War, including a fire that left a lasting mark on its structure. Subsequent renovations aimed to preserve the building's historical significance while adapting it to modern needs. One remarkable aspect of this preservation effort was the conservation of Pere Pruna's frescoes on the domed ceilings, which serve as both artistic treasures and acoustic challenges.

Today, the hall not only stands as a symbol of art and history in the area but also plays a crucial role for the residents and families of the neighbourhood. Here, they find a sense of community and the opportunity to engage in enriching and stimulating cultural initiatives.

The cultural centre houses a diverse array of activities, from chamber music concerts to art exhibitions and conferences. However, the architectural features that make it an aesthetic marvel, such as its vaulted ceilings, robust and reflective walls, frescoes, and stained glass, also pose significant challenges for effective acoustic treatment. The fundamental goal of this treatment project is to optimize the acoustic environment of the Centre Civic Pere Pruna, transforming it into a versatile and acoustically superior venue capable of hosting a myriad of artistic activities.

To achieve this, a strategic approach is required, given the architectural constraints and the need to preserve the historical and artistic significance of the hall. The main strategy involves selectively adding sound-absorbing materials, in areas where they can enhance acoustics without compromising the hall's historical and artistic value. This approach maintains a delicate equilibrium between acoustic performance and the preservation of historical and artistic elements.

In this intricate process, maintaining a critical eye is paramount. Every proposed intervention must undergo rigorous evaluation to ensure it aligns with the project's overarching goal. Prior to making any recommendations, thorough pre-proposal phases are necessary to consider all available options and their potential impact.

The critical aspect of this approach lies in the meticulous planning and execution of the interventions. Detailed plans, sections, and elevations are essential to ensure that every modification aligns with the hall's aesthetics and historical significance. Flexibility and adaptability are the imperatives of this project; in this regard, the concept of variable acoustics will be explored in depth. Variable acoustics holds the potential to cater to a wide range of needs and activities within the space. Whether it's hosting classical music concerts, lectures, art exhibitions, or community gatherings, the ability to adjust the acoustic environment according to the specific event is invaluable. It allows the hall to transform seamlessly, ensuring an optimal acoustic experience for each occasion and maximizing its utility for the community.

Having provided this general overview of the contextual background within which the research is situated, let’s now delve into a detailed exposition of the thesis project, focusing on an in-depth analysis of the case study: the Centre Civic Pere Pruna.

1 Fundamentals of Room Acoustics

The initial segment of the thesis is dedicated to elucidating a variety of pivotal elements intertwined with room acoustics. The purpose is to foster enhanced comprehension of the subject matters subsequently expounded in the second section concerning the acoustic intervention project.

1.1 Principles of physical acoustics

Whether it's concert halls, theatres, classrooms, or offices, the acoustic properties of a room significantly impact the way sound behaves and is perceived by occupants. To create spaces that fulfil their intended purpose, it is essential to understand the physical mechanisms underlying architectural acoustics projects. By unravelling these mechanisms, designers and engineers can make informed decisions about room design, materials, and sound management strategies.

For this reason, it is necessary to explore the importance of understanding the physical mechanisms in architectural acoustics and how it directly influences the success of a project. We will delve into key considerations, methodologies, and challenges faced in achieving optimal sound performance in built environments.

1.1.1 The science of Acoustics

Acoustics is a fascinating interdisciplinary field that deals with the behaviour of sound waves in elastic media. It encompasses various scientific disciplines such as physics, engineering, psychology, physiology, and music. By combining knowledge from these areas, acoustics provides insights into the behaviour of sound and its applications in numerous fields. Here are some key aspects of acoustics to consider for the purpose of this thesis:

1. *Physics of Sound*: Acoustics heavily relies on the principles of physics to understand the nature of sound. It involves the study of wave mechanics, vibration, resonance, and the interaction of sound with different materials and environments.
2. *Engineering Acoustics*: Acoustical engineering focuses on the practical application of acoustics in various fields. It involves the design and optimization of sound systems, architectural acoustics for room design, noise control and reduction, audio signal processing, and the development of acoustic measurement techniques and instruments.
3. *Psychoacoustics*: Psychoacoustics investigates how humans perceive and interpret sound. It combines principles from psychology, physiology, and acoustics to understand

how the human ear and brain process sound stimuli. Psychoacoustic research helps in areas such as noise masking, audio compression algorithms, and the design of audio equipment to enhance sound perception.

By integrating knowledge from these multiple disciplines, acoustics aims to comprehend the intricate process involved in the generation, propagation, and reception of sound waves:

- *Sound generation*: Sound originates from the vibrations of objects or bodies. The field of Rational Mechanics explores the behaviour of solid objects undergoing vibration, while Fluid Dynamics investigates the characteristics of fluid jets that can generate sound.
- *Sound propagation*: The study of electromagnetic wave propagation in Mathematical Physics provides a foundation for understanding the propagation of acoustic waves. Complex formulations and principles from electromagnetic wave theory are applied to analyse the behaviour of sound waves as they propagate through various media.
- *Sound reception*: The realm of Physiology and Psychology comes into play when examining the reception of sound. Factors such as the anatomical structure of the auditory system, the perception of different sounds (which can vary significantly), and psychological influences (such as distinguishing between sound and noise) all impact the reception and interpretation of sound.

Having established this overview, let us now delve deeper into the mechanisms involved in the generation and propagation of sound.

1.1.2 Sound generation and propagation

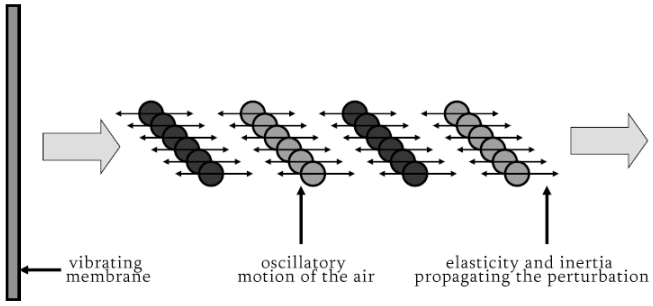

Figure 2. Sound generation and propagation from a vibrating source

Consider a vibrating membrane, such as a fibre or window glass (Fig.1). As this membrane oscillates, it imparts motion to the adjacent air particles in contact with it. The oscillations of the membrane cause the air particles to also oscillate, thereby transmitting the disturbance to

neighbouring air particles. This sequential transfer of motion leads to the propagation of the perturbation through the medium. In this context, the medium of propagation is air, which possesses specific properties, namely elasticity and inertia.

Sound pressure can be defined as the oscillation, relative to atmospheric pressure, of the air pressure that arises when an object undergoes vibration. For instance, considering the two prongs of a tuning fork, when set in motion, they generate waves that cause fluctuations in the atmospheric pressure. These small variations, known as sound pressure, combine with the static atmospheric pressure (101,325 Pa) to produce the overall pressure at a given point. Although sound pressure is characterized by its relatively small magnitude, it exhibits rapid variations in space and time, with frequencies reaching up to thousands of oscillations per second (Hz).

In contrast, atmospheric pressure is commonly regarded as static, both spatially and temporally, due to its imperceptible and minuscule variations. On the other hand, sound pressure exhibits quantifiable fluctuations in both space and time.

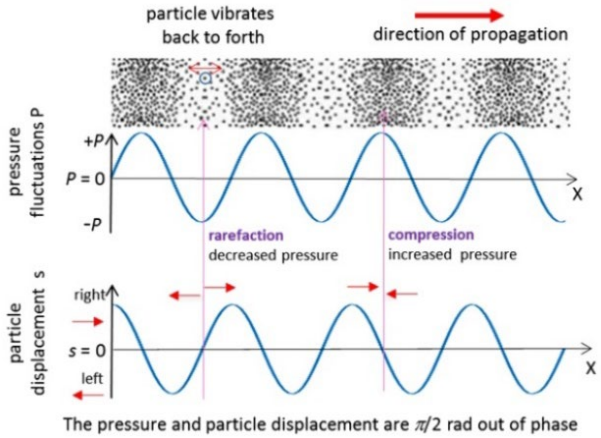

Figure 3. Sound pressure fluctuation

Therefore, the total pressure experienced at a specific point is the sum of the static atmospheric pressure, denoted as p_0, and the wave-induced fluctuation in pressure, referred to as p:

$$p_{tot} = p + p_0 \,, \qquad p \ll p_0$$

The acoustic wave can be classified into two fundamental types:

- *Compression waves*, also referred to as longitudinal waves, are characterized by particle motion in the same direction as the wave propagation.
- *Shear waves*, also known as transverse waves, exhibit particle motion perpendicular to the direction of wave propagation.

Mixed waves are formed through the combination of compression and shear waves. This type of wave is commonly observed in flexural waves that occur on a membrane.

In solids, both longitudinal and transverse waves, as well as their combinations, can propagate. However, in fluids, only longitudinal waves are possible, given the condition of very low viscosity. Transverse shear waves do not propagate in fluids. This characteristic presents an advantage in studying the transmission of waves in the air, where only longitudinal waves exist.

Nevertheless, if the aim is to investigate the transmission of waves through solids, such as building structures, the study becomes considerably more complex due to the presence of multiple wave types.

1.1.3 The wave equation

In the context of air, longitudinal waves are governed by the wave equation for small oscillations, commonly known as the D'Alembert equation, which was proposed in the latter half of the 1700s. This equation represents the Laplacian of the acoustic pressure ($\nabla^2 p$) subtracted by a term of ($\frac{1}{c^2}$) multiplied by the second partial derivative of the pressure with respect to time (t) squared, where c represents the speed of wave propagation.

$$\nabla^2 p - \frac{1}{c^2}\frac{\partial^2 p}{\partial t^2} = 0$$

The derivation of this equation is based on a series of assumptions: the fluid is considered homogeneous, isotropic – exhibiting the same properties in all directions –, ideal – with no viscosity – and non-dispersive. Additionally, the equation applies to the linear regime, where the relationship between the acoustic pressure and the corresponding disturbances remains linear:

$$p \ll p_0, \quad \rho \ll \rho_0, \quad u \ll u_0$$

Where:

p is the sound pressure, in Pa;

p_0 is the atmospheric pressure, in Pa;

ρ is the local density fluctuation of the air as the wave passes, in kg/m^3;

ρ_0 is the static pressure density, in kg/m^3;

u is the particle oscillation speed, in m/s;

u_0 is the average oscillation speed of the fluid, in m/s;

c is the sound propagation speed, in m/s.

The term u_0 can also be omitted if we consider the average speed equal to 0.

Indeed, it is crucial to highlight that the local oscillation speed of the particles, denoted as u (particle speed), does not coincide with the overall propagation speed of the waves, represented as c (wave speed). These two quantities also exhibit different orders of magnitude, and as a result, we primarily perceive the overall propagation speed of the waves and not the local particle speed.

	$\boldsymbol{p}$ [Pa]	$\boldsymbol{u}$ [m/s]
Hearing threshold	$2 \cdot 10^{-5}$	$4{,}82 \cdot 10^{-8}$
Calibration	1	$2{,}42 \cdot 10^{-3}$
Pain threshold (1)	20	$4{,}82 \cdot 10^{-2}$
Pain threshold (2)	200	$4{,}82 \cdot 10^{-1}$

Table 1. Sound pressure and particles oscillation speed referred to plane waves in the air

The magnitudes presented in the adjacent table, expressed in Pascals (Pa), are remarkably small. The minimum sound pressure that falls within the range of our auditory perception is approximately 2 hundred thousandths of a Pascal, which represents a value nearly 10 orders of magnitude below atmospheric pressure. Further details about the dynamic range of the human hearing system will be explained later (see par. 1.1.6).

For what concerns the propagation speed of the sound wave in the air, denoted as c, it can be determined through thermodynamic considerations. It corresponds to the square root of the ratio γ between the specific heat capacities of air, c_p and c_v. Multiplying this by the ratio of the static pressure p_0 to the static density ρ_0, which is obtained from the equation of state for perfect gases, yields the propagation speed.

$$c = \sqrt{\gamma \frac{p_0}{\rho_0}} = \sqrt{\gamma R T}$$

Where:

γ is the ratio between the specific heat capacities: $\gamma = \frac{c_p}{c_v} = 1{,}4$

p_0 is the atmospheric pressure, in Pa;

ρ_0 is the static pressure density, in kg/m^3;

R is the characteristic gas constant;

T is the absolute temperature, in K.

By expressing the temperature in Celsius, the formula can be further simplified. Consequently, the value of the sound wave's propagation speed in air is given by the following equation:

$$c \approx 331{,}6 + 0{,}6t \ \ [m/s]$$

This implies that the speed of sound increases gradually with the rise in absolute temperature, specifically by 0.6 m/s for each degree of temperature change.

Considering the elastic properties of the several media we can obtain different speeds of the longitudinal and transversal waves. The Table 2 shows a brief series of materials with the respective sound transmission speeds.

Materials	Speed of sound [m/s]	
	Longitudinal wave	Transverse wave
Air	340	-
Water	1500	-
Lead	1960	690
Gold	3240	1220
Iron	5920	3240
Titanium	6100	3120
Aluminum	6380	3130
Beryllium	12890	8880

Table 2. Sound wave speed in some media materials

1.1.4 Fundamental wave models

In the study of physical acoustics, it is usual to employ simple wave models to establish a foundational understanding of the physical characteristics involved. These insights lay the groundwork for further exploration and analysis of more intricate wave phenomena in various fields of physics and engineering.

We explore three essential waves models: plane waves, spherical waves and cylindrical waves.

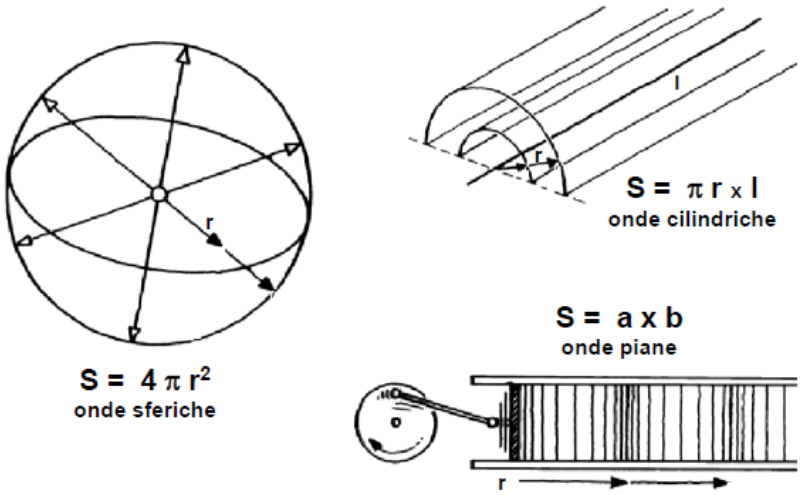

Figure 4. Fundamental wave models representation

Plane waves. These waves serve as a fundamental concept in current harmonic analysis, which is an extension of Fourier analysis (originating in the early 1800s). In a plane wave, the wavefronts are flat and parallel, resembling an infinite, unending plane. The wave travels uniformly in one direction and is characterized by a constant phase and amplitude across any plane perpendicular to its direction of propagation. While plane waves are a theoretical abstraction and not easy to physically create – as it requires visualizing the wave in a one-dimensional space –, they are valuable in simplifying complex waveforms.

Let's consider an oscillating piston located at one end of a tube, moving back and forth. When the piston moves forward, it generates a compression, increasing the density and pressure of the air. Conversely, when it moves backward, it causes a rarefaction, reducing the density and pressure. This motion creates a sinusoidal wave pattern inside the tube, which travels at the speed of sound (approximately 340 m/s in air). We can represent this wave in two ways:

1. *Plane wave in time domain*: At a fixed point in space, we observe the behaviour of the wave over time. The wave function can be described as follows:

$$p(t) = P_0 \cos(\omega t)$$

Where:

$p(t)$ is the sound pressure in the time domain, in Pa;

P_0 is the amplitude, in Pa;

t is time, in s;

ω is the angular frequency – also called pulsation – in rad/s; it corresponds to:

$$\omega = 2\pi f$$

f is the frequency, in s^{-1} (or Hertz, Hz).

2. *Plane wave in space domain*: At a specific instant in time, we take a snapshot of the wave pattern across all available space. The wave function can be expressed as follows:

$$p(t) = P_0 \cos(kr)$$

Where:

r is the

k is the wavenumber, in rad/m; it corresponds to:

$$k = \frac{2\pi}{\lambda}$$

λ is the wavelength, in m.

To summarize, the most general representation of a plane wave, accounting for both space and time, involves an amplitude for a sinusoidal function:

$$p(t) = P_0 \cos(\omega t \pm kr)$$

Given a fixed speed of sound (c) in a medium, as the wavelength increases, the frequency decreases, and vice versa. Very low frequencies, near the lower limit of our auditory system (around 20 Hz), have wavelengths exceeding 10 meters. As the frequency increases, the wavelength becomes smaller. At 1000 Hz – a fundamental frequency in speech and music –, the wavelength drops below 1 meter (approximately 34 cm).

The relationship between frequency, wavelength and speed of sound is expressed by the formula:

$$c = \lambda f$$

This relationship is crucial in understanding how sound behaves as it propagates through different mediums. By knowing the frequency and wavelength of a sound wave, we can infer

important characteristics of its propagation, such as the spatial distribution of sound energy and how it interacts with various obstacles and boundaries.

Spherical waves. These are waves that emanate from a point source, and their wavefronts take on the shape of concentric spheres centred at the source. Consider a sound source emitting sound waves equally in all directions. At a substantial distance from the source, the sound waves can be approximated as spherical waves. This is because, from a distance, the curvature of the wavefronts becomes negligible, and the waves propagate uniformly in all directions, similar to the way plane waves do.

The mechanism of a spherical wave involves considering a small pulsating sphere as the source of the wave. As the sphere expands, it compresses the air around it, generating a compression wave that forms a spherical shell enveloping the sphere. Subsequently, as the sphere contracts, it generates a wave of rarefaction that also forms a spherical shell around the sphere. These alternating spherical compression and rarefaction shells continuously move away from the source, exhibiting spherical symmetry.

Mathematically, spherical waves satisfy a wave equation represented as:

$$p(t) = \frac{1}{r} P_0 \cos(\omega t \pm kr)$$

Unlike plane waves, spherical waves have an amplitude that is not constant but decays as it propagates away from the source. This attenuation is a function of the radial distance, making the spherical wave much more realistic in real-world situations.

Cylindrical waves. Cylindrical waves are waveforms that exhibit cylindrical symmetry. They propagate along the axis of the cylinder while maintaining constant phase and amplitude across any circular cross-section perpendicular to the axis. Imagine an infinitely long line source, like a highway with vehicles moving at a constant speed and emitting sound. The sound waves generated by each vehicle can be approximated as cylindrical waves. The waves spread outward from the source along a cylindrical surface, and the sound pressure remains uniform across any circular section perpendicular to the highway.

The mathematical representation for the cylindrical wave is analogous to the spherical wave and maintains the same relationship between pressure variation, radial distance, and time. However, the attenuation of the amplitude in cylindrical waves is proportional to the square root of the distance:

$$p(t) = \frac{1}{\sqrt{r}} P_0 \cos(\omega t \pm kr)$$

The following graph depicted in Figure 5 represents a concise comparison between plane waves, spherical waves, and cylindrical waves as a function of the distance from the source. The plotted quantity is the square of the amplitude; this is because, from a physical perspective, the energy carried by a wave is proportional to the square of its amplitude.

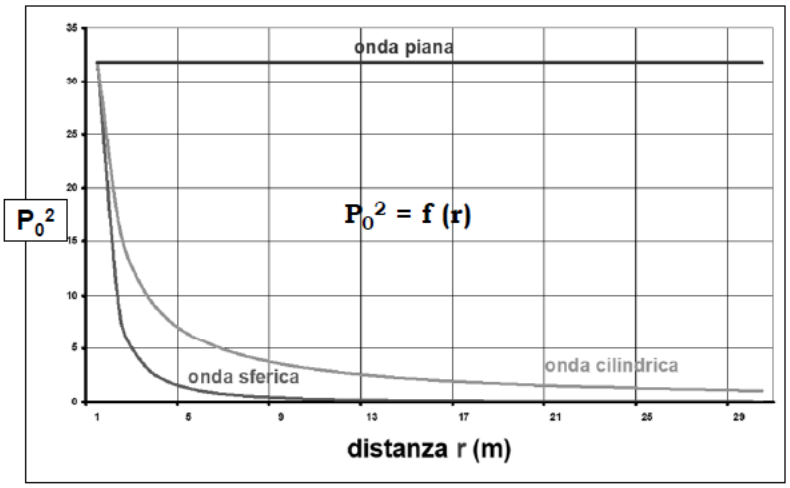

Figure 5. Sound energy variation with increasing distance in plane, spherical and cylindrical waves

The plane wave always carries the same energy that remains constant over distance; this is an idealized construction. The spherical wave attenuates with the square of the distance from the source ($1/r^2$). The cylindrical wave, on the other hand, decays with 1/r.

With these foundational concepts and relationships, we can now introduce and work with acoustic magnitudes that play a crucial role in practical problem-solving. These quantities help us analyse and understand various acoustic phenomena encountered in real-world scenarios.

1.1.5 Acoustic magnitudes

First of all, it is notable to clarify the difference between *sound power* and *sound pressure*. They represent different aspects of sound energy and have distinct units of measurement.

Sound power refers to the total amount of acoustic energy radiated by a sound source per unit of time. It represents the rate at which energy is emitted in the form of sound waves. Sound power is measured in watts (W) and is an intrinsic property of the sound source, meaning it is independent of the distance from the source or the environment in which the sound propagates.

Sound pressure, on the other hand, is a measure of the local instantaneous pressure variation caused by sound waves in a particular medium (usually air). Unlike sound power, sound

pressure depends on the distance from the source, the propagation environment, and any reflecting surfaces.

Another important acoustic quantity is the *sound intensity*. Sound intensity is the rate at which sound energy passes through a unit area in a specified direction per unit of time. It can be expressed as the product of the oscillating particle speed and the acoustic pressure p:

$$I = pu\ [\frac{W}{m^2}]$$

As sound waves propagate away from the source and spread out over a larger area, the sound intensity decreases due to the increased area over which the energy is distributed.

Sound power, sound pressure, and sound intensity are extremely interrelated and provide valuable insights into the acoustic characteristics and energy distribution of sound waves.

Sound Power to Sound Pressure. In *plane waves*, the sound power generated by a source contributes to the sound pressure in the surrounding medium. As sound waves spread out from the source, the sound power is distributed over an increasing area, resulting in a decrease in sound pressure with distance.

$$W = \frac{{P_0}^2}{2\rho_0 c} S$$

Where:

W is the sound power, in W;

P_0 is the pressure amplitude, in Pa;

$\rho_0 c$ is a characteristic quantity that relates the static density of the medium (in kg/m^3) with the sound speed (in m/s). Thus, it is the *acoustic resistance* of the medium.

S is the effective radiation area of the source, in m^2.

In the case of *spherical waves*, the effective radiation area is a sphere and the amplitude decays with the increasing distance.

$$W = \left(\frac{{P'_0}^2}{r}\right)\frac{4\pi r^2}{2\rho_0 c} = \frac{2\pi {P'_0}^2}{\rho_0 c}$$

These equations show that the sound power is directly proportional to the square of the sound pressure at a given distance. As the sound pressure increases, the sound power increases exponentially.

Sound Power to Sound Intensity. Sound intensity is inversely proportional to the area over which the sound power is distributed, resulting in a ratio between two constants. For *plane wave* sources, the power flow remains constant across all positions.

$$I = \frac{W}{S} = cost$$

Where:

I is the sound intensity, in W/m^2;

W is the sound power, in W;

S is the area through which the sound power is radiated, in m^2

For *spherical waves*, the dispersion of power on the spherical surface increases as we move farther away from the source. Consequently, the intensity diminishes in proportion to the square of the radius, signifying the distance from the source to the receiver.

$$I = \frac{W}{4\pi r^2} \propto \frac{1}{r^2}$$

Sound Pressure to Sound Intensity. In the time domain, the intensity is directly proportional to the square of the acoustic pressure and inversely proportional to the density and speed of sound in the medium.

$$I(t) = \frac{p^2(t)}{\rho_0 c}$$

Where:

$I(t)$ is the sound intensity as a function of time, in W/m^2;

p is the sound pressure, in Pa;

$\rho_0 c$ is the acoustic resistance of the medium.

1.1.6 Sound reception: the human hearing system

The human hearing system is a complex and remarkable sensory mechanism that allows us to perceive and interpret sound waves from our environment. It consists of three main components: the outer ear, the middle ear, and the inner ear.

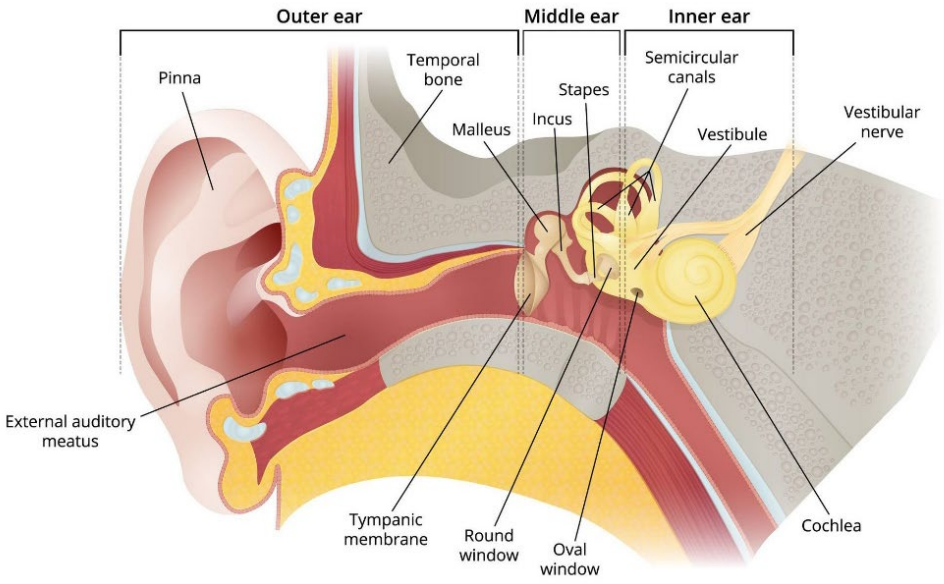

Figure 6. Human auditory system representation

Outer Ear. The outer ear is the visible part of the ear and serves as the initial gateway for sound waves to enter the auditory system. It consists of two primary structures:

- Pinna (Auricle): The pinna is the external, fleshy, and cartilaginous structure on the side of the head. It helps in capturing sound waves from the surrounding environment and directing them into the ear canal.
- Ear Canal (External Auditory Canal): The ear canal is a tube-like structure that extends from the pinna to the eardrum (tympanic membrane). It serves to amplify and channel sound waves towards the middle ear.

Middle Ear. The middle ear is an air-filled cavity located between the eardrum (tympanic membrane) and the inner ear. It contains three small bones known as the ossicles, which transmit sound vibrations from the eardrum to the fluid-filled inner ear. The middle ear includes the following components:

- Tympanic Membrane (Eardrum): The eardrum separates the outer ear from the middle ear. When sound waves strike the eardrum, it vibrates, transmitting the mechanical energy of sound to the ossicles.

- Ossicles: The ossicles consist of three tiny bones – the malleus (hammer), incus (anvil), and stapes (stirrup). They form a chain of bones that amplify and transmit the sound vibrations from the eardrum to the inner ear. The malleus is connected to the eardrum, while the stapes is connected to another vibrating membrane (oval window) that transmits the vibrations to the inner ear.
- Eustachian Tube: This tube connects the middle ear to the back of the throat. It helps maintain equal air pressure on both sides of the eardrum and regulates the conditions within the middle ear.

Inner Ear. The inner ear is the complex structure responsible for converting mechanical vibrations (sound) into neural signals that the brain can interpret as auditory sensations. It comprises two primary components:

- Cochlea: The cochlea is a spiral-shaped, fluid-filled structure resembling a snail's shell. It is a complex system composed by three section – scala vestibuli, scala tympani and scala media – separated by two membranes. The scala media contains the sensory cells (hair cells) responsible for converting sound vibrations into electrical signals. Different parts of the cochlea are sensitive to different frequencies, allowing us to perceive a wide range of sounds.
- Vestibular System: The vestibular system is adjacent to the cochlea and is responsible for maintaining balance and spatial orientation. It contains structures like the semicircular canals and the utricle and saccule, which detect head movement and acceleration.

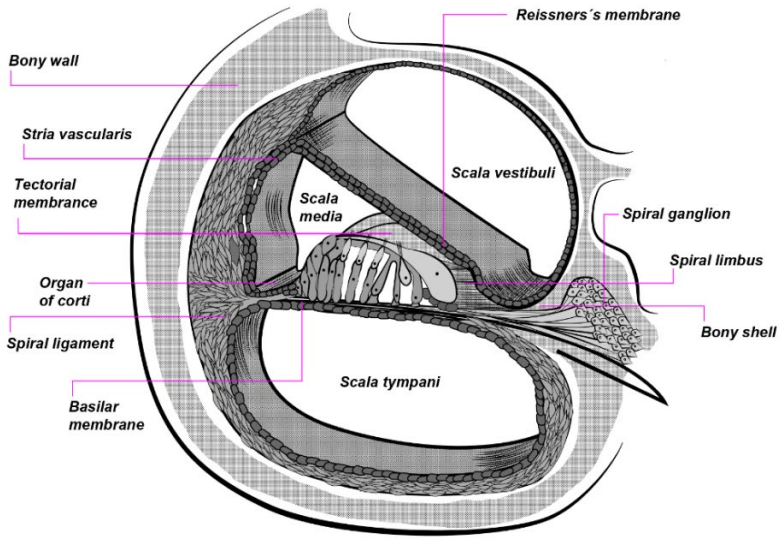

Figure 7. Sectional view of the cochlea

The complex interaction between the outer ear, middle ear, and inner ear allows us to perceive sound, from the moment sound waves enter the ear canal to the conversion of those waves into neural signals that our brain interprets as meaningful auditory experiences. Any disruptions or issues within these components can lead to hearing impairments or balance problems, underscoring the delicate and intricate nature of the human hearing system.

1.1.6.1 Equal-loudness contours

Our hearing system is sensitive within a frequency range spanning approximately from 20 Hz to 20,000 Hz. Frequencies below 20 Hz are categorized as infrasounds, while those above 20,000 Hz are classified as ultrasounds. Notably, these are sound ranges beyond human auditory perception.

The dynamics of the human auditory system pertain to the range of sensitivity between the minimal and the most intense signals that can be detected. In controlled conditions, individuals with healthy hearing can perceive a pure tone at 1000 Hz with a minimum detectable sound pressure level of 20 μPa – equivalent to $2x10^{-5}$ Pa. This sensitivity is exceptionally high, being ten orders of magnitude below atmospheric pressure. On the other hand, 200 Pa marks the pain threshold, causing irreversible damage to the auditory system. This damage includes potential eardrum perforation, dislocation of ossicles, and most significantly, the death of hair cells, which are crucial nerve-type cells that do not regenerate.

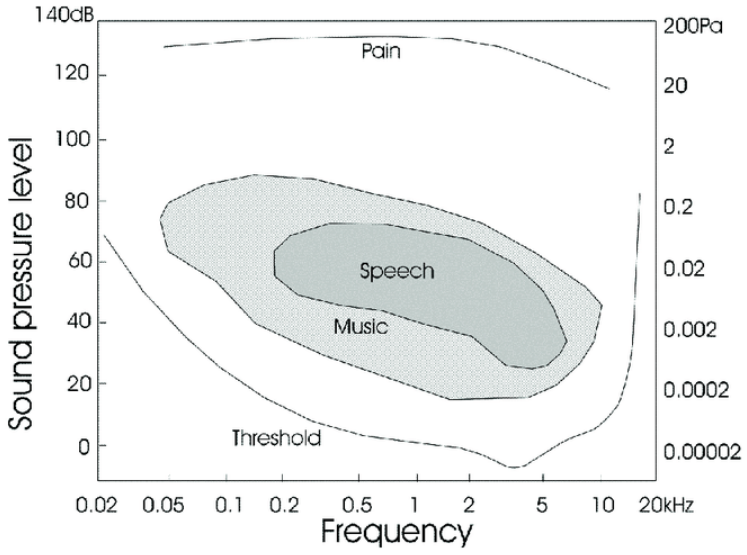

Figure 8. Human hearing area, with audibility and pain thresholds

The dynamics of the human auditory system play a crucial role in our perception of sound, including how we interpret the information provided by *equal-loudness contours*.

Equal-loudness contours illustrate the sound pressure levels across different frequencies that are perceived as equally loud to the human ear. These curves are derived from extensive psychoacoustic studies that take into account the varying sensitivity of our ears to different frequencies. The threshold level, acknowledged as the minimum audible sound, is normalized to 20 μPa (at 1000 Hz).

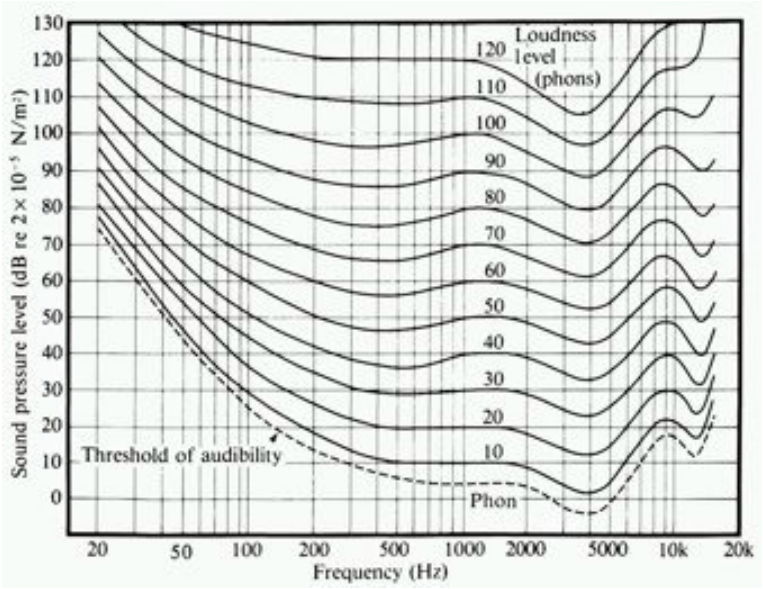

Figure 9. Equal-loudness contours according to ISO 226 standard. Both axes are in logarithmic scale

Our hearing is more sensitive to certain frequencies, particularly in the midrange frequencies around 1000 Hz. Consequently, isophonic curves exhibit the characteristic shape depicted in Figure 9, with elevated sensitivity in the medium region and reduced sensitivity at both lower and higher frequencies. This unique response to different frequencies directly influences how we perceive sounds at varying intensities.

Moreover, the knowledge of our auditory system's sensitivity to different sound pressure levels is pivotal in designing sound systems and spaces that aim to provide optimal listening experiences. Equal-loudness contours aid in calibrating audio systems to deliver balanced and accurate sound across different frequencies, considering the varying loudness perception of our ears.

1.1.6.2 The Weber-Fechner principle

The Weber-Fechner Law is a fundamental principle in psychology that helps explain the non-linear relationship between the physical intensity of a stimulus and our psychological perception of that stimulus. Specifically, in the context of auditory perception, the Weber-Fechner Law states that the perceived loudness of a sound is not directly proportional to its physical intensity – measured in decibels or other units.

Mathematically, the Weber-Fechner Law can be expressed as follows:

$$\Delta S \approx k \frac{\Delta P}{P}$$

Where:

ΔS is the just noticeable difference (JND) in perception (e.g., loudness)

ΔP is the magnitude variation of the stimulus (e.g., sound intensity)

P is the physical intensity of the last stimulus

k is a constant factor

In practical terms, this law explains why we perceive small changes in loudness more acutely at lower sound levels and are less sensitive to similar changes at higher sound levels. If we examine this phenomenon through the lens of a differential relation and perform a visual integration, the outcome can be expressed as:

$$S \approx klnC$$

Wherein the absolute sensation correlates with the logarithm of the stimulus, subject to certain constants. Consequently, it becomes evident that our perception of loudness follows a logarithmic relationship with the physical intensity of the sound.

The Weber-Fechner Law has important implications for fields such as psychophysics, perception, and the design of sensory experiments. It helps us understand how our auditory system processes and interprets sound stimuli, accounting for the non-linear nature of our perception of loudness and other sensory attributes.

1.1.7 Sound levels

To summarize the aforementioned aspects:

- Sound power is proportional to the square of sound pressure, thus indicating a lack of linearity in this relationship;
- The dynamic range of human auditory sensitivity spans from $2x10^{-5}$ Pa to 200 Pa, encompassing a six-order magnitude disparity, which consequently leads to notable measurement uncertainties;
- The subjective perception of sound exhibits a non-linear nature, manifesting a logarithmic connection with the physical stimulus.

Given these physical considerations, it becomes apparent that linear assessments are unsuitable for computations and acoustic measurements. Consequently, the introduction of *sound levels*, acoustic magnitudes on a logarithmic scale, becomes necessary to simplify the interpretation of measured values, mitigate their uncertainties, and more accurately approximate the non-linear response of the human auditory system.

The process of formulating this definition can be broken down into several steps:

1. **Derivation from pressure**: The objective is to measure energy, which cannot be directly measured. Instead, energy is derived from pressure (p). Once pressure is measured, it is squared using a simple microphone.
2. **Normalization with reference value**: Due to increased variability, the squared results are further normalized using the audibility threshold as a reference value (p_0). This transition transforms the consideration from p^2 to [p/p0]^2, yielding a dimensionless value devoid of specific units.

$$\left[\frac{p(t)}{p_0}\right]^2, \qquad p_0 = 20\ \mu Pa$$

3. **Logarithmic compression**: To accommodate the broad auditory range, a logarithmic transformation is applied to the normalized value. A base 10 logarithm is used, effectively compressing the numerical field while retaining physical significance. This operation is given a label, called *bel* [B], which is a pure non-dimensional unit that serves as a quantification of the logarithmic transformation.
4. **Amplification and final definition**: Due to its excessive compression, the process was adjusted to provide more room for variation. The first submultiple of the bel, its tenth, was employed for this purpose – resulting in *decibels*. Numerically, this involves multiplying the logarithmic value by 10, ultimately forming the conclusive definition referred to as sound pressure level (L_p).

$$L_p = 10log\left[\frac{p(t)}{p_0}\right]^2 \ decibel\ [dB]$$

This nuanced process not only simplifies the measurement process but also acknowledges the non-linear nature of our auditory perception.

The illustration in Figure 10 depicts a concise comparison between pressure levels (in Pa) and sound pressure levels (in dB) values associated with acoustic waves, ranging from low pressures indicative of faint sounds to high pressures generated by very loud noises. The logarithmic scale provides a more compact and manageable scale.

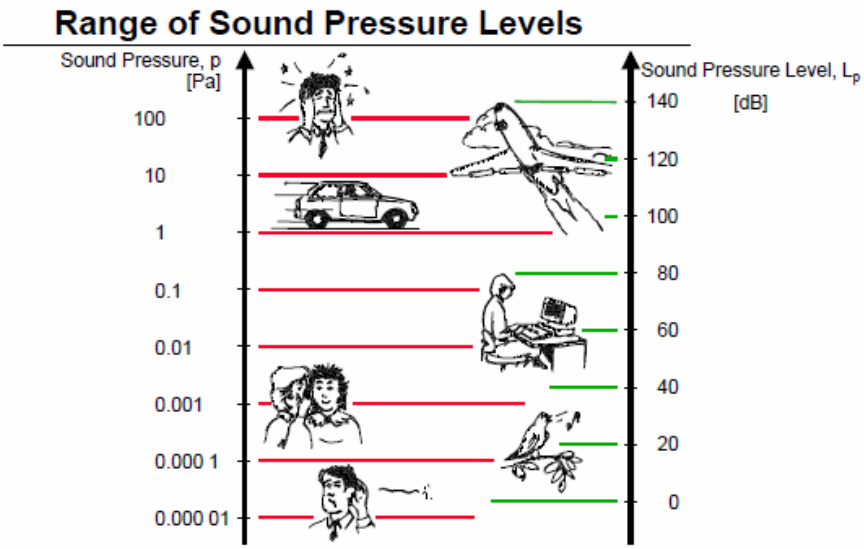

Figure 10. Range of sound pressure levels

It is crucial to note that the scale's logarithmic nature must be kept in mind during operations, ensuring adherence to logarithmic principles.

Upon establishing the decibel scale for sound pressure levels, it is equally feasible to extend this definition to more fundamentally energetic parameters such as *sound power* and *sound intensity*. These extensions are defined as follows:

- Sound power level (Lw):

$$L_W = 10log\left[\frac{W(t)}{W_0}\right] dB, \quad W_0 = 10^{-12}\ W$$

This parameter, which pertains to energy, cannot be directly measured by instruments; however, established standards provide guidance on its determination. In this context, there is no requirement for exponentiation, as power inherently signifies an energy measure.

- Sound intensity level (L_I):

$$L_I = 10log\left[\frac{I(t)}{I_0}\right] dB, \quad I_0 = 10^{-12}\, W/m^2$$

1.1.8 FFT and CPB passband filters

Passband filters are usually implemented into electronic or digital devices allowing a certain range of frequencies to pass through while attenuating or blocking frequencies outside that range. They are commonly used in signal processing and communication systems to isolate specific frequency components from a larger spectrum of frequencies.

A passband filter is characterized by two main parameters: the centre frequency and the bandwidth. The centre frequency is the frequency around which the filter allows the most energy to pass, while the bandwidth specifies the range of frequencies that are permitted to pass through.

There are mainly two different types of passband filters:

1. **FFT (Fast Fourier Transform) filter**: FFT is a mathematical algorithm used to transform a time-domain signal into its frequency-domain representation. It allows us to analyse the frequency components present in a signal. FFT filters have a fixed or constant bandwidth in Hertz (Hz) around a central frequency. This means that as the centre frequency changes, the absolute bandwidth remains the same.
2. **CPB (Constant Percentage Bandwidth) filter**: CPB refers to a bandwidth that remains a constant percentage of the centre frequency. This concept is particularly relevant in *octave* and *fractional octave filters*, where the centre frequency and bandwidth are related logarithmically. CPB ensures that filters maintain consistent characteristics across different frequency ranges; furthermore, it offers notable convenience when operating across an extensive spectrum of frequencies.

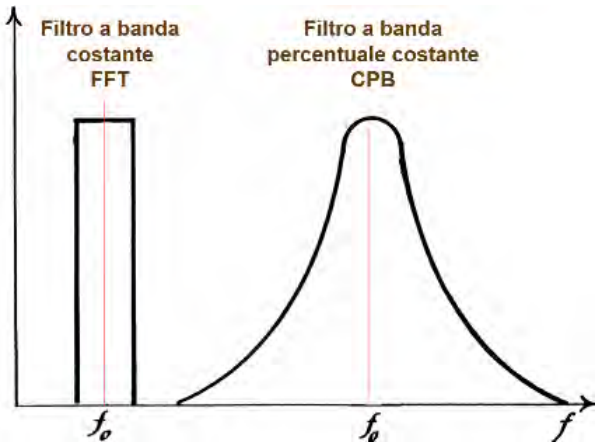

Figure 11. FFT and CPB passband filters

1.1.9 Reflection, absorption and transmission

When energy waves interact with a material surface, they experience reflection, absorption, and transmission. This holds true for various energy forms, including sound and light. The reflected portion contributes to what we hear, while the transmitted part gains significance in distant spaces. Mathematically, this is expressed as:

$$W_i = W_r + W_a + W_\tau$$

Where:

W_i is the incident sound power, comprising reflected (W_r), absorbed (W_a), and transmitted (W_τ) energies.

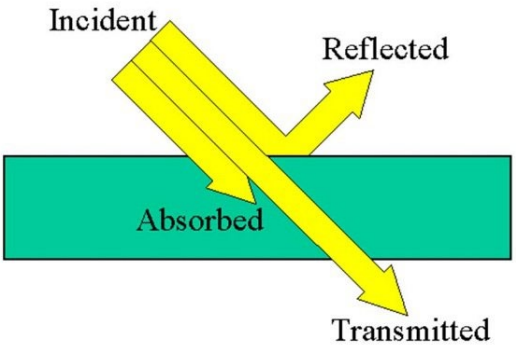

Figure 12. Incident sound wave interacting with a surface

To quantify these interactions, reflection (r), absorption (a), and transmission (τ) coefficients are introduced as power ratios: $r = \frac{W_r}{W_i}$, $a = \frac{W_a}{W_i}$, $\tau = \frac{W_\tau}{W_i}$. The sum of these coefficients is 1, revealing their interdependence.

$$r + a + \tau = 1$$

In the field of acoustics, a novel coefficient, denoted as α, is introduced. In light of the interrelated nature of these coefficients, α represents the combined power of absorbed and transmitted energy. In other worlds, it corresponds to all the non-reflected sound power:

$$\alpha = a + \tau = 1 - r = \frac{W_a + W_\tau}{W_i}$$

Practically, α is utilized as the primary indicator of sound absorption, superseding the absorption coefficient 'a'. This is a common practice among material vendors, who often refer to α as the sound absorption coefficient.

From α, a quantity related to surface area is derived. By multiplying the surface area (S) of a material by its absorption coefficient, the value A is obtained. A is known as the *sound absorbing power* or equivalent sound absorption of the surface. It is quantified in square meters (m^2), sometimes also referred to as "Sabin," named after Wallace Clement Sabine, a pioneer in modern acoustics.

$$A = \alpha S \ \ [m^2] \ or \ [Sabin]$$

Now, let us delve into the central theoretical aspect that holds the greatest significance for the purpose of this thesis: the study of acoustics within enclosed spaces.

1.1.10 Sound waves in enclosed spaces

Unlike open environments, reflections between walls significantly shape the distribution of sound waves and their perception. These reflections impact both the energy distribution across frequencies and the perception of reverberation, thus requiring careful consideration for effective acoustic design.

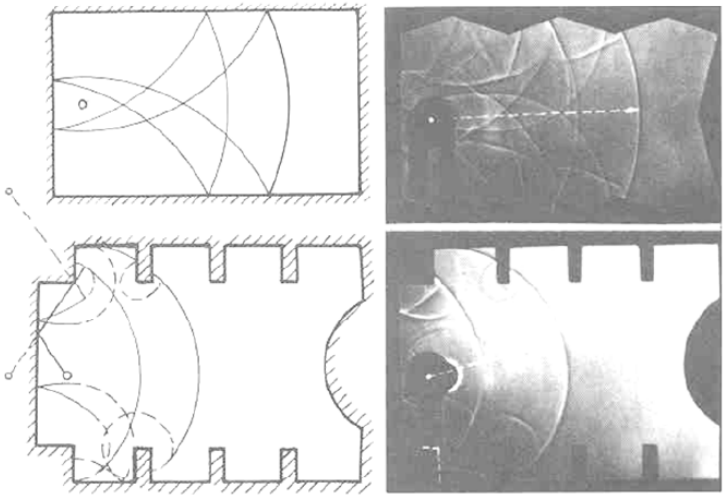

Figure 13. Simulation of sound wave propagation within enclosed spaces, involving the utilization of predictive models that replicate the phenomenon of wave reflection against walls. On the right, a physical experiment was conducted, employing water-filled bowls and propelled stones to observe the progression of the wave front.

Moreover, t's imperative to acknowledge the significant variability in the wavelength of sound waves within the audible frequency rang. For instance, at 20 Hz, the wavelenght is 17.2 meters, whereas at 20 kHz, it reduces to 0.17 meters. Consequently, distinct methodologies are required for treating low and medium-high frequencies.

These approaches utilize various methods to analyse sound propagation and interactions within architectural environments.

Wave Theory. The wave theory involves treating waves as solutions to the wave equation. D'Alembert's wave equation can be used as a foundational concept, expanded with a non-homogeneous term that characterizes the effects of sound sources. Analytical solutions are feasible for simpler geometries like spheres, cylinders, and parallelepipeds. However, for more complex environments, especially those with irregular shapes, numerical methods are essential. These techniques, facilitated by modern computers, provide insights into how sound waves interact with various surfaces and structures.

For instance, let's consider a parallelepiped-shaped environment with perfectly reflective surfaces (α=0, ρ=1). The pressure field p – as a function of spatial coordinates and time – can be separated into a spatial part P(x,y,z) and a harmonic temporal term $e^{i\omega t}$:

$$p(x, y, z, t) = P(x, y, z)e^{i\omega t}$$

One can focus only on the spatial component's progress within this idealized environment. The spatial behaviour of the sound field can be described by the *Helmholtz equation*:

$$\nabla^2 P(x,y,z) + k^2 P(x,y,z) = 0$$

Where:

∇^2 is the Laplacian of P

k^2 is the wavenumber.

To solve the Helmholtz equation, appropriate boundary conditions must be established. These conditions are governed by the fact that the walls are perfectly rigid. Consequently, at the boundaries, the pressure experiences a maximum and momentarily freezes before rebounding.

Without delving into intricate mathematical steps, it is feasible to establish that within a closed environment, the distribution of the sound field is not uniform; rather, it is characterized by the presence of three cosines, each corresponding to a distinct spatial direction. These cosines exhibit maxima and minima as dictated by the boundaries and spatial configuration.

$$p(x,y,z,t) = C \cdot \cos\left(\frac{n_x \pi}{L_x}\right) \cdot \cos\left(\frac{n_y \pi}{L_y}\right) \cdot \cos\left(\frac{n_z \pi}{L_z}\right) \cdot e^{i\omega t}$$

Where:

p is the pressure field as a function of time and spatial coordinates;

C is an arbitrary constant;

$\frac{n_x \pi}{L_x} = k_x$ is the solution of P_x after imposing the boundary solutions (same for k_y and k_z);

$e^{i\omega t}$ is the harmonic temporal term.

Thus, if a sound field is generated within an enclosed space, it inherently responds by establishing these sinusoidal waves, dependent on a set of three integer values (n_x, n_y, n_z). The frequencies at which these *stationary waves* are established correspond to the natural frequencies of the environment. These frequencies are derived from the roots of a highly symmetrical equation, which can be expressed as follows:

$$f_{n_x,n_y,n_z} = \frac{c}{2}\sqrt{\left(\frac{n_x}{L_x}\right)^2 + \left(\frac{n_y}{L_y}\right)^2 + \left(\frac{n_z}{L_z}\right)^2}$$

In summary, within an enclosed space stationary waves are established, characterized by points of maxima and minima. These patterns are referred to as the *normal modes of the environment*,

contributing to the non-uniform distribution of energy. This phenomenon is rooted in the wave nature of sound, resulting in the presence of points where the sound wave exhibits maximum amplitude as well as points where it reaches zero amplitude.

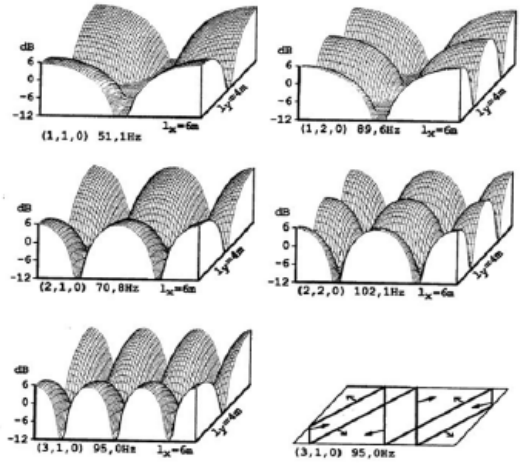

Figure 14. Representation of normal modes within a parallelepiped-shaped room.

Geometric Approximation. Geometric approximation, often referred to as ray acoustics or geometric acoustics, simplifies the complex behaviour of sound waves by treating them as rays that reflect, refract, and diffract. This approach is particularly effective for higher-frequency sound waves, where the normal modes exhibit a significant overlapping, rendering them indistinguishable from one another. To determine the cross-over frequency at which a shift occurs from the modal regime to the statistical regime, conventionally, the *Schroeder frequency* formula is employed (M. Schroeder, 1987). This formula is expressed as:

$$f_s = 2000\sqrt{\frac{T}{V}}$$

Where:

f_s is the Schroeder frequency, in Hz;

T is the averaged reverberation time, in s;

V is the total room volume, in m^3.

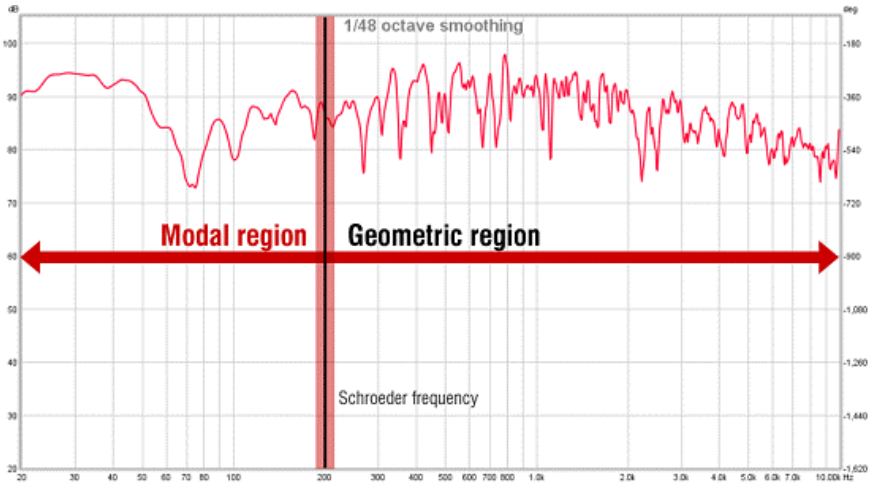

Figure 15. Transition between modal region and geometric-statistic region through Schroeder frequency

The geometric approximation is commonly used in numerical methods to predict sound propagation paths in spaces with complex geometries. Image Source Method (ISM) and Stochastic Ray Tracing (SRT) techniques help estimate sound reflections, absorption, and diffusion, enabling the design of optimal acoustic environments for specific purposes. Such methodologies are integrated into the most reliable acoustic simulation software, such as CATT-Acoustic or Odeon. For more comprehensive insights, please refer to section 4.1.

Energetic-Statistic Approximation. In this approach, the average behaviour of sound energy is analysed statistically, as it considers diffuse field conditions in enclosed spaces. *Reverberation time*, which measures the time sound takes to decay by 60 dB in a space, is a key parameter studied in this approach (see par. 1.3.1). Acoustic treatments such as adding absorptive materials and diffusers are designed to manipulate reverberation time and enhance sound clarity.

These three approaches are not mutually exclusive; they often complement each other to provide a comprehensive understanding of sound behaviour in enclosed spaces across different frequency ranges. By applying these methods, architects, engineers, and acousticians can create environments that cater to specific acoustic requirements, whether it's achieving optimal sound quality for music, reducing noise in office spaces, or creating immersive experiences in theatres and auditoriums.

1.2 Introduction to ISO 3382 standards

This chapter provides a concise overview of the guidelines set forth in the international technical standard for measuring room acoustic parameters. Additionally, a brief list of these criteria – which are extensively described in the standard – will aid in establishing a general framework for understanding the quantities necessary for a comprehensive description of the acoustic conditions of concert halls.

The series of standards, collectively titled "Measurement of Room Acoustic Parameters," is organized into three sections:

- ISO 3382-1: Performance spaces
- ISO 3382-2: Reverberation time in ordinary rooms
- ISO 3382-3: Open plan offices

This chapter will specifically focus on ISO 3382-1, as the second and third parts are deemed irrelevant to the scope of this thesis.

1.2.1 ISO 3382-1: General rules for the execution of measurements

The first part of ISO 3382-1 outlines the measurement of the reverberation time, which will be defined mathematically in the subsequent paragraph.

Measurement conditions. An accurate description of the *states of occupancy* of the room is essential to establish the results obtained with the reverberation time measurement. All habitual states of occupation and variable settings of the acoustical conditions must be defined and clearly distinguished from each other.

Equipment to be used.

- **Sound source.** The sound source shall be as omnidirectional as possible, with a sound pressure level sufficient to provide a complete decay curve in the required frequency range, without contamination from background noise.
- **Microphone.** The microphone to be used in measuring the reverberation time shall be omnidirectional, or better for a diffuse sound field for most criteria, except for the measurement of the lateral fraction (JLF) and IACC. In addition, it should be as small as possible, with a maximum diaphragm diameter of 13 millimetres. The distance between the sound source and the microphone shall not be less than 1.5 meters during the measurements.

- **Recording device.** The recording time of each sound decay shall be sufficiently long to enable determination of the final background level following the decay; the international standard recommends five seconds plus the expected reverberation time as a minimum. The dynamic range shall be sufficient to allow the required minimum decay curve range.

Apparatus for forming the decay record of level. It is possible to use exponential or linear averaging, with continuous curve or successive discrete sample points as output. The averaging time, i.e. time constant of an exponential averaging device, shall be less than, but as close as possible to, T/30.

Measurement positions. The source positions should be situated where the natural sound sources in the room would commonly be located. At the very least, two source positions must be employed. Additionally, the height of the acoustic centre of the source ought to be at 1,5 meters above the floor.

In terms of microphone placement, the measurement positions should coincide with representative locations where listeners would typically be situated. Furthermore, they should sample the entirety of the space and be selected in a manner that accounts for the significant influences that are likely to cause differences in RT throughout the room. Examples of such influences may include seating areas situated close to walls or beneath balconies.

In order to ensure accurate measurement of the room's acoustic criteria within the typical frequency range, microphone positions should be spaced at a minimum of 2 meters apart. Additionally, the distance from each microphone position to the nearest reflecting surface, including the floor, should be approximately 1 meter. The height of the microphones should be 1.2 meters above the floor, corresponding to the average ear height of listeners seated in typical chairs. The ISO 3382 also provides a reference in the Annex A for the minimum recommended number of receiver positions, as a function of hall size:

Number of seats	Minimum number of microphone positions
500	6
1 000	8
2 000	10

Table 3. Minimum number of receiver positions as a function of auditorium size. ISO 3382-1, Annex A

Measurement procedures. In this section of ISO 3382, two methods for measuring reverberation time are outlined: the interrupted noise method and the integrated impulse response method. For all other acoustic criteria, the second method is recommended.

For the engineering and precision methods, the frequency range should cover at least 125 Hz to 4000 Hz in octave bands.

- **Interrupted noise method.** The loudspeaker utilized for exciting the room should derive from broadband random or pseudo-random electrical noise. To ensure accurate results, the source must produce a sound pressure level adequate enough to initiate a decay curve with a minimum of 35 dB above background noise - for measuring T30, it must be at least 45 dB. The duration of the excitation of the room should be adequate enough for the sound field to reach a stable state before the source is turned off. Due to the inherent randomness of the source signal, ISO 3382 stresses the need to average over multiple measurements at each position to obtain acceptable measurement uncertainty.
- **Integrated impulse response method.** The meaning of the impulse response will be expounded later in more detail (see par. 1.3.2). There exist various methods of measuring the impulse response, including the use of pistol shots, spark gap impulses, noise bursts, chirps or maximum-length sequences (MLS) as signals. It is required that the impulse source is capable of producing a peak sound pressure level sufficient to ensure a decay curve initiating at least 35 dB above the background noise in the corresponding frequency band. For T30, the required level is 45 dB. The decay curve for each octave band is generated by a backward integration of the squared impulse response, as per the following equation:

$$E(t) = \int_{t}^{+\infty} p^2(\tau)d\tau = \int_{+\infty}^{t} p^2(\tau)d(-\tau)$$

  The physical and mathematical explanation of the above equation is provided in the following chapter (see par. 1.2.2.1.2).

1.2.2 ISO 3382-1: Acoustic criteria

For numerous years, the sole measure of acoustic quality in concert halls was considered to be the reverberation time, due to its well-understood nature and simple calculability. Nevertheless, since its initial release in 1975, ISO 3382-1 has established a quantitative framework for a set of acoustic quantities, referred to as acoustic criteria, that are mathematically derived from the

impulse response and associated with subjective factors that link the room's acoustics to the listener's psychoacoustic perception. Annex A classifies these criteria into five distinct types (refer to Table 4).

Subjective listener aspect	Acoustic quantity	Single number frequency averaging [a] Hz	Just noticeable difference (JND)	Typical range [b]
Subjective level of sound	Sound strength, G, in decibels	500 to 1 000	1 dB	–2 dB; +10 dB
Perceived reverberance	Early decay time (EDT) in seconds	500 to 1 000	Rel. 5 %	1,0 s; 3,0 s
Perceived clarity of sound	Clarity, C_{80}, in decibels	500 to 1 000	1 dB	–5 dB; +5 dB
	Definition, D_{50}	500 to 1 000	0,05	0,3; 0,7
	Centre time, T_S, in milliseconds	500 to 1 000	10 ms	60 ms; 260 ms
Apparent source width (ASW)	Early lateral energy fraction, J_{LF} or J_{LFC}	125 to 1 000	0,05	0,05; 0,35
Listener envelopment (LEV)	Late lateral sound level, L_J, in decibels	125 to 1 000	Not known	–14 dB; +1 dB

[a] The single number frequency averaging denotes the arithmetical average for the octave bands, except for L_J which shall be energy averaged [see (A.17)].

[b] Frequency-averaged values in single positions in non-occupied concert and multi-purpose halls up to 25 000 m^3.

Table 4. List of acoustic criteria extracted from ISO 3382-1, Annex A.

Prior to introducing these descriptors, it is necessary to delve into the concept of reverberation time and its evolution over time.

Reverberation Time RT

According to ISO 3382, the reverberation time is defined as the time, expressed in seconds, which takes the sound pressure level to decrease by 60 dB after the source emission has stopped. This value is extracted from the decay curve – which can be obtained by squaring the impulse response – and corresponds to Sabine's original definition of the T_{60}.

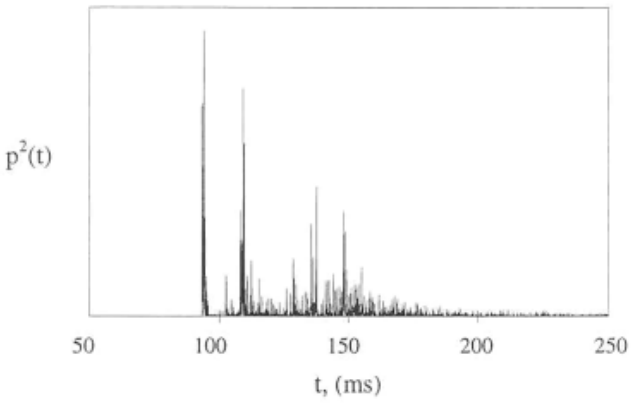

Figure 16. Echogram of the impulse response, from which the RT is extracted

The duration of the reverberation time is dependent on frequency and therefore must be assessed in each octave or third octave band. Typically, the duration of reverberation time is shorter at higher frequencies, owing to the greater range of materials capable of absorbing them and the absorptive qualities of air.

RT formulas

Sabine formula.

$$T_{60}(f) = 0{,}16\frac{V}{A} = 0{,}16\frac{V}{\bar{\alpha}(f)S} \ \ [s]$$

Where the factor 0.16 is related to the speed of sound. Furthermore:

V is the volume of the room in m^3;

$\bar{\alpha}(f)$ is the average absorption coefficient of the room surfaces, which varies according to the frequency of the sound wave;

S is the total surface area of the room, in m^2;

A it is defined as equivalent sound absorption, in sabins;

Sabine's equation is valid under the following assumptions:

- Sound energy is distributed uniformly in the room;
- Sound waves propagate in completely random directions, i.e. equally in every direction.

Norris-Eyring formula. Norris-Eyring's formula, developed in the 1930s, provides significant corrections to the Sabine formula, especially in the case of very absorbent rooms. An average reflection coefficient is introduced, which is also valid for non-uniform diffusion of sound energy: $\bar{r} = 1 - \bar{\alpha}$.

$$T_{60}(f) = -0{,}16\frac{V}{S\ln\bar{r}\,(f)} = -0{,}16\frac{V}{S\ln(1-\bar{\alpha})\,(f)} \ \ [s]$$

Where the minus sign allows to bring it back the formula to positive values. Furthermore:

V is the volume of the room in m^3;

$\bar{r}(f)$ is the average reflection coefficient of the room surfaces, which varies according to the frequency of the sound wave;

S is the total surface area of the room, in m^2;

The Norris-Eyring equation gives more accurate results in highly absorption conditions ($\alpha \rightarrow 1$) minimizing the errors and approximations inherent in the Sabine's formula (Eyring, 1930).

Schröder integral for evaluating RT

In the 1960s, Schröder introduced a new approach for measuring reverberation time with the emergence of the impulse response technique. This method involves obtaining the sound decay curve by performing a backward integration of the squared impulse response. (M. R. Schroeder, 1965).

$$E(t) = \int_{t}^{+\infty} p^2(\tau)d\tau = \int_{+\infty}^{t} p^2(\tau)d(-\tau)$$

Where:

$E(t)$ is the sound field energy as a function of time;

$p^2(\tau)$ is the square of sound pressure as a function of a fictitious time.

The method proposed by Schröder provides a more precise estimation of the reverberation time and has since become a standard technique for its computation. Unlike Sabine's method, which required a stationary noise source, the Schröder method allows for the use of various sound sources, such as impulsive sources and exponential sweeps.

T_{20} and T_{30}

To be valid, the T_{60} assumes a very low background noise which is not supposed to alter the measurement result. Since this condition is nowadays not ensured due to traffic noise or similar, it is usually preferred to select a small portion of the decay curve, then extrapolated to a 60 dB decay time. If we consider a decay of 30 dB, in the range from -5 dB to -35 dB, the parameter is defined as T30; then multiplied by 2, it returns the decay time of 60 dB. Similarly, if we consider a decay of 20 dB in the range from -5 dB to -25 dB, the parameter is defined as T20 and multiplied by 3.

Note that, to avoid the fluctuations from stationary state to decay which cause greater uncertainty in the measurement, the reverberation time is estimated starting from 5 dB and not from 0 dB, that is, from when the decay has already started.

There is an exception to this approach, which is EDT.

Early Decay Time (EDT)

The definition of EDT is similar to that of the reverberation time. The difference between the two lies in the time interval evaluated in the decay curve. In the case of EDT, the slope of the curve is determined in the initial 10 dB (from 0 dB to -10 dB) of decay. The EDT is then extracted by multiplying the found value by 6; this allows a "direct comparison between EDT and RT" (Beranek, 2004).

Therefore, EDT represents the very first impression of Reverberance, closer to the subjective sensation of the listener than to the physical properties of the room, although subject to more uncertainty due to the initial fluctuations.

Moreover, while the RT normally presents the same value in all positions, the EDT varies as the source-receiver distance changes.

ISO 3382-1 establishes the need to measure both RT and EDT.

Sound strength G

Sound Strength is a logarithmic ratio of energies that expresses the reinforcement – or damping – of sound in an enclosed space. This comparison relates the sound energy emitted by a source as measured within the enclosed environment to that same sound energy as measured in a free field at a distance of 10 meters:

$$G = 10 \lg \frac{\int_0^\infty p^2(t)\, dt}{\int_0^\infty p_{10}^2(t)\, dt} = L_{pE} - L_{pE,10}\ dB$$

Where:

$p(t)$ is the instantaneous sound pressure of the impulse response measured at the measurement point;

$p_{10}(t)$ is the instantaneous sound pressure of the impulse response measured at a distance of 10 m in a free field. This is measurable within an anechoic chamber (see par. 3.2.4 for further information);

p_0 is 20 μPa;

L_{pE} is the sound pressure exposure level of $p(t)$;

L_{pE} is the sound pressure exposure level of $p_{10}(t)$.

- When the Sound Strength value is less than 0, it signifies that the enclosed space is absorbing the sound energy, resulting in a damping effect. Such a room is commonly referred to as a "dead" room due to its high level of absorption.
- On the other hand, a Sound Strength value greater than 0 indicates that the enclosed space is amplifying the sound energy relative to the free field. Such a room is known as a "live" room due to its ability to reinforce sound.

Clarity parameters

The criteria used to evaluate the clarity of speech or music in an enclosed space are defined as *energy fractions*. They are determined by dividing the impulse response of the enclosed environment into two components – "useful" energy and "harmful" energy – based on the arrival time of reflections in milliseconds.

The parameters are designed to assess the impact of early reflections, which are considered crucial in determining speech or music clarity within the enclosed environment.

Definition D50. The following descriptor is an Early-to-Total Ratio, a quantitative measure of the proportion of sound energy represented by early reflections, relative to the total sound energy within an enclosed environment. This ratio is expressed on a linear scale and is commonly used to evaluate speech conditions within the space.

The Early to Total Ratio is specifically evaluated at 50 milliseconds, as this time interval is considered crucial for assessing the contribution of early reflections to speech intelligibility within the enclosed environment.

$$D_{50} = \frac{\int_0^{0,050} p^2(t)\,dt}{\int_0^{\infty} p^2(t)\,dt}$$

The D_{50} takes values within the range of 0 and 1 inclusive, where:

- A value closer to 0 indicates that a larger proportion of the sound energy arrives during the first 50 milliseconds. This indicates a relatively high amount of energy from early reflections within the enclosed space.
- Conversely, a value closer to 1 indicates that a larger proportion of the sound energy arrives after the first 50 milliseconds. This indicates a relatively low amount of energy from early reflections within the enclosed space.

Clarity C_{80}, C_{50}. The Clarity parameter is a metric used to quantify the ratio of early sound energy to late sound energy within an enclosed environment, i.e. an Early-to-Late Ratio. This is expressed on a logarithmic scale and is calculated over an initial time limit of 50 milliseconds for speech conditions (C_{50}) and 80 milliseconds for music conditions (C_{80}), according to the following formula:

$$C_{t_e} = 10 \lg \frac{\int_0^{t_e} p^2(t)\, dt}{\int_{t_e}^{\infty} p^2(t)\, dt}\ dB$$

Where:

C_{t_e} is the early-to-late index;

t_e is the early time limit of either 50 ms or 80 ms (C_{80} is usually "clarity");

$p(t)$ is the instantaneous sound pressure of the impulse response measured at the measurement point.

- A value greater than 0 dB indicates that the largest amount of sound energy arrives in the first t_e ms, so there is good clarity (better for opera);
- A value of less than 0 dB indicates more energy in late reflections, so it denotes poor clarity (better for symphonic music).

C_{50} is closely linked to D_{50} through the expression given by the following formula:

$$C_{50} = 10 \lg \left(\frac{D_{50}}{1 - D_{50}} \right) dB$$

According to ISO 3382-1 it is sufficient to measure only one of this two criteria.

Center Time Ts

The final descriptor in this series is the Center Time, which is designed to provide a measure of the overall balance between useful and harmful energy within an enclosed space. To calculate the Center Time, a barycentric time of the square of the impulse response is determined. This corresponds to a weighted average of the arrival times of sound energy, and is used to eliminate the clear distinction between useful and harmful energy.

$$T_S = \frac{\int_0^\infty t p^2(t)\, dt}{\int_0^\infty p^2(t)\, dt}\ dB$$

The value of the Center Time can provide insight into the character of an enclosed space's acoustic environment. A Center Time that is shifted towards shorter times indicates a dry acoustic environment, where the majority of sound energy arrives quickly. Conversely, a Center Time that is shifted towards longer times indicates a more reverberant environment, where sound energy arrives later and persists for longer periods.

Now, it is important to briefly delve into another aspect and consider a distinct standard, specifically focused on speech intelligibility: the IEC 60268-16, referred to the STI parameter.

1.2.3 IEC 60268-16: Speech Transmission Index (STI)

Given the multifunctional nature of the room under investigation, which will be extensively discussed in the latter part of this thesis (see chapter 2), it is pertinent to highlight the methodologies used for measuring the Speech Transmission Index (STI).

The Speech Intelligibility Index (STI) is a widely used objective measure in the field of acoustics and audio engineering to quantify the intelligibility or clarity of speech in various listening environments. It assesses how well speech can be understood by listeners in different acoustic conditions, such as rooms, auditoriums, or other spaces. Unlike the acoustic criteria applied for evaluating musical quality, the STI serves as a practically ubiquitous descriptor specifically for speech intelligibility due to its comprehensive and precise definition. Moreover, its universality across various communication systems, whether amplified or not, contributes to its widespread adoption.

The STI descriptor is standardized within the electroacoustic domain by EN IEC 60268-16, titled "Sound system equipment - Part 16: Objective rating of speech intelligibility by speech transmission index". This standard encompasses the comprehensive description of the index, its extraction procedures, and the methodologies employed for its measurement within enclosed

environments. It takes into account factors like background noise, reverberation, and other acoustic characteristics that can affect speech comprehension (IEC 60268-16:2020).

The STI model represents an idealised situation in which a talker with the standardised male speech spectrum is speaking with good articulation (clear speech) at a nominal word rate of 3 to 4 syllables per second and assumes listeners have normal hearing.

A speech signal level varies rapidly with time producing variations (or fluctuations) in the intensity envelope of the sound. Slower fluctuations of this intensity envelope correspond with word and sentence boundaries, while faster fluctuations coincide with individual phonemes within words. Phonemes are the fundamental elements of speech and connected discourse can be considered as a sequence of phonemes. The STI concept is based on the empirical finding that these fluctuations carry the most relevant information relating to speech intelligibility, and preservation of the intensity envelope is considered to be of the utmost importance. Time-domain distortions within a transmission channel (such as reverberation, echoes and automatic gain control) along with noise can degrade the fluctuating speech-signal and reduce the intelligibility. The extent of degradation in the fluctuations determines the potential speech intelligibility and the STI model measures the degree to which the fluctuations are preserved.

According to the IEC standard, the STI measurement determines the degree to which the intensity envelope of the speech signal is affected by a transmission channel. A modulation transfer function (MTF) is determined, which quantifies how the channel affects the intensity envelope or fluctuations of the speech signal.

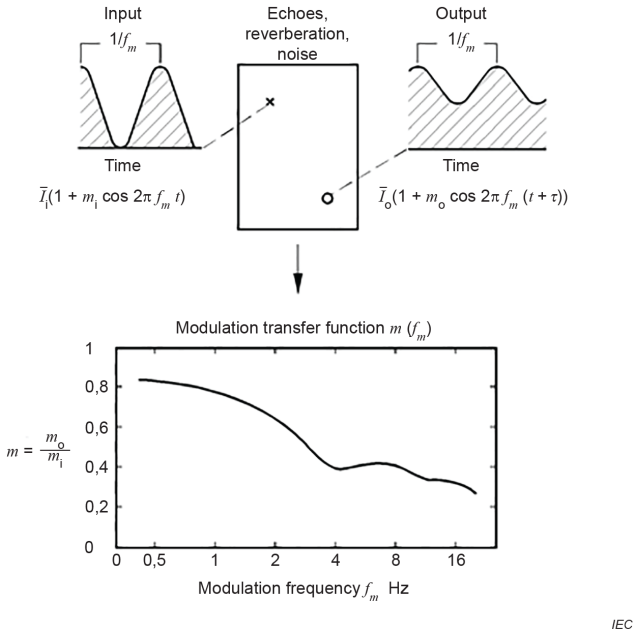

Figure 17. Graphic illustration of Modulation Transfer Function (MTF): m_i and m_o are the modulation depths of the input and the output signals, respectively. I_i and I_o are the input and output intensities, the intensities being equal to the square of the sound pressure levels (p^2).

The MTF quantifies the extent of the reductions in the modulations of the original material as a function of the modulation frequency. The modulations are defined by the intensity envelope of the signal, as it is in the intensity domain that interfering noise or reverberation normally affects only the depth of modulation of a sinusoidal modulation without changing its shape.

In addition to this fundamental premise, various refinements are introduced into the STI calculation. These refinements encompass considerations such as auditory masking and the assessment of critical bands, which also contribute to the reduction in the modulations.

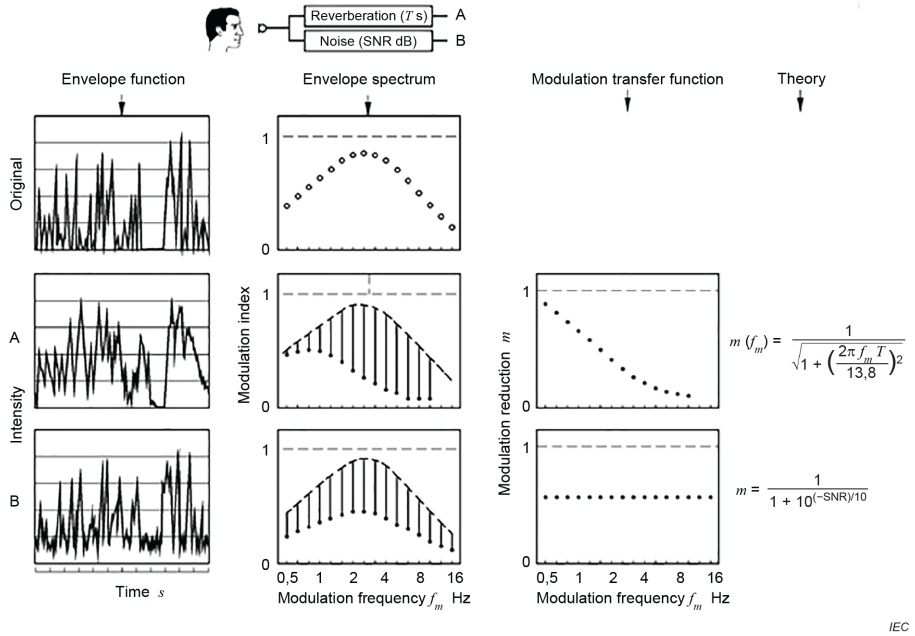

Figure 18. Effect of reverberation and background noise. The picture illustrates this for the octave-band centred on 250 Hz for two simple transmission systems, one with exponential reverberation only (case A: T = 2,5 s) and the other with only interfering noise (case B; signal-to-noise ratio SNR = 0 dB) (the vertical lines in the envelope spectrum indicate the reduction in modulation index at each modulation frequency).

The STI produces a metric on a scale of 0 to 1 – based on weighted contributions from seven octave frequency bands present in speech – where higher values indicate better speech quality. Typically, an STI value exceeding 0,45 indicates satisfactory levels of speech intelligibility.

Giudizio	STI
Bad	$0 \leq STI \leq 0{,}30$
Poor	$0{,}30 < STI \leq 0{,}45$
Fair	$0{,}45 < STI \leq 0{,}60$
Good	$0{,}60 < STI \leq 0{,}75$
Excellent	$0{,}75 < STI \leq 1$

Table 5. STI evaluation

It's important to note that the STI is just one tool in the field of room acoustics and speech intelligibility assessment. Other methods, such as the Rapid Speech Transmission Index (RASTI), are also used for similar purposes. Additionally, while the STI provides valuable quantitative information, the subjective experience of listeners is also crucial in evaluating the overall quality of speech communication in a given space.

1.3 A summary of modern architectural acoustics

The field of architectural acoustics emerged as a response to the growing need for optimizing sound environments within various architectural spaces. Its inception can be traced back to a time when architectural designs were evolving, introducing novel materials and structures, but often neglecting the acoustic consequences of these changes. This nascent field of study, although relatively young compared to some other branches of science, quickly gained significance due to its direct impact on human comfort, communication, and overall well-being within constructed spaces.

As buildings evolved in complexity and purpose, from concert halls to lecture rooms and places of worship, the importance of architectural acoustics became increasingly evident. Early researchers like Wallace Clement Sabine laid the foundation by developing fundamental acoustic principles and measurement techniques. These pioneers paved the way for a more systematic and scientific approach to shaping the acoustic characteristics of architectural spaces.

Today, architectural acoustics stands as an interdisciplinary field, drawing knowledge from physics, engineering, and architecture. Its goals include not only optimizing sound quality but also addressing environmental noise concerns. In a world where our surroundings play a critical role in our daily lives, the study of architectural acoustics remains ever-relevant, continually adapting to the changing landscape of architectural design and technological advancements.

1.3.1 Wallace C. Sabine and the Reverberation Theory

The birth of modern architectural acoustics is commonly attributed to the theory of Wallace Clement Sabine, who developed a scientific method for analysing and solving acoustic defects in the Fogg Art Museum’s Hall, where he worked as an assistant professor at Harvard University in the early 1900s. Sabine's method revolutionized the way of conceptualizing and studying room acoustics and gained significant success in the following decades. His theory on reverberation time, which is still used in most validated architectural acoustics projects and international technical standards, is the first scientific theory in the field of acoustics based on an objective formulation of sound behaviour in a closed environment (Sabine, 1922). Prior to Sabine's work, acoustic-architectural design relied primarily on empirical approaches and the imitation of existing models.

Sabine's method is characterized by:

- a quantitative evaluation, from which the definition of the famous Reverberation Time parameter is born;
- a search for the causes: excessive reverberation of the sound indicates a poor absorption capacity of the room;
- a correction proposal: increase absorption.

Sabine's innovative ideas led him to work on some of the world's most renowned concert halls, including the Boston Symphony Hall (see par. 1.4.1).

Despite Sabine's significant contributions to the field, his theory has some limitations:

- it is based on a drastic approximation of the behaviour of sound waves, such as the hypothesis of a uniformly diffuse field;
- it is characterized by a single descriptor, the reverberation time, even if it was evident the existence of other acoustic effects that this descriptor is not able to express;
- it almost totally neglects the subjective perception of the phenomenon, which today we know is very important for describing the acoustic qualities of an enclosed space.

Despite these limitations, Sabine's theory was immensely successful, and no significant progress was made in the study of room acoustics until the early 1960s.

1.3.2 Leo Beranek and the impulse response

Leo Leroy Beranek is a widely acknowledged figure in the field of modern architectural acoustics, owing to his significant contributions to its evolution. Beranek, who was a renowned acoustics expert and a former professor at MIT, dedicated his life to analysing the finest concert halls in the world, with the support of experts from the domains of music, architecture, and physical acoustics. Today, his published works are considered classic textbooks in the field of acoustics (Beranek, 1996, 2004).

Beranek's theory is an extension of Sabine's theory, which overcame several of its well-known limitations. Beranek's theory is characterized by:

- a multiparametric analysis of rooms, which involves considering interdependent physical acoustic criteria in addition to the reverberation time;
- opinions of qualified individuals such as musicians, music critics, conductors, architects, and so on;

- a correlation between physical descriptors and psychoacoustic judgments, from which evaluation scales have been derived.

1.3.2.1 Evaluation scales and ITDG

In his efforts to correlate objective descriptors with subjective opinions, Beranek attempted to develop scales for evaluating the acoustic quality of a room – these scales were ultimately deemed too arbitrary and ambiguous and were abandoned –. The scoring system was based on a range of 0 to 100.

The parameters presented in Table 6 have undergone significant revisions and refinements over the years. Nevertheless, they are generally regarded as a solid foundation for establishing a common ground between acousticians and musicians in terms of terminology and concepts.

Parameter	Physical quantity	Rating points	Max. point
Intimacy	Initial time delay gap (ms)	0-20 ms: 40 pts. >70 ms: 0 pts.	40
Liveness	Reverberation time (s) at mid frequencies (500-1000Hz)	Longer or shorter time than optimum gives lower points	15
Warmth	Average RT at 125 and 250Hz divided by RT at 500-1000Hz	RT larger or smaller than 1,2-1,25 gives lower points	15
Loudness of direct sound	Distance between listeners and the sound source	18 meters (1 point reduction for each extra 3 meters)	10
Loudness of reverberant sound	(RT / V) x 10^6	3.0 (larger or smaller gives lower points)	6
Diffusion	Irregularities on the walls and ceilings	If satisfactory	4
Balance and blend	Balance between sections of the orchestra	If satisfying	6
Ensemble	The orchestra's capability to hear each other	If convenient	4

Table 6. Evaluation scales for symphonic music (Beranek 1962)

Beranek assigns the highest score to the physical descriptor of Initial Time Delay Gap (ITDG), which he considers the most important parameter. ITDG is associated with the subjective perception of Intimacy of sound, which refers to the sensation of being in the optimal listening position in the room where the music arrives as intended for the audience. ITDG is defined as the time delay in milliseconds between the first reflections and the direct sound, as perceived from the listener's position.

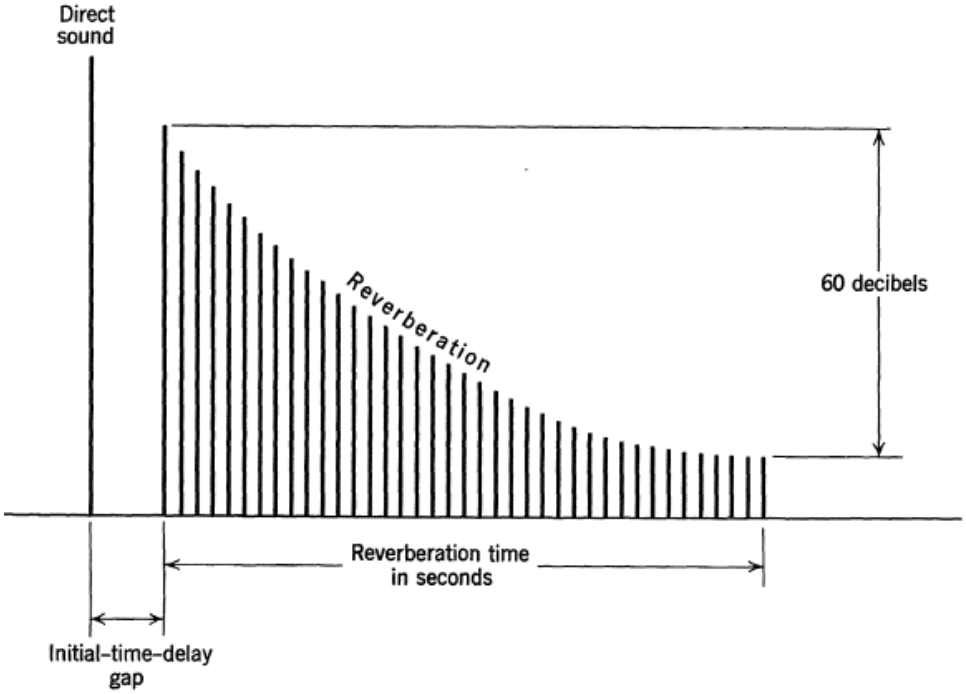

Figure 19. Graphic representation of the ITDG. (Beranek 1962)

The impulse response technique, which was introduced in the same period, enables the extraction of the ITDG and other acoustic criteria. This technique is now widely used in various fields of engineering and physics.

1.3.2.2 Impulse response

The impulse response (IR) refers to the output response in the time domain of a system, such as an acoustic system, when subjected to an impulsive stimulus that is very short in time. In an ideal scenario, the signal should be a Dirac delta function (Dirac, 1930). The signal generated by a sound source reaches the receiver, which could be a microphone or a listener, after interacting with the environment or system. The system responds according to its characteristics, delaying, repeating, and distorting the input signal. In a standard graph of the IR, as depicted in Figure 20, the measured output is the sound pressure as a function of time, making it possible to distinguish the direct sound from the sound reflections in the room that arrive later and with a smaller amplitude. This is due to the absorption of sound by the air and surrounding surfaces.

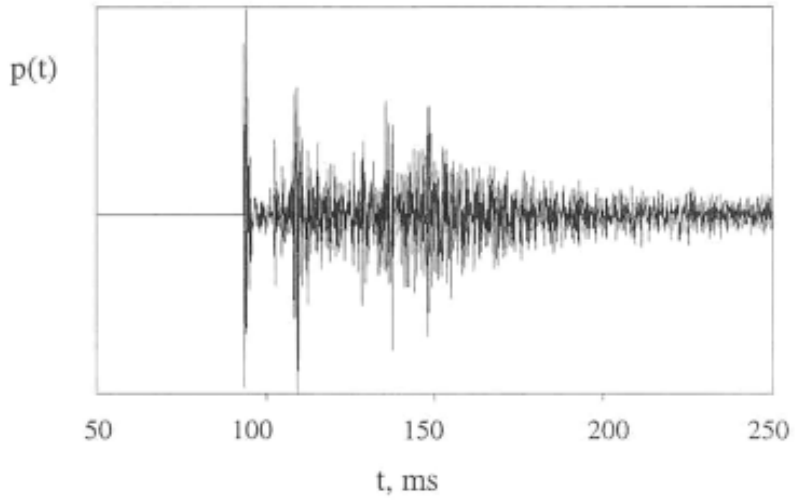

Figure 20. Example of acoustic impulse response

The acoustic impulse response offers significant advantages in that it contains a broad range of information, including the decay of sound over time, the signal-to-noise ratio, and the frequency content of direct sound and reflections. It is also valid and reproducible for any type of input signal, meaning that once the IR has been measured, the response to any other acoustic solicitation can be reconstructed using harmonic analysis. This allows for the use of multiple types of sound sources.

Today, most instruments on the market can perform impulse response measurements automatically, enabling the direct extraction of many acoustic criteria prescribed in the standards for analysing the acoustic conditions of enclosed spaces (see Appendix A).

1.3.3 Michael Barron's Revised Theory

Michael Barron's contributions to the field of architectural acoustics in the 1980s are noteworthy, particularly in his multi-parametric analysis of renowned concert halls, primarily in Britain and New Zealand, which he documented in a seminal manual on architectural acoustics (Barron, 1993). Unlike Beranek, Barron adopted a more direct approach to the evaluation of acoustic spaces by using descriptors outlined in the newly released ISO 3382 standard (see par. 1.2). He carried out:

- an objective analysis of the sound field, which involved a revision of Sabine's theory for reverberation time, which he called the Revised Theory;
- using specific and repeatable laboratory-based conditions.

Barron's theory posits that reverberated sound, i.e., reflections, is not uniformly diffused in the environment and, therefore, not constant, as Sabine's theory suggests, but decays with distance, like direct sound (Barron & Lee, 1988). This hypothesis is based on the concept that, as the distance between the sound source and the listener increases, the sound pressure level decreases, leading to a decline in the perceived loudness of the sound.

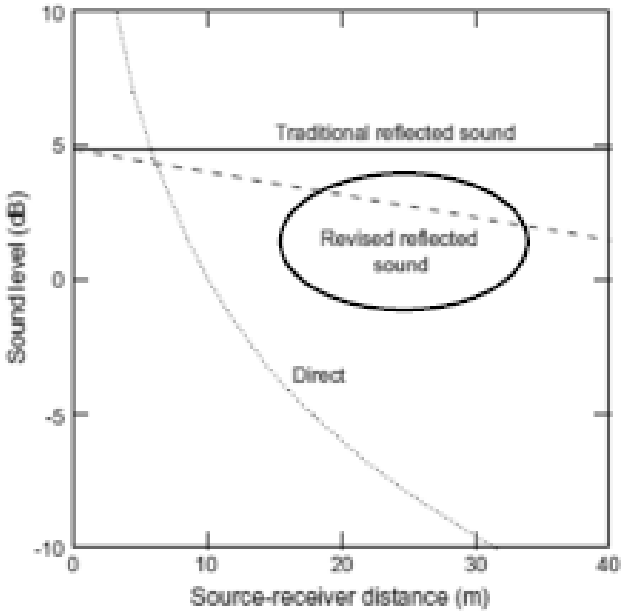

Figure 21. Reflected sound in Barron's Revised Theory

Based on the idea that reverberated sound is not uniformly diffused in the environment and decays with distance, Michael Barron redefined several acoustic descriptors, including the reverberation time, sound pressure level (SPL), sound strength (G), and clarity (C80), all as a function of the source-receiver distance (Barron, 2013). As a result of the Revised Theory, a maximum source-receiver distance value of 40 m is established to achieve good acoustic quality at each location in the hall. Notably, the best concert halls do not exceed 40 meters in length.

1.3.4 Yoichi Ando

At the University of Göttingen in Germany, Yoichi Ando, while pursuing his PhD program under the guidance of Professor Schröder at the University of Göttingen in Germany, developed the Inter Aural Cross-Correlation Coefficient (IACC) with the goal of determining the subjective quality of the spatial impression of a listener in a concert hall (Ando, 1983, 1985).

Ando's parameter aims to express the mechanism of human hearing, which processes acoustic signals in a binaural manner by means of cross-correlation between the two ears.

Subsequently, Ando formulated his own theory based on a cognitive model of the human auditory system and the autocorrelation function of brain waves, seeking to establish a relationship between these and the subjective preference of the sound field as the IACC varies (Ando & Nishio, 1996). According to Ando, there are four fundamental descriptors sufficient to describe the subjective quality of the sound field of a room (Ando, 1998):

1. The Sound Pressure Level (SPL), then replaced with the Listening Level (LL);
2. The Initial Time Delay Gap (ITDG);
3. The Reverberation Time (RT);
4. The Inter Aural Cross-Correlation Coefficient (IACC).

These are defined by Ando as *orthogonal factors* that are linearly independent of each other. The current formulation comprises two temporal and monoaural descriptors (ITDG, RT) and two spatial and binaural descriptors (LL, IACC).

Ando's work has significantly contributed to the definition of acoustic descriptors, confirming the notion that the sensation of both temporality and spatiality of the environment provides substantial information for assessing the acoustic quality of rooms.

1.4 Typologies of concert halls

Although the boundaries between the various types of music halls may not always be well defined and there are exceptions, several primary configurations of concert and multifunctional halls exist, with distinctive characteristics in their form and design that have been utilized and replicated throughout history (refer to Figure 22). Beranek's comprehensive book documents many of these halls (Beranek, 2004).

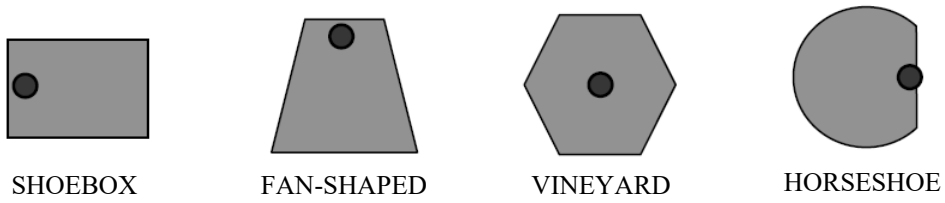

Figure 22. Main types of concert halls

1.4.1 Shoebox concert hall

The rectangular room, often embellished with balconies, was originally utilized as a ballroom for the noble class in the 1600s and proved to be very effective for the performance of symphonic music concerts due to its commendable acoustic quality. Despite having been constructed in the late 1800s when little attention was paid to the management of acoustic properties, the Boston Symphony Hall and the Wien Grosser Musikvereinssaal, widely regarded as the world's best concert halls from an acoustic standpoint, feature this type of layout.

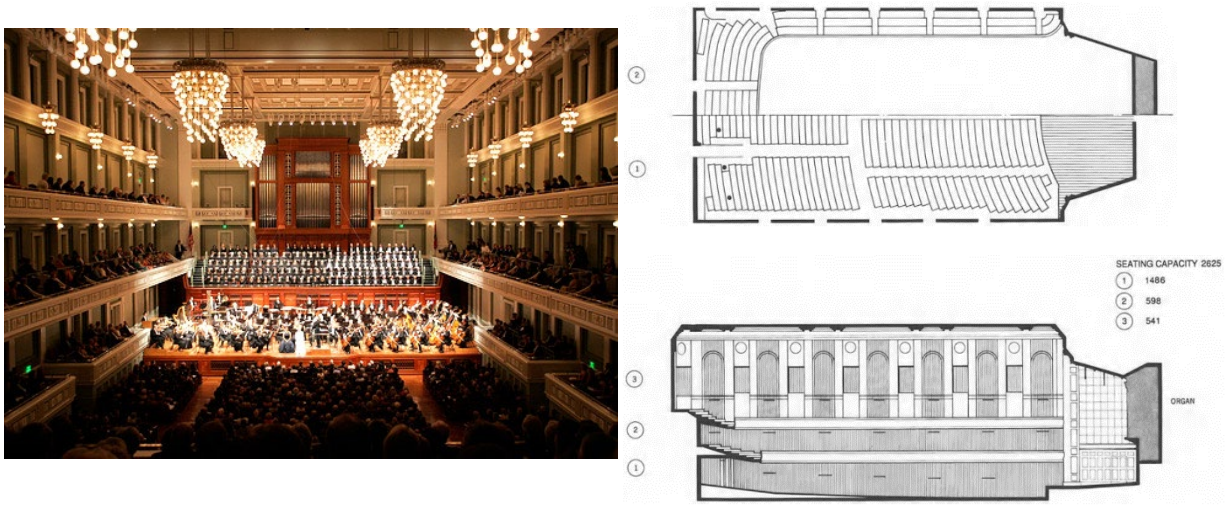

Figure 23. Boston Symphony Hall, McKim, Mead and White (W. Sabine), 1900. V = 18750 m3, seats 2625 (Beranek, 2004)

Presently, we recognize that the shoebox hall generally possesses exceptional acoustic properties, provided it complies with certain parameters regarding maximum size and audience capacity. Isbert, for instance, claims that the world's top-rated rooms acoustically have a volume

between 10,000 and 30,000 m^3, and can accommodate up to 1,000 to 3,700 people (Isbert, 1998).

In a shoebox hall, which usually boasts balconies, the stage is located in front of the audience, while the orchestra is positioned on one side of the room, and the public occupies the remaining area.

To summarize, the fundamental characteristics of a shoebox hall are as follows:

- High degree of sound diffusion thanks to the existence of irregular surfaces and decorations;
- First abundant lateral reflections due to the proximity of the public to the side walls;
- High sound strength (G);
- High acoustic intimacy (ITDG);
- Good spatial impression (IACC).

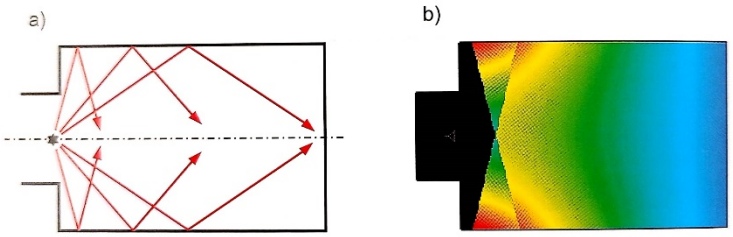

Figure 24. Shoebox Hall: a) generations of lateral reflections; b) map of sound pressure levels corresponding to the sound reflected by the side walls. (Isbert 1998)

1.4.2 Fan-shaped concert hall

The fan-shaped concert hall is a more contemporary evolution of the rectangular hall and is characterized by walls that diverge in a way that can accommodate a greater number of spectators. However, the divergence of the walls generates considerable problems for lateral reflections that tend to slide towards the back of the room, thereby affecting the overall acoustic quality. Therefore, the geometry of the side walls is normally modified with the addition of facets to correct these acoustic defects.

The Beethovenhalle in Bonn is among the first examples of a fan-shaped concert hall, built in 1959. The acoustic consultant, Kuttruff, corrected the acoustic defects of the hall by fragmenting the side walls and inserting 1760 acoustic elements on the ceiling, filled with absorbent material, which allowed for effective scattering of the sound as well as a reduction of reverberation, especially at low frequencies (125 Hz).

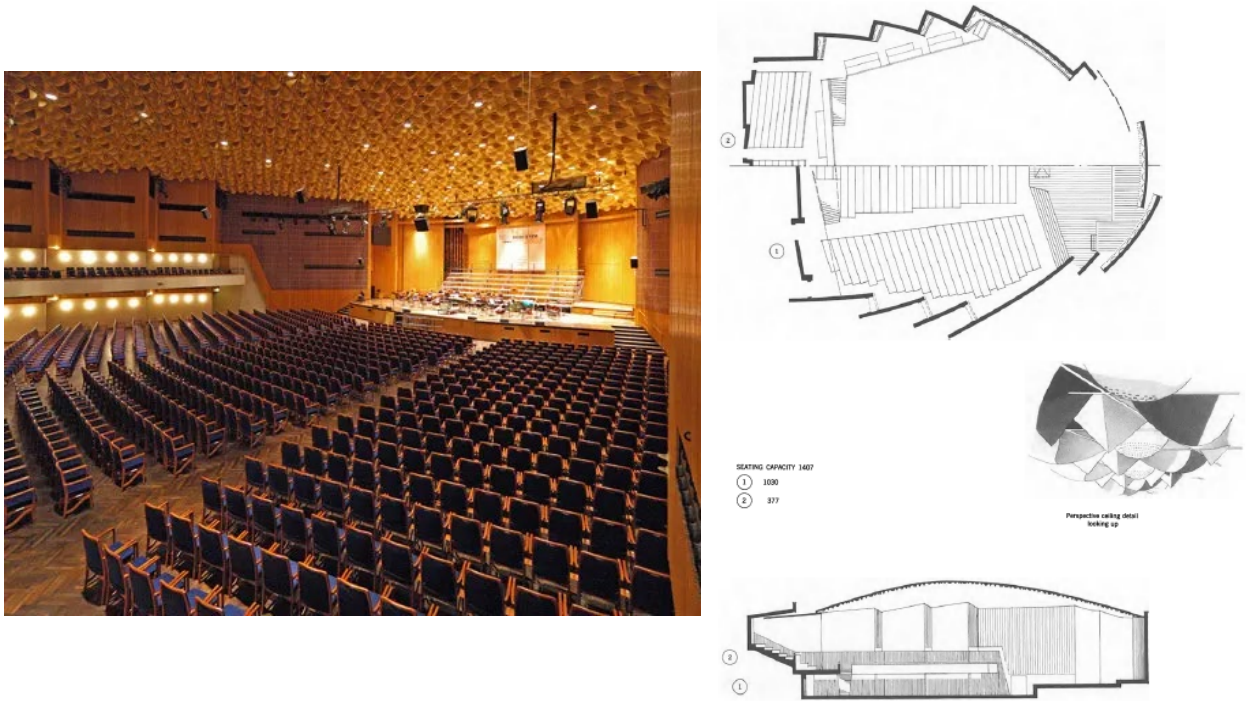

Figure 25. Bonn Beethovenhalle, Siegfried Wolske (E. Meyer, H. Kuttruff), 1959. V = 15728 m3, seats 1407 (Beranek 2004)

In summary, the features of the fan-shaped hall are as follows:

- Absence of early lateral reflections in the central part of the room;
- Limited spatial impression and acoustic intimacy, especially in the central area;
- At a greater angle of the fan, more unfavourable acoustics;
- Possibility of a large seating capacity.

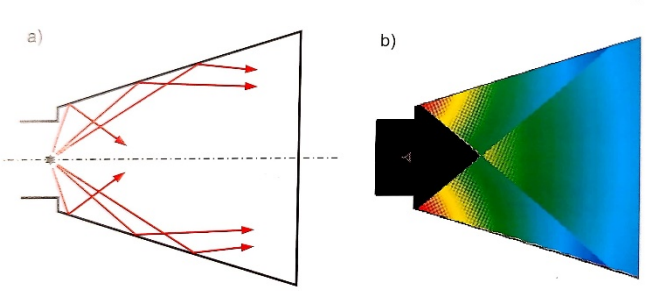

Figure 26. Fan-shaped Hall: a) generations of lateral reflections; b) map of sound pressure levels corresponding to the sound reflected by the side walls. (Isbert 1998)

1.4.3 Vineyard concert hall

This type of hall is intimately linked to the Berliner Philharmonie, the first example of Vineyard Hall. It was designed by the architect Hans Scharoun and built in 1963, with the help of acoustic expert Lothar Cremer. According to Beranek, “Philharmonie Hall has become one of the models of successful acoustical designs, pioneering the concept of the "vineyard" style hall” (Beranek, 2004).

The central idea behind this design is to place "music at the center", creating an intimate and direct communication between the orchestra and the audience. The final result is surprising.

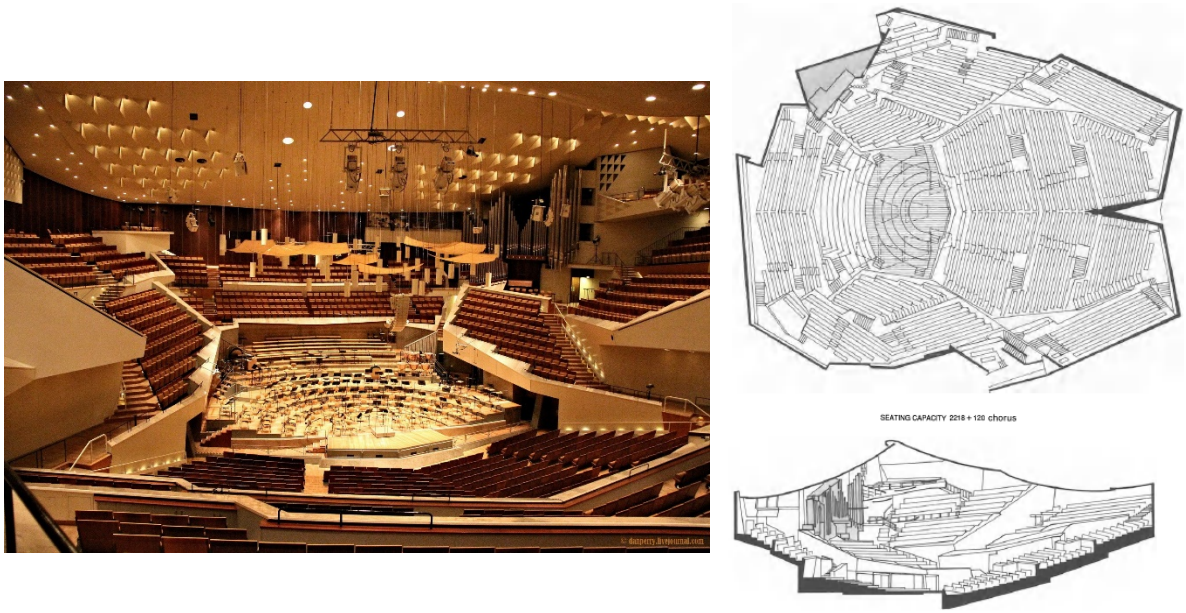

Figure 27. Berliner Philharmonie, Hans Scharoun (L. Cremer), 1963. V = 21000 m3, seats 2215 (Beranek 2004)

While such a design offers many advantages, including an excellent and suggestive visual impression, it also poses a significant challenge in terms of acoustic design, which must be carefully studied to mitigate potential defects.

Some key features of the vineyard hall include:

- Good spatial impression of sound and good acoustic intimacy;
- Complex design of reflective, diffuser and absorbent surfaces for an effective control of side reflections and reverberation across the entire frequency spectrum;
- Personalized listening in each seat, also due to the directivity of the instruments;
- Ability to accommodate a large seating capacity.

1.4.4 Horseshoe concert hall

This term typically refers to European and particularly Italian opera houses, which have maintained a consistent horseshoe-shaped configuration since the 1700s, with some minor variations.

The Teatro alla Scala in Milan, completed in 1778, is considered among the world's best opera houses from an acoustic standpoint, with its horseshoe shape reaching its apogee. However, acoustic measurements show that excellent acoustic quality exists only in the cavities of the boxes, not on the ground floor (Beranek, 2004).

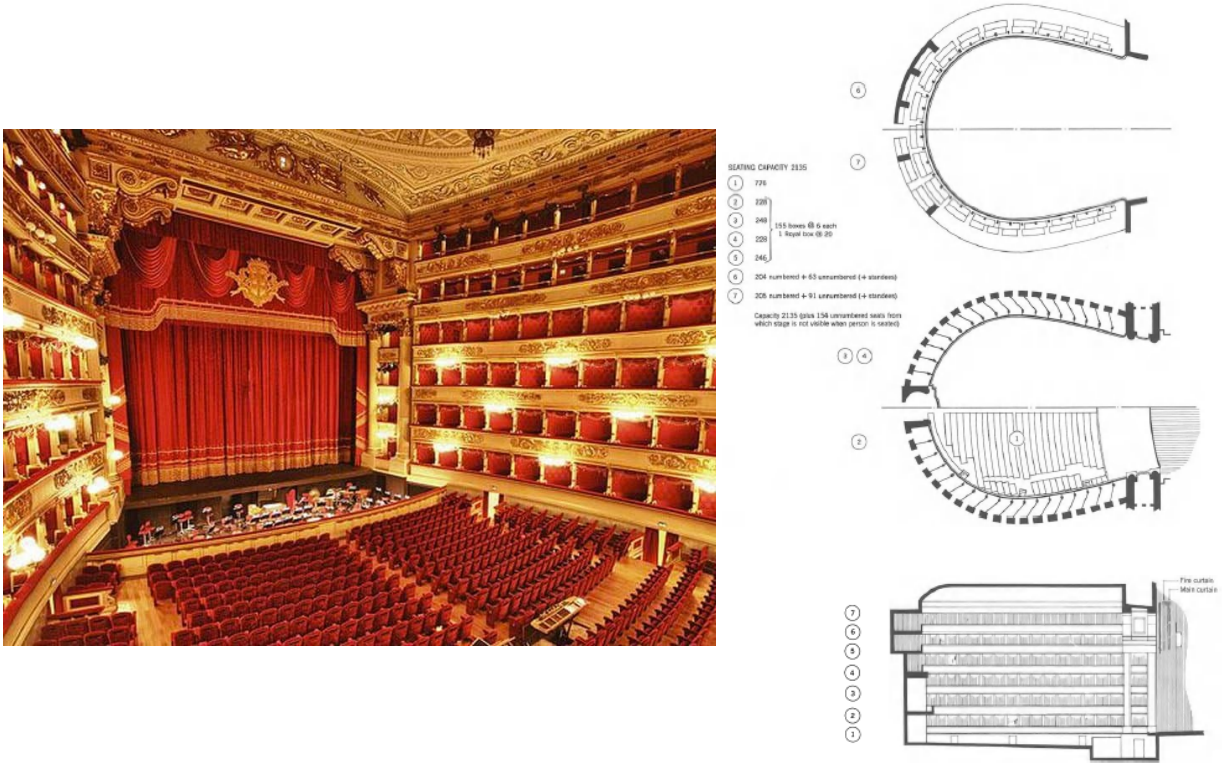

Figure 28. Teatro alla Scala di Milano, Giuseppe Piermarini, 1778. V = 11252 m3, seats 2489 (Beranek 2004)

The opera house traditionally reflected the division between the social classes of the time. In fact, it always consists of:

- a central audience where the middle class sat;
- rings of boxes superimposed on each other where the nobility sat;
- an upper crowning gallery with seats at low prices where the commoners sat.

The acoustical requirements of opera differ from those for orchestral concerts. The vocal part plays a fundamental role, and the listeners must be able to understand the words clearly. In order to preserve the intelligibility of speech, especially at the musical speeds of Mozart and Rossini, the reverberation of the sounds must not mask the successive syllables. These needs

are mostly satisfied in the most famous opera houses, primarily thanks to the absorbing power of the boxes.

Some general characteristics of the horseshoe concert hall include its profile, which is typically used for opera, a lower reverberation time compared to symphonic music concert halls, the possible existence of sound focalization due to the concavity of the posterior wall, and low energy associated with the first lateral reflections due to the divergence of the walls, often compensated by a reflecting strip on the walls at audience height.

Some general characteristics of the horseshoe concert hall include:

- Profile typically used for the opera;
- Lower reverberation time compared to symphonic music concert halls;
- Possible existence of sound focalization due to the concavity of the posterior wall;
- Low energy associated with the first lateral reflections due to the divergence of the walls, often compensated by a reflecting strip on the walls at audience height.

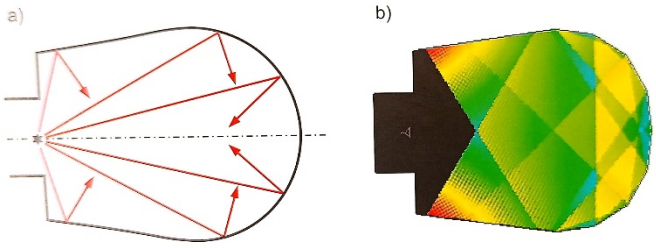

Figure 29. Horseshoe hall: a) generations of lateral reflections; b) map of sound pressure levels corresponding to the sound reflected by the side walls. (Isbert 1998)

2 The case study: Centre Civic Pere Pruna

The selection of the cultural association centre Pere Pruna, based in Barcelona, as the subject of study for this work was not an immediate decision. There were numerous concert halls in the city available for examination, including two concert halls at the Palau de la Musica Catalana and three halls at the Conservatorio Municipal de Musica de Barcelona (CMMB). Acoustic measurements were conducted in all of these venues to assess their current conditions.

The final choice of the Pere Pruna Civic Centre was primarily based on two factors. Firstly, its historical and architectural significance added value to the space under investigation. In fact, The Pere Pruna Civic Centre stands as a unique and captivating architectural space that has undergone various structural and functional changes throughout its history, assimilating diverse artistic influences from the 20th century. Secondly, and more significantly, the room exhibited notable acoustic challenges and lacked proper treatment for its current usage as a chamber music hall. The complex acoustic conditions make it particularly intriguing for the purposes of this study. Additionally, the management of the cultural centre has expressed a keen interest in an acoustic improvement intervention, which provides a tangible practical application for this project.

Considering these aspects, the other rooms were excluded from further consideration, and the focus was shifted to an in-depth exploration of the Pere Pruna Civic Centre. In the subsequent paragraphs, a brief contextualization of the analysed space will be provided.

2.1 Historical and architectural context

The Centre Civic Pere Pruna is a cultural centre situated in the Sant Gervasi neighbourhood, in the northwest area of Barcelona, within a primarily residential district. This facility offers a diverse cultural program that is accessible to all, serving as a central gathering place for local residents. Through its cultural offerings, the centre has fostered a strong sense of community and active participation among the residents. It has become a focal point where people come together to engage in meaningful and enriching activities, contributing to the development of a vibrant and closely-knit community.

Figure 30. Location of the Centre Civic Pere Pruna in the city of Barcelona

In 1904, the Juncadella family donated land to the congregation of the Mares Reparadores – Repairing Mothers – to construct a monastery in the Sant Gervasi area of Barcelona. Construction of the monastery began the same year and occupied half a block of the current buildings on Carrer Ganduxer. The chapel, added to the convent later in 1928, was designed by Enric Sagnier, author of the Tibidabo temple and Casa Sagnier. He was a prominent architect known for his eclectic style, drawing inspiration from various architectural movements.

During the Spanish Civil War, the monastery was collectivized following a fire, resulting in the loss of much of its furniture. Over the years, the chapel underwent changes and faced challenges. In 1970, the nuns decided to sell both the monastery and the chapel for speculative development. However, thanks to the efforts of Fernando Rubió i Tudurí and the local neighbours, the Rubió i Tudurí Foundation was established to save the chapel, due to its symbolic value and significance as a community gathering place.

In 1984, the chapel came under the ownership of the City Council and was classified as a heritage asset. An important restoration project, including the preservation of Pruna's frescoes, was carried out in 1998.

Figure 31. Restoration project of Pere Pruna Civic Center, 1998

The Pere Pruna Civic Centre has an architectural background rooted in its original function as a religious building. The chapel's design likely reflects the prevailing architectural influences of the early 20th century, which include elements of historicism and Catalan modernism.

Regarding the decoration of the chapel, the artist Pere Pruna was commissioned to undertake the work in the 1950s. Pruna, trained in Paris and influenced by the avant-garde, combined a conservative mentality with elements of modern artistic expression. The frescoes painted by Pruna, advised by Eugeni d'Ors, incorporated images related to Eucharist, with angelic figures with a unique feature of depicting their gender. The cold blue colour of the painting is contrasted with the warmer tones of seven precious stained-glass windows – among the last made in Barcelona after the modernist period – which Pruna created in honor of Casa Geroni Graells.

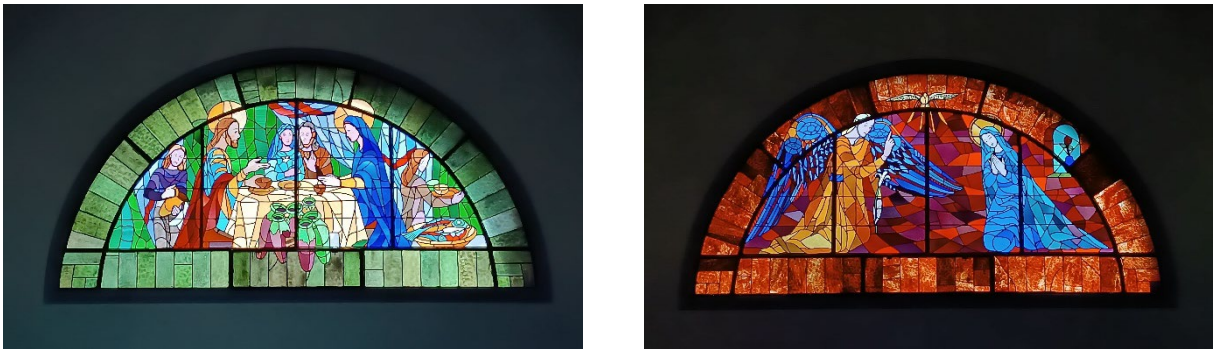

Figure 32. Stained-glass windows located on the sides of the hall

In 1998, the City Council initiated a restoration project, with a particular focus on preserving the frescoes painted by Pere Pruna. Although the high altar was not preserved, the painting of the maredeu was saved using the strappo technique and is displayed in another location within the civic centre.

Figure 33. Restoration of the frescoes painted by Pere Pruna

2.1.1 The Pere Pruna Civic Centre today

Today, the Pere Pruna Civic Centre is a former church serving as a cultural facility, offering chamber music performances and used as a community space for residents to enjoy. It stands as a testament to the collaborative efforts of the Rubió i Tudurí Foundation, local residents, and the City Council in preserving a significant historical and architectural landmark in the neighbourhood.

Throughout the rehabilitation process, utmost care was taken to preserve the original layout of the church, including its external facade and the frescoed chapels. However, significant modernization efforts were concentrated on the lower floor. Light brick walls were installed to accommodate the display of paintings, and an intermediate floor was constructed within the small side aisles encircling the central nave, allowing visitors to traverse the entire space. Additionally, a modest stage was incorporated to facilitate concerts and conferences.

Figure 34.
Above: Restored ground floor, with paintings placed on the left wall, a little stage located at one side of the hall.
Below: Intermediate floor, with a corridor that surrounds the central nave.

2.2 Geometric and acoustic features of the hall

The Pere Pruna Hall is designed in the typical rectangular shoebox shape. It features a spacious central nave where the seating for the audience is arranged, while the orchestra stage is situated to one side of the hall. The architectural elements, such as the pillars and open spaces, define two smaller side aisles located on an intermediate level. These side aisles can be accessed via the staircases adjacent to the stage. The intermediate level comprises a corridor encircling the central audience area, providing a pathway around it. This arrangement creates balconies with interesting listening and visual points towards the lower level of hall. However, these balconies are currently not utilized for audience purposes. The Table 7 provides some useful geometric data for acoustical purposes.

Feature	ID	Value
Length (m)	L	27.50
Width (m)	W	14
Height (m)	H	11
Total volume (m^3)	V	2600
Total surface (m^2)	S	2100
Floor surface (m^2)	S_{floor}	385
Stage area (m^2)	S_S	20
Audience area (m^2)	S_A	74
Number of seats	N	83

Table 7. Geometrical features of the hall

It is noteworthy to observe that the audience area S_A = 74 m^2 yields a ratio V/S_A = 35 (m), a value that surpasses those obtained in the study conducted by Hidaka and Nishihara for chamber music halls (Hidaka & Nishihara, 2004). This outcome reflects the characteristic geometric condition of a church: the analysed room exhibits a limited space designated for the audience, enclosed within a considerably spacious volume and characterized by a substantial reverberation. Nevertheless, despite these factors, the room is utilized for chamber music and conferences. Thus, it may be justifiable to contemplate expanding the surface area available to the audience, considering the space availability (see Figure 35). Further details of this intervention will be explained in chapter 5.

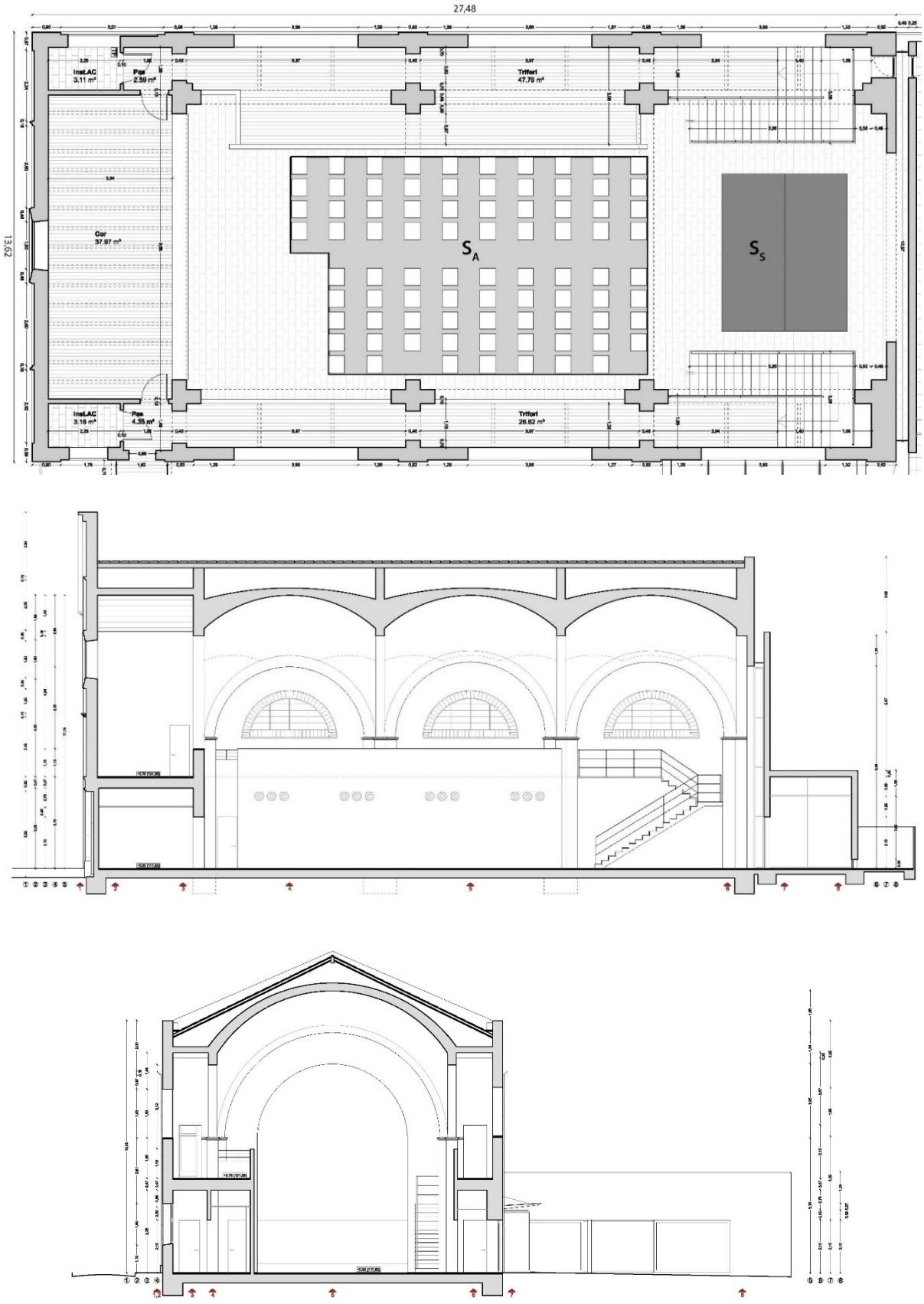

Figure 35. Above: plan of the hall. Stage area S_S and actual audience area S_A
Below: longitudinal and transversal section of the hall. Vaults and intermediate corridor level

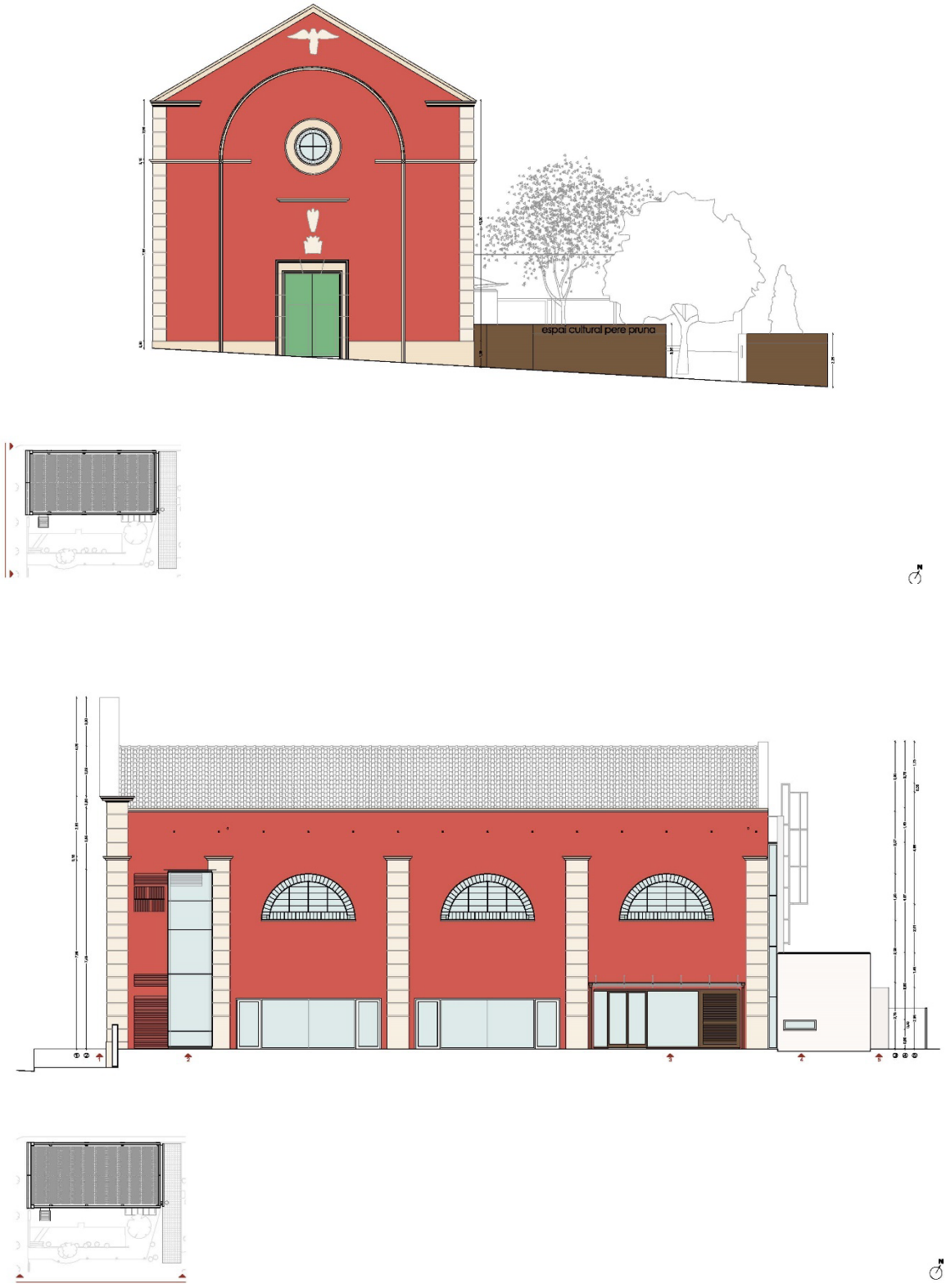

Figure 36. Above: transversal view of the building.
Below: longitudinal view of the building

Although the Pere Pruna Hall has undergone a transformation in its function, its structural arrangement still maintains the characteristic features of a religious building. The hall boasts high and reflective walls, a vaulted and painted ceiling, and expansive stained-glass windows that invite ample natural light. All these elements, combined with the modernization project, create a captivating fusion of the spiritual and contemporary worlds.

From an acoustic standpoint, the hall has remained largely untreated and unchanged, apart from the addition of a partial curtain and small speakers positioned alongside the audience. Consequently, it retains the acoustic characteristics typically associated with a church environment – long reverberation and diminished sound clarity – making it less than ideal for chamber orchestra concerts or conferences.

The aim of this thesis, therefore, is to enhance the acoustical properties of the space to optimize its suitability for its intended functions. The hall is envisioned as a multifunctional venue capable of accommodating various activities, including exhibitions, conferences, and concerts encompassing diverse musical genres, primarily choral performances and chamber orchestras. Consequently, the analysis will encompass the monaural descriptors that define sound quality from the listener's perspective, involving both musical and speech intelligibility aspects.

Given these aspects, an ideal treatment will require the presence of variable acoustics, characterized by specific configurations tailored to specific requirements.

3 Acoustic measurements

3.1 General overview

The in-situ measurements were conducted on February 10, 2023, in collaboration with the acoustics group of the Campus La Salle, from the Ramon Llull University. A preliminary inspection was carried out the day before, during which guidelines were established for the configuration of the room. These guidelines included considerations regarding the objects and materials to be taken into account or excluded, as well as the precise placement of the microphones and sound sources.

The objective of the acoustic measurements was to obtain the impulse responses (IRs) and extract monaural time parameters that enable the evaluation of the room's acoustic properties from the listener's perspective.

Additionally, the research directed by the acoustics group aimed to assess the effectiveness of their newly developed experimental loudspeaker, the OPL (Omnidirectional Parametric Loudspeaker), and its performance in measuring acoustic criteria in enclosed environments. The OPL is a new device that aims to overcome the limitations of the conventional dodecahedral loudspeaker, specifically regarding the pronounced directionality of high frequencies sound waves. For further details on this matter, please refer to Appendix A, which provides an explanation of the distinctions between this device and the traditional dodecahedron.

The entire procedure was conducted in strict adherence to the guidelines outlined in the ISO 3382 standard, which provides comprehensive instructions and specifications for the methods to be employed (ISO 3382-1:2009).

The measurements were carried out with the hall arranged in its customary configuration for concerts or conferences. The chairs were positioned in their usual locations within the audience area. Regarding the curtains situated on one side of the room, it was determined that leaving it open and disregarding its presence would be appropriate, as only one of the curtains was operational during the measurement day, while the other had been removed due to a malfunction.

In order to ensure the integrity of the acoustic environment and prevent sound leakage into adjacent spaces, all doors were securely closed.

Figure 37. Above: Audience area, seats located within the central part of the hall
Below: curtains left opened due to a malfunction.

3.2 Measurement execution

3.2.1 Equipment

The equipment used for the measurement campaign was supplied by the HER research group of the La Salle acoustics department; it includes:

- A Windows operating system computer (i7 processor, 32 GB RAM) that launched the Exponential Sine Sweep and performed the post processing work
- Two different sound sources:
    - Omnidirectional dodecahedral sound source CESVA BP012
    - Omnidirectional Parametric Loudspeaker (OPL) built by the HER research group of La Salle (see Appendix A for further information)
- Monoaural half inch free-field calibrated microphone (Random Incidence G.R.A.S. 40 AQ), with diffuse field compensation at least 1 dB at 4000 Hz
- Software:
    - MATLAB custom code from HER group of La Salle, developed to carry out all measurements.
    - ITA-Toolbox
- Hardware:
    - ECLER XPA3000 amplifier for signal generation
    - B&K Nexus conditioning amplifier for signal capture
    - DT9847 Sound Card
- Cables
- Thermohydrometer
- Oscilloscope
- Laser distance meter

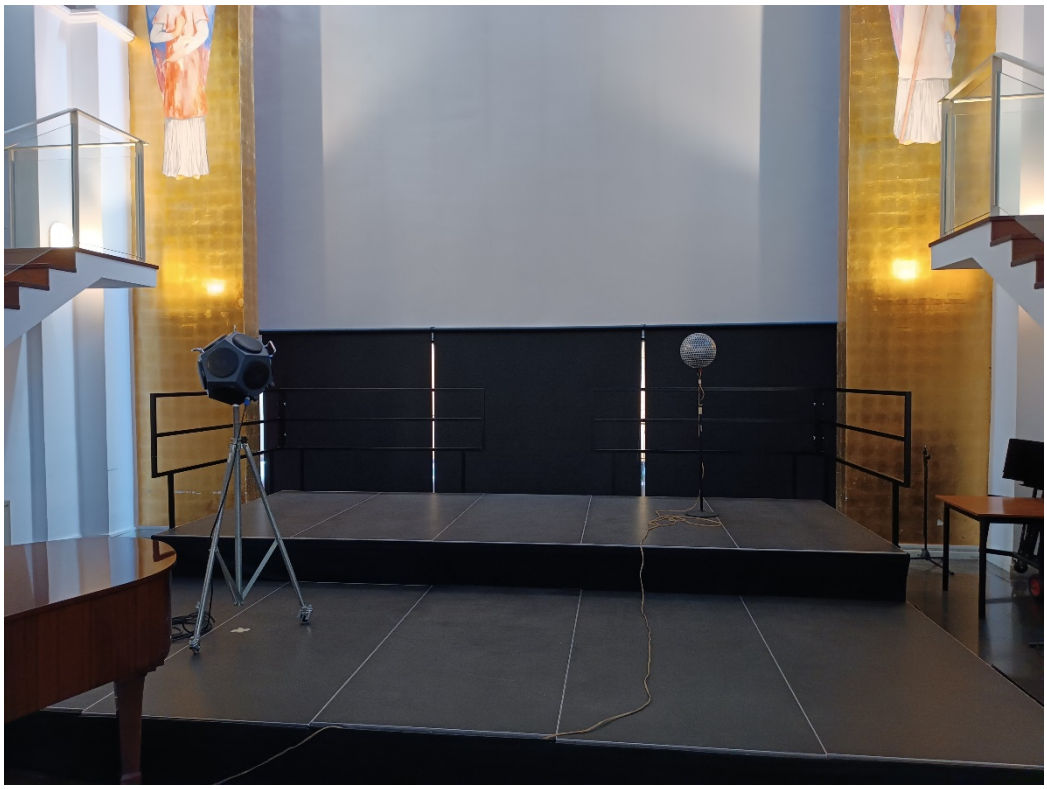

Figure 38. Sound sources located on the stage. On the left the dodecahedron, one the right the OPL.

3.2.2 Signal generation and signal capture: ESS and IR

The Exponential Sine Sweep (ESS), also known as the logarithmic sine sweep or swept sine, is a widely used technique in acoustic measurements to characterize the frequency response of a system.

The basic principle behind the ESS is to generate a continuous sinusoidal signal that sweeps through a range of frequencies logarithmically over a specific time duration. The logarithmic sweep is achieved by exponentially increasing the frequency of the sinusoid over time.

In the context of room acoustic measurements, the Exponential Sine Sweep can be used as a type of emission signal for the purpose of measuring room impulse response.

Compared to other emission techniques commonly used in room acoustic measurements, such as the starter pistol or maximum length sequence (MLS), the ESS offers several advantages:

- Linear Frequency Response: The ESS utilizes a logarithmic sweep, which covers a wide frequency range evenly. This results in a linear frequency response in the measured signal, allowing for accurate analysis of the room's behaviour across different frequencies.

- Spectral Resolution: The logarithmic frequency sweep of ESS provides excellent spectral resolution, meaning that the measurements can capture fine details in the room's response at different frequencies. This is particularly important for identifying resonances, room modes, and other frequency-dependent effects.
- Energy Efficiency: The ESS can achieve higher energy efficiency compared to other techniques like MLS. This is because the ESS focuses energy on the frequencies of interest, reducing energy waste at frequencies outside the desired range. It allows for more efficient use of limited sound source power and reduces the risk of sound source overload or distortion.
- Time-Domain Accuracy: The ESS generates a continuous sweep in the time domain, ensuring a precise and consistent excitation signal throughout the entire frequency range. This helps in obtaining accurate time-domain responses and impulse responses, which are critical for analysing early reflections and spatial characteristics of the room.
- Audibility: The ESS is typically designed to be audibly pleasant or imperceptible, making it more suitable for subjective listening tests or measurements involving human listeners. In contrast, other techniques like starter pistol or MLS may produce loud and abrupt signals that can be disruptive or uncomfortable.

By utilizing the Exponential Sine Sweep technique, it becomes possible to obtain a comprehensive characterization of a system's frequency response in a single measurement, making it a powerful tool in acoustic analysis and engineering.

A custom code written by the La Salle acoustic research group was used to generate the ESS.

The ESS has been configured with the following settings:

- Emitted frequency range: 100 - 4000 Hz
- Sampling Rate:
    - Dodecahedron: 100 kHz
    - OPL: 150 kHz
- Measurement averaging time:
    - Dodecahedron: 30 seconds, two repetitions
    - OPL: 50 seconds

The emitted signal from the loudspeaker was subsequently captured by the microphones, undergoing modifications due to the room's reflections. The analogue signal has been converted

into a digital format using a sound card and stored within the computer for further analysis and processing.

The IRs were saved in *.mat format using other custom code written by the acoustics group, with the following nomenclature:

- Format of Filename: S*X*_R*Y*_M*Z*.mat
    - S*X*: *X* first or second source position
    - R*Y*: *Y* number of the Receiver position
    - M*Z*: *Z* first or second measurement

The notation "*S2_R1_M2.mat*" means therefore:

- *S2:* second position source
- *R1:* receiver in the first position
- *M2*: second measurement.

3.2.3 Sound sources and receivers mapping

Fifteen selected points has been established to accommodate the placement of microphones, alternating seats and creating a receiver's grid. Thirteen of these points are situated within the audience area, as depicted in Figure 39. It should be noted that the last two positions at the rear of the room are presently situated beyond the current designated audience area due to the absence of chairs. However, there are intentions to incorporate additional seating and expand the audience area accordingly (see chapter 5).

Two additional receiver positions have been included within the church choirs. Although these choir positions are not designated listening areas, their inclusion allows for an assessment of sound behaviour in those specific locations. However, they will not be considered for the extraction of the results.

All microphones have been positioned at a height of 1.2 meters above the floor and at least 1 meter away from any reflective surfaces, in adherence to legislative requirements. For the sound sources, two positions on the stage have been identified. These positions correspond to different sections of the stage, distinguished by varying heights. The first position, located towards the front, aligns with the strings or piano area, while the second position, located further towards the rear, coincides with the percussion and wind section. Adhering to legislative guidelines, the sound source has been placed 1.5 meters above the ground floor.

Considering the utilization of 15 receiver positions for each of the two source positions, a total of 30 measurements would be expected. However, as the experimentation incorporates two distinct sound sources, the entire process has been duplicated, yielding a cumulative total of 60 measurements. Furthermore, two repetitions have been carried out for each position.

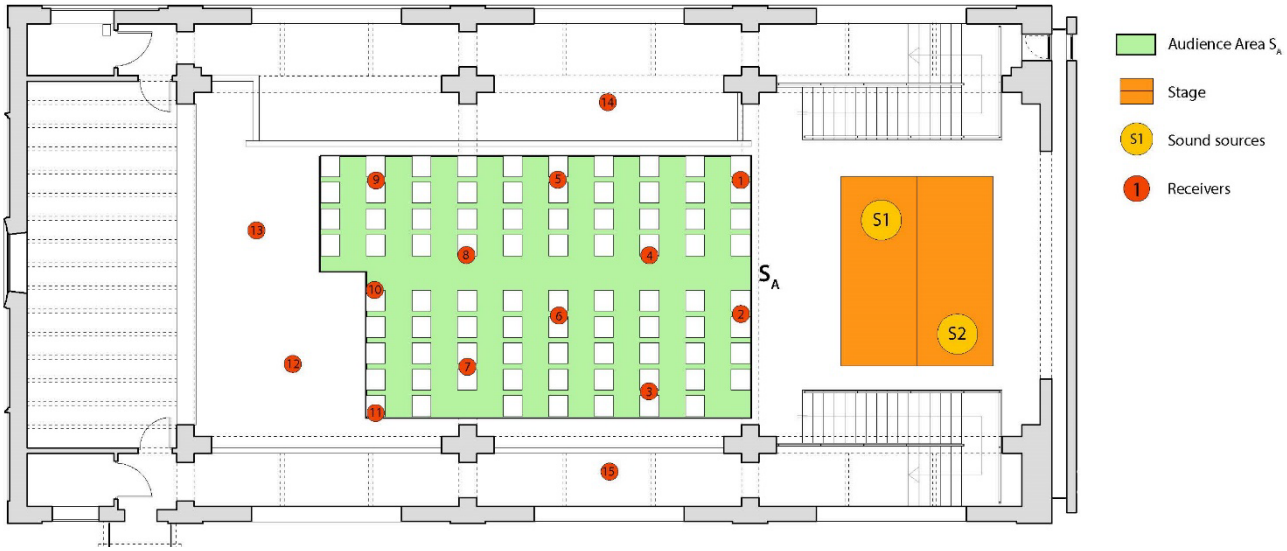

Figure 39. Sound sources and receivers mapping

3.2.4 SPL measurement within the anechoic chamber

After completing the room measurements, an additional phase of measurements was conducted in an anechoic chamber to acquire the Sound Strength parameter (G). As previously explained (refer to section 1.2.2.3), the G parameter denotes the difference between the sound pressure level (SPL) recorded at a specific point within the room (L_{pE}) and the same sound pressure level measured in open field conditions at a distance of 10 meters from the sound source ($L_{pE,10}$):

$$G = L_{pE} - L_{pE,10}\ dB$$

For each receiver location in the Pere Pruna Hall, the L_{pE} was derived from the measured impulse responses used for all the other criteria. As for the second value mentioned, ISO 3382-1 standard offers comprehensive guidelines for the measurement procedures. These measurements can be performed within an anechoic chamber, a space designed to resemble open field conditions by employing sound-absorbing materials on walls, ceiling, and floor to minimize sound reflections. This controlled environment ensures minimal sound reflections, facilitating precise measurements.

According to ISO 3382-1, Annex A, if a sufficiently large anechoic room is available, $L_{pE,10}$ can be directly measured using a source-to-receiver distance of 10 meters. In cases where this

condition cannot be met, as in our scenario where the anechoic chamber lacks such a distance, the sound pressure exposure level at a point located at a distance d (⩾3 m) from the source ($L_{pE,d}$) may be measured. $L_{pE,10}$ can then be derived using the following equation:

$$L_{pE,10} = L_{pE,d} + 20\log\left(\frac{d}{10}\right)\ dB$$

Following the guidelines of the standard, measurements were conducted at every 15° intervals around the sound source, and subsequently, the energy-mean value of the sound pressure exposure levels was computed to average the sound source's directivity. The sound source was positioned on one side of the room, and the sound receiver – microphone – was placed on the opposite side at a distance of d = 4.8 m. The source was mounted on a rotating mechanical support capable of a 360° rotation and automatic movement of 15° after each measurement. A total of 24 measurements were performed.

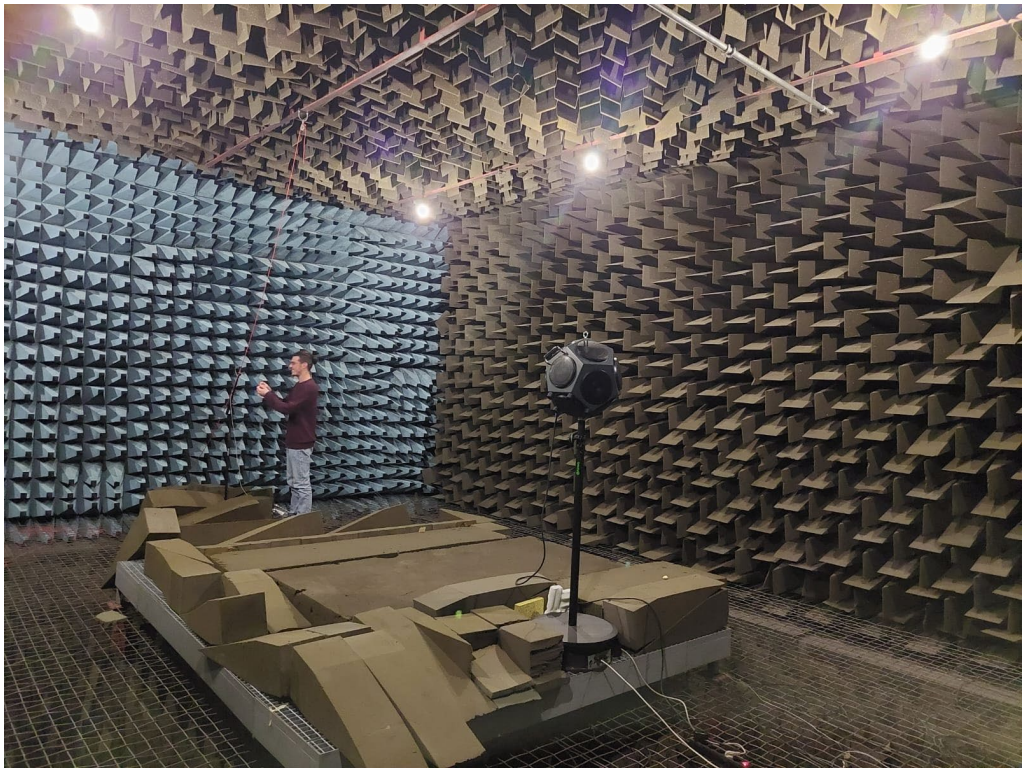

Figure 40. SPL measurement setup within the anechoic chamber

The extracted impulse responses were processed using MATLAB, and the sound pressure levels (SPLs) were initially calculated for each of the 24 source angles, in one-third octave bands. Subsequently, to obtain levels in the central octave bands, adjacent sound levels were summed – for instance, levels at 100, 125, and 160 Hz were summed to obtain the SPL for the central

octave band at 125 Hz. Finally, the SPL from each angle were averaged to obtain a single value of the mean SPL for each octave band.

The obtained SPL corresponds to the sound pressure exposure level $L_{pE,d}$ at a distance of 4.8 meters from the source. As a final step, $L_{pE,10}$ was derived using the formula mentioned above.

Following the calculations, the sound level $L_{pE,10}$ at a distance of 10 meters from the source was found to be approximately 6 dB lower than the sound level measured in the anechoic chamber at 4.8 meters. This value will then be subtracted from the sound pressure exposure level L_{pE} measured in the Pere Pruna Hall, and subsequently, the Sound Strength (G) will be extracted. The results will be summarized in the next section, along with the other monaural parameters under examination.

3.3 Post-processing and results

The collected data was processed in the research laboratory of the university. The recorded impulse responses (IRs) were normalized to the highest sound pressure value among all measurements. To facilitate the extraction of acoustic criteria, the data files in *.mat format were converted to *.wav format and transferred to ITA-Toolbox. This software is a MATLAB toolbox, developed by the Institute of Technical Acoustics (ITA) at the RWTH Aachen University, created to solve common post-processing tasks in the field of acoustic research (Dietrich et al., 2012).

ITA-Toolbox effectively interfaces with MATLAB, enabling the automation of criteria extraction using simple code scripts.

The results of the monaural acoustic criteria, including EDT, T_{30}, T_S, C_{80}, D_{50}, and G, are presented in Table 8.

Additionally, the Speech Transmission Index (STI) values related to speech intelligibility are provided. To ensure reliability, only the results for the male voice are reported, as it typically exhibits lower values.

Source	$T_{30,M}$ (s)	EDT_M (s)	$C_{80,3}$ (dB)	$D_{50,3}$ (%)	$T_{S,3}$ (ms)	G_M (dB)	STI_{male}
S1	3.63	3.65	-4.3	0.16	253	3.5	0.40
S2	3.63	3.67	-4.2	0.18	253	3.6	0.40

Table 8. Measured room criteria. Results are provided for S1 and S2 source positions, averaged all over the receiver points. The subscript "M" and "3" mean that the octave band average is, respectively, for 500 and 1000 Hz, and 500, 1000 and 2000 Hz.

A series of graphs are presented to provide a comprehensive and detailed depiction of the trends observed in each individual criteria, measured within their respective octave bands. These graphical representations offer a deeper understanding of the data and facilitate a more thorough analysis of the findings.

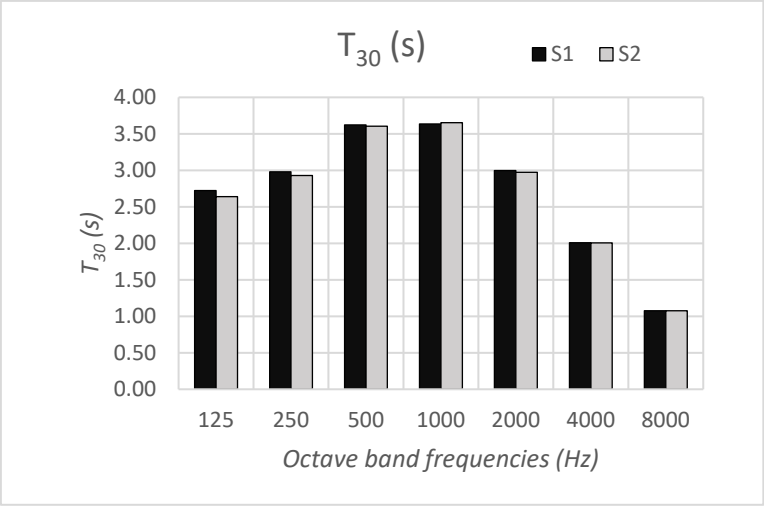

Figure 41. Octave band graph of measured T_{30}, considering both source positions.

The obtained results indicate inappropriate reverberation time values that exceed the desired levels for the intended functions of the room. The graph shown in the Figure 41 illustrates a notable trend in the reverberation time (T_{30}) of the room. It reveals an increase in reverberation towards the medium frequencies, followed by a subsequent decrease towards the high frequencies. This observation suggests a higher level of absorption at medium-low frequencies within the room. This phenomenon can likely be attributed to the absorbing properties of certain elements in the room, such as the wooden panels on the stage or the entrance glass panels. These elements act as elastic membranes, partially attenuating the low frequencies.

Moreover, the subjective perception of sound is compromised by excessively high EDT and T_S values, resulting in diminished clarity and low definition.

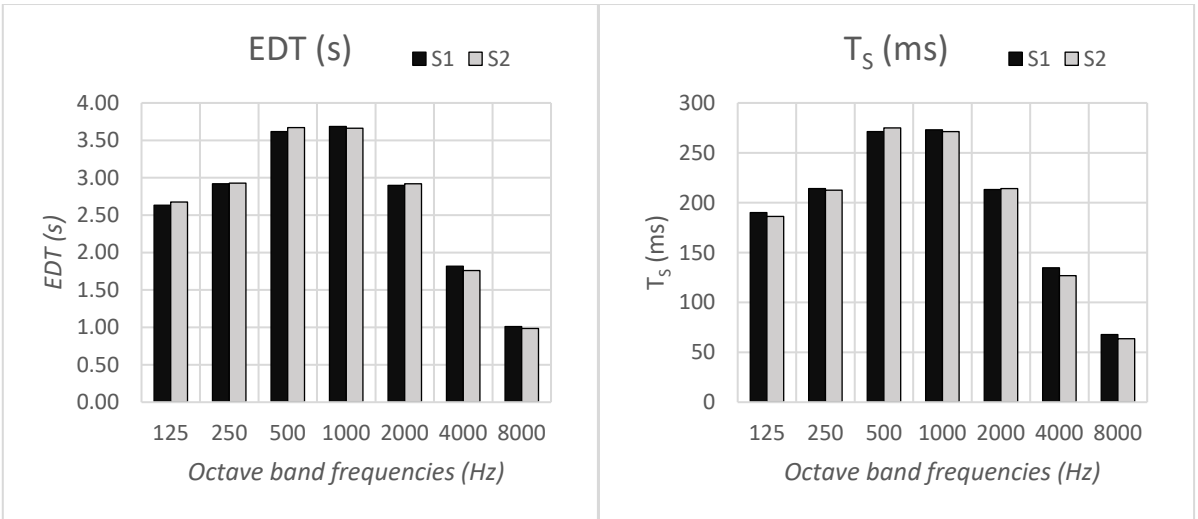

Figure 42. Octave band graph of measured EDT and Ts, considering both source positions.

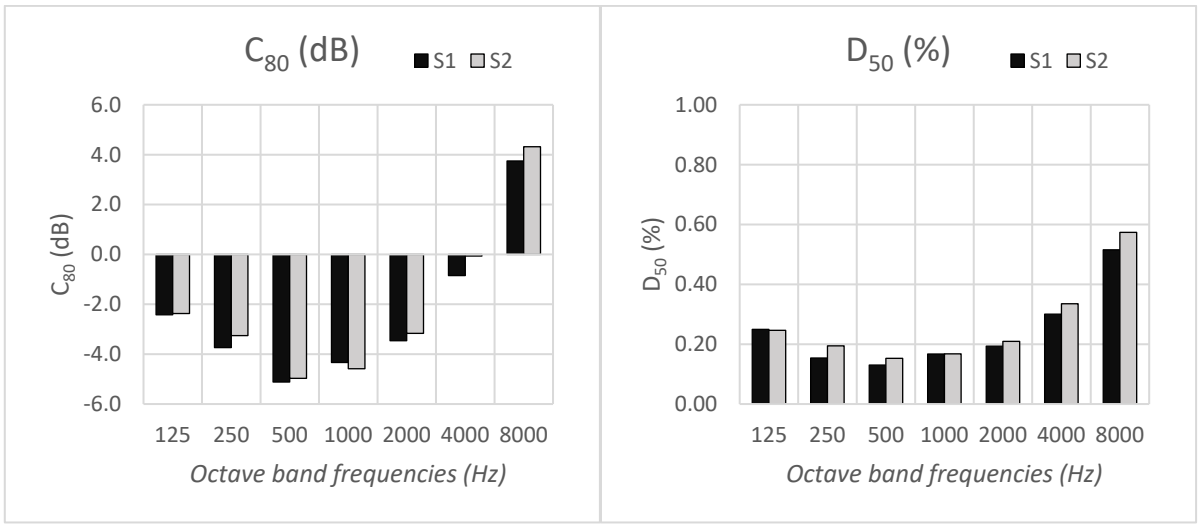

Figure 43. Octave band graph of measured clarity criteria, considering both source positions.

Furthermore, the STI values fall significantly below the thresholds required for optimal speech intelligibility.

Therefore, it is necessary to revise the current room criteria to align them with the target values suitable for chamber orchestras and conferences. Based on the analysis, the acoustic quality of the hall is deemed unsuitable, thus prompting the need for an intervention design aimed at improving its acoustic performance. Enhancing the room's absorption characteristics is a key objective of this work.

To facilitate this task, a numerical model of the hall was developed. The comparison of results involved utilizing two software tools provided by collaborating universities: CATT-Acoustic, supplied by the University of Barcelona, and ODEON, supplied by the University of Bologna. This allowed for a comprehensive evaluation and comparison of the outcomes obtained from both modelling approaches.

4 Acoustic simulation

4.1 Room Acoustics software: CATT-Acoustic and ODEON

CATT-Acoustic and ODEON are two of the most popular and reliable acoustic simulation software programs used by acoustic consultants, architects, and engineers to model and analyse the acoustics of various spaces.

CATT-Acoustic was developed in the late 1980s by Bengt-Inge Dalenbäck and his Swedish company CATT AB, specializing in room acoustics software and consulting services, then released in 1992 and has since undergone continuous development and updates (Dalenbäck, 2011). ODEON was initially developed and released in 1986 by the company ODEON A/S, which is based in Denmark. It was created by a team led by Dr. Eckhard Kahle. Since its inception, ODEON has undergone several updates and advancements, with new versions being released over the years to enhance its capabilities and features (Christensen, 2020).

While both software programs have similar goals, there are some key differences between the two:

- User Interface: CATT-Acoustic has a user-friendly interface with a 3D modeling environment, whereas ODEON has a more complex interface that requires some level of expertise in acoustics.
- Simulation Capabilities: CATT-Acoustic is better suited for simulating room acoustics, while ODEON is more versatile and can simulate a wider range of acoustical scenarios, including outdoor spaces, concert halls, and auditoriums.
- Sound Sources: both CATT-Acoustic and ODEON support a variety of sound sources, including point, line, and surface sources.
- Material Modeling: CATT-Acoustic has more advanced material modeling capabilities – including a material catalogue taken from several studies – allowing for the simulation of complex materials such as porous absorbers and diffusers, while ODEON's material modeling is more simplistic.
- Calculation Speed: ODEON is generally faster than CATT-Acoustic in terms of calculation speed, which is important for large-scale simulations.

4.1.1 Calculation principles

In the field of acoustics, two primary approaches are used to analyse and model sound propagation: wave-based methods and geometrical acoustic methods.

Wave-based methods, such as the *Finite Element Method* (FEM) and the *Boundary Element Method* (BEM), delve into the physical nature of sound waves. They solve the wave equation to provide a detailed understanding of how sound waves behave in different acoustic environments. These methods take into account complex phenomena like diffraction and wave interference, offering highly accurate results. However, due to their computational intensity, wave-based methods require significant computational resources.

Geometrical acoustic methods, on the other hand, focus on the geometric paths of sound rays and their interactions with surfaces. These methods are particularly useful in architectural spaces and room acoustics, since they are computationally efficient and can simulate large spaces more quickly than wave-based methods. However, geometrical acoustic methods do not capture fine details of wave phenomena and are limited to macroscopic characteristics.

Both CATT-Acoustic and ODEON are Geometrical Acoustic (GA)-based software, meaning that sound waves are represented by rays. As clearly explained in the ODEON manual, a ray can be understood as a straight line connecting a source and a receiver. Reflections are represented by image and secondary sources, where the sound is still considered as rays. These simplified – but reliable – assumptions make it possible to calculate the acoustic response in large spaces, while maintaining a short computation time and a high level of accuracy. Nevertheless, phase information is not included in the propagation of sound. Recent studies are showing the benefits of implementing wave-based algorithm like FEM or BEM into the room acoustics simulation programs, creating a hybrid model that allows to minimize the drawback of each simulation approach (Fratoni et al., 2022).

Therefore, both simulation software programs use hybrid ray-tracing algorithms to simulate and analyse the acoustics of various spaces, including *Image Source Method* (ISM) and *Stochastic Ray Tracing* (SRT):

- **The Image Source Method (ISM)** is a technique commonly used to calculate the early reflections in a space. ISM involves tracing sound rays from the source to the receiver and considering the reflections off surfaces such as walls, floors, and ceilings. It assumes that sound reflections can be represented by virtual image sources created by mirror-like reflections. ISM is computationally efficient and provides valuable information about the early sound field, including the direct sound and the first-order reflections.
- **Stochastic Ray Tracing (SRT)** extends the calculations beyond the early reflections considered in ISM. Ray tracing traces sound rays as they propagate through the space,

accounting for multiple reflections, diffraction, scattering, and other interactions with the environment. Unlike ISM, ray tracing can capture higher-order reflections and more accurately model complex sound paths. It is computationally more intensive than ISM but provides a more detailed representation of the sound field, especially for complex and irregularly shaped spaces.

Each algorithm has its strengths and limitations, and their suitability depends on the specific requirements and complexity of the acoustic simulation.

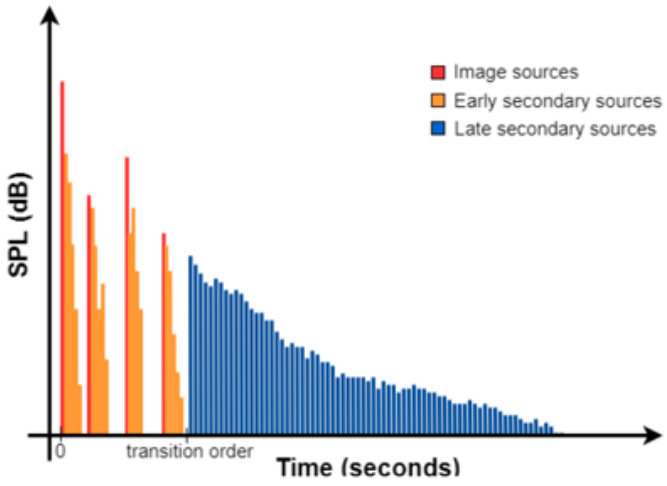

Figure 44. Hybrid GA algorithms in the time domain

In general, the transition from ISM to SRT occurs when the contributions from higher-order reflections become less significant or negligible compared to the statistical fluctuations or uncertainties in the sound field. At this point, the statistical or stochastic ray-tracing method can provide a more accurate representation of the sound field by considering the statistical variations in the reflections.

The decision to switch from one method to another is typically based on the determination of a transition order. Acoustic simulation software typically employs a default transition order of second order, utilizing the ISM for the direct sound and first order reflections, and subsequently employing SRT for all higher order reflections.

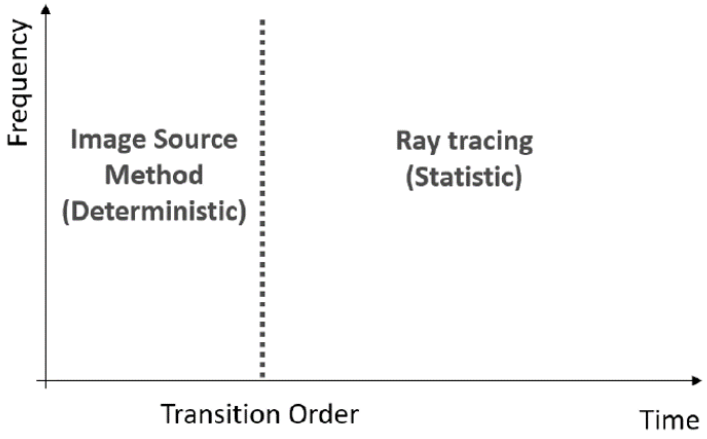

Figure 45. Transition order in acoustic simulation software

4.1.2 Tools comparison

While both programs share common techniques, their specific implementation and feature differ. This section will provide a concise analysis of the main tools and coefficients employed within the two software applications, to observe the manner in which they are handled.

4.1.2.1 Absorption coefficient α

Within CATT-Acoustic, a comprehensive catalogue of materials extracted from various manuals and publications is readily available, enabling users to edit them manually. Alternatively, users can input custom materials, assigning absorption coefficient values in octave bands ranging from 125 Hz to 4000 Hz. The software automatically assigns values for the 8000 Hz and 16000 Hz bands based on the trend of the preceding values. However, it doesn't consider the 63 Hz octave band.

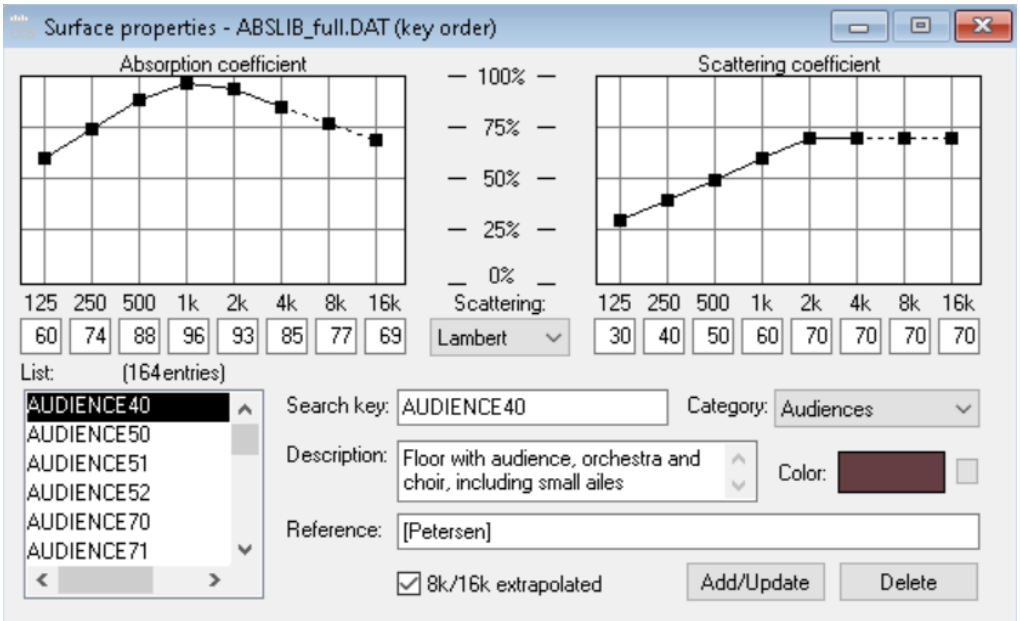

Figure 46. CATT-Acoustic materials catalogue: both absorption and scattering coefficient can be set

On the other hand, ODEON also include an internal catalogue extracted from distinct references but it's more user-friendly for manual creation of materials. Users must assign absorption coefficient values for octave bands spanning from 63 Hz to 8000 Hz. The 16000 Hz band is not taken into consideration within the software.

4.1.2.2 Scattering coefficient s

The scattering coefficient, in the context of room acoustics, represents the degree of scattering or diffusion of sound waves when they interact with surfaces. It quantifies how much the sound energy is scattered in different directions upon reflection from a surface. In other words, it is a measure of the total amount of scattered sound – for random incidence – in relation to specular sound. A scattering coefficient of 0 indicates a perfectly specular reflection, where the sound waves are reflected like a mirror. On the other hand, a coefficient of 1 represents completely diffuse scattering, where the sound energy is equally distributed in all directions upon reflection.

Both CATT-Acoustic and ODEON software are based on Lambert 1D distribution (see par. 1.2).

CATT-Acoustic allows users to assign for each octave band different scattering coefficients to surfaces based on their material properties and characteristics, as depicted in Figure 46. This enables the simulation of surfaces with varying degrees of scattering, such as diffusers or other materials designed to disperse sound energy.

In ODEON instead, users can only assign one value of scattering coefficient per surface. This value corresponds to 707 Hz (the exact middle between 63 Hz and 8000 Hz, in a logarithmic scale). The ODEON manual provides a very useful table with suggested scattering values for different types of material. For example, a value of 0.7 – which is high scattering – has been assign to the audience area in this work (see par. 4.2).

Material	Scattering coefficient at mid-frequency (707 Hz)
Audience area	0.6–0.7
Rough building structures, 0.3–0.5 m deep	0.4–0.5
Bookshelf, with some books	0.3
Brickwork with open joints	0.1–0.2
Brickwork, filled joints but not plastered	0.05–0.1
Smooth surfaces, general	0.02–0.05
Smooth painted concrete	0.005–0.02

Table 9. Suggested scattering coefficient for different materials, from ODEON manual

The scattering coefficient is frequency dependent. Each value determines a curve, which is extrapolated towards high and low frequencies, and is used for the frequency dependent calculations in ODEON.

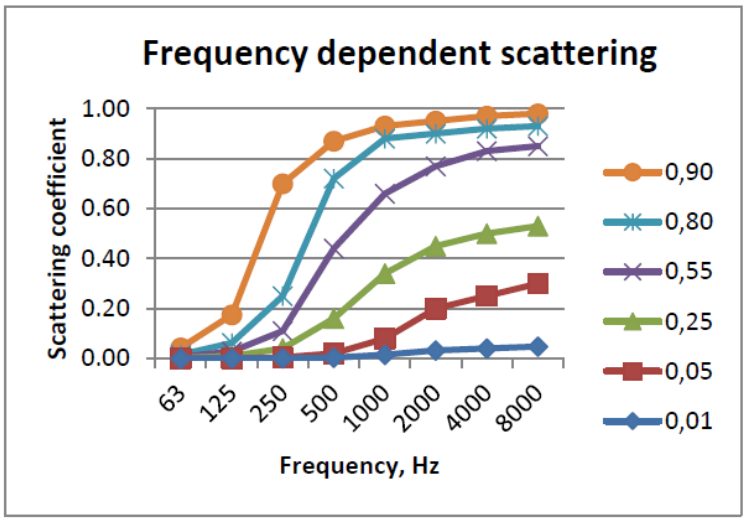

Figure 47. Frequency dependent scattering curves, extracted from ODEON manual

4.1.2.3 Sound strength G

A noteworthy consideration is warranted regarding the sound strength parameter G, as it is calculated using two distinct methods in the two simulation programs.

The G descriptor investigates how much the reflections contributes to the SPL level (see par. 1.2.2.3). In a very reflective room, there will be a high contribution, in an absorptive space there will be a low contribution. As explained in the ODEON manual, this is in short done by measuring an SPL and subtracting the Sound Level of the source, but with a reference. The reference point at 10 meters distance is the standard according to ISO 3382-1, 2009. This means that, from the measured SPL, one should subtract SPL of the source in 10 meters distance in free field. This equals a Sound Power of an omnidirectional point source of 31 dB.

In ODEON, G parameter can be found by setting the value of 31 dB within the sound source "overall gain". Following this, the SPL value and G value will be the same anywhere in ODEON, but the G value will only be displayed as SPL.

On the other hand, in CATT-Acoustic, the G parameter is automatically calculated through the external room criteria prediction tool known as TUCT (The Universal Cone-Tracer), eliminating the need for additional adjustments.

Both software applications require the presence of only one active source, which must be omnidirectional for the G descriptor calculation to function effectively.

It is important to note that the parameter G will not be considered for acoustic calibration. Instead, the distribution of sound energy within the room, obtained from both simulations and measurements, will be qualitatively analysed in comparison with Barron and Lee's theory on sound reflections decay (see paragraph 4.3.1).

4.2 Acoustic calibration

4.2.1 Room modelling

Initially, the room was subjected to modelling procedures utilizing SketchUp, a highly user-friendly 3D modelling software that demonstrates seamless compatibility with both CATT-Acoustic and ODEON.

Numerous studies emphasize the significance of taking precautions in geometry modelling, suggesting the implementation of various tests before importing the final model into acoustic simulation software. This approach facilitates the easy identification of errors and helps minimize the time invested in corrections. Modelling inaccuracies, such as warped, overlapping, reversed, or missing planes, are common pitfalls that may arise. Consequently, a rigorous examination and debugging process becomes indispensable, though it is often disregarded, in constructing and verifying models (James, 2016).

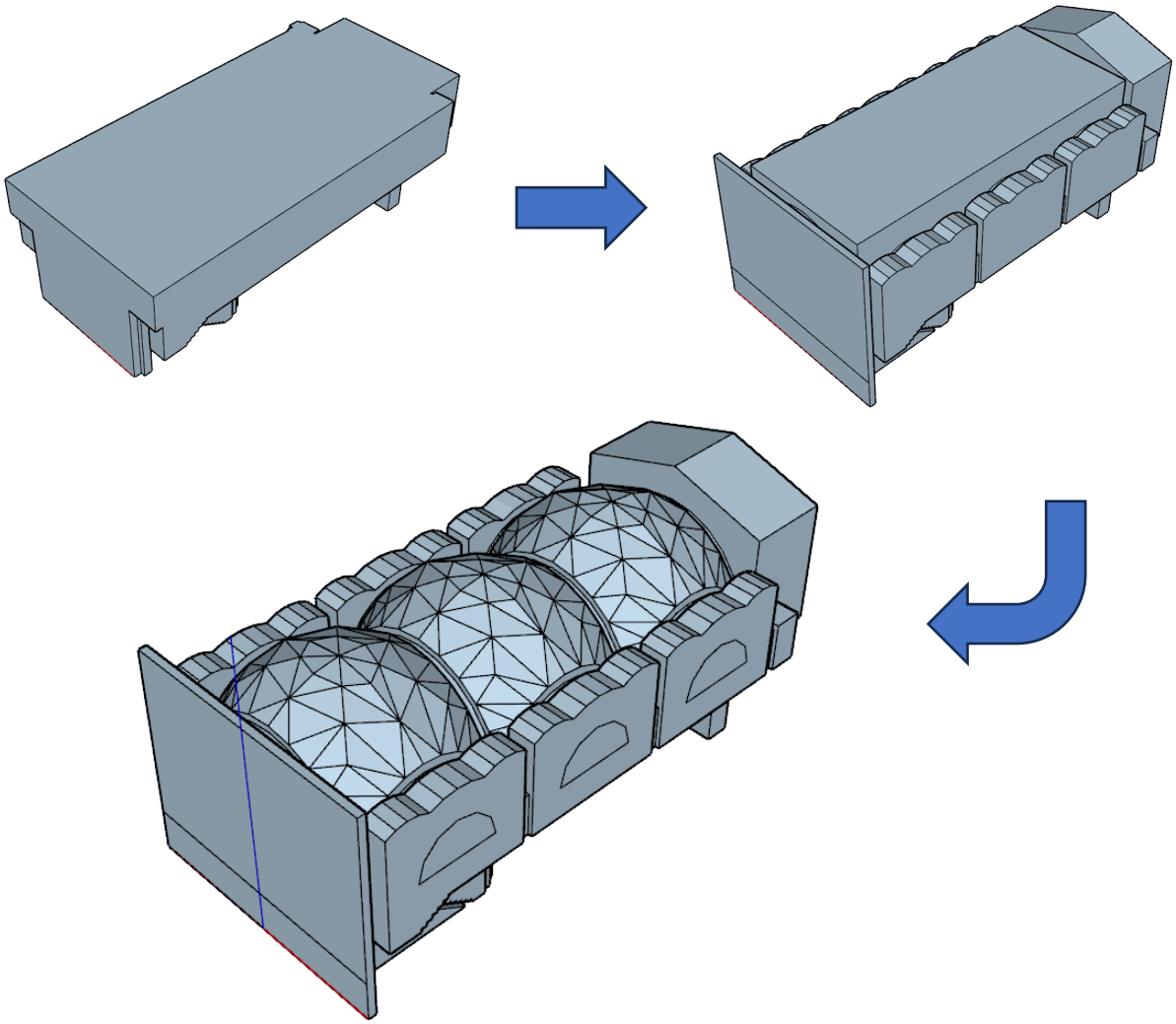

Figure 48. SketchUp modelling process. Final result is shown below.

As depicted in the Figure 49, all curved surfaces were meticulously discretized and subdivided into flat surfaces, aiming to strike an optimal balance between geometric accuracy and model simplification to facilitate computational calculations. Indeed, excessively complex or small surfaces can be redundant and detrimental to the simulation process. Regarding the vaults, a comprehensive effort of refinement and simplification was necessary.

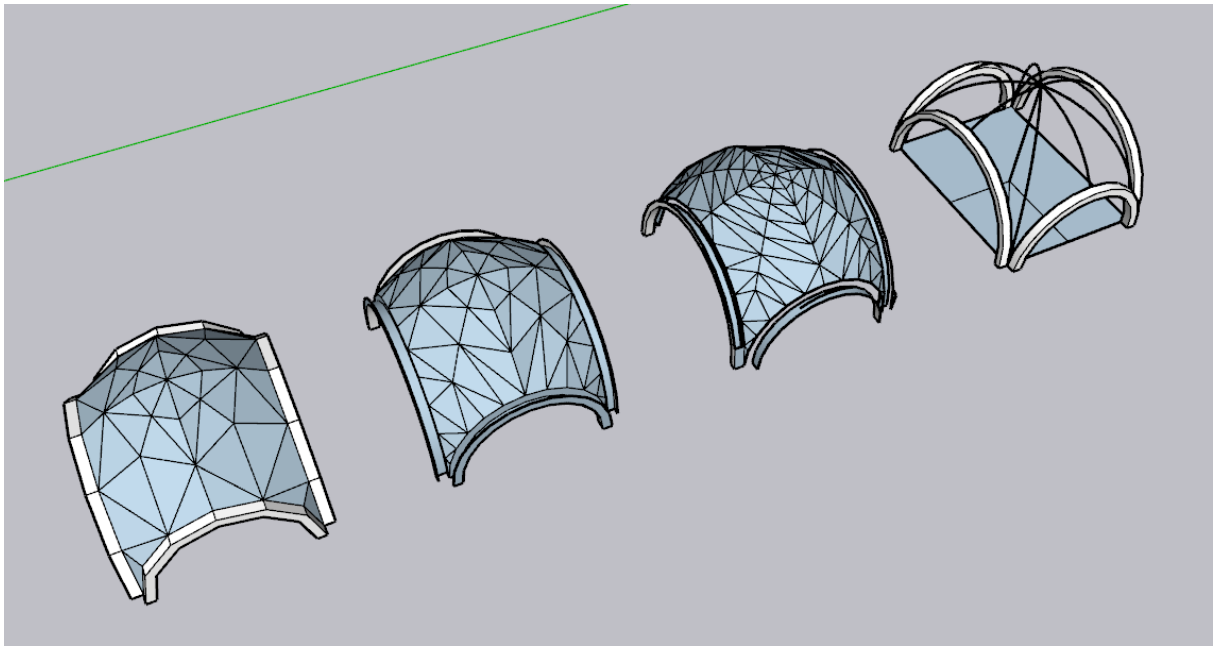

Figure 49. Refinement process of the vaults

Consequently, a meticulous process was undertaken to verify the model's integrity at various steps. This systematic approach facilitated the identification of errors, especially as the geometry progressively assumed a more complex configuration.

It is pertinent to mention that surfaces in SketchUp are assigned positive and negative versors: by default, planes with a positive versor (reflective surfaces) are displayed in white, while those with a negative versor appear in blue-gray. Therefore, ensuring correct orientation of the planes was crucial: before exporting, the entire model should appear blue-gray when viewed from outside. Only the inner faces of the surfaces – the white ones – were assigned the corresponding material, while the external faces (the blue-gray ones shown in the figure) were left without material. Notably, CATT-Acoustic is particularly sensitive to this aspect: even a single incorrectly oriented surface results in an error, preventing the simulation from starting.

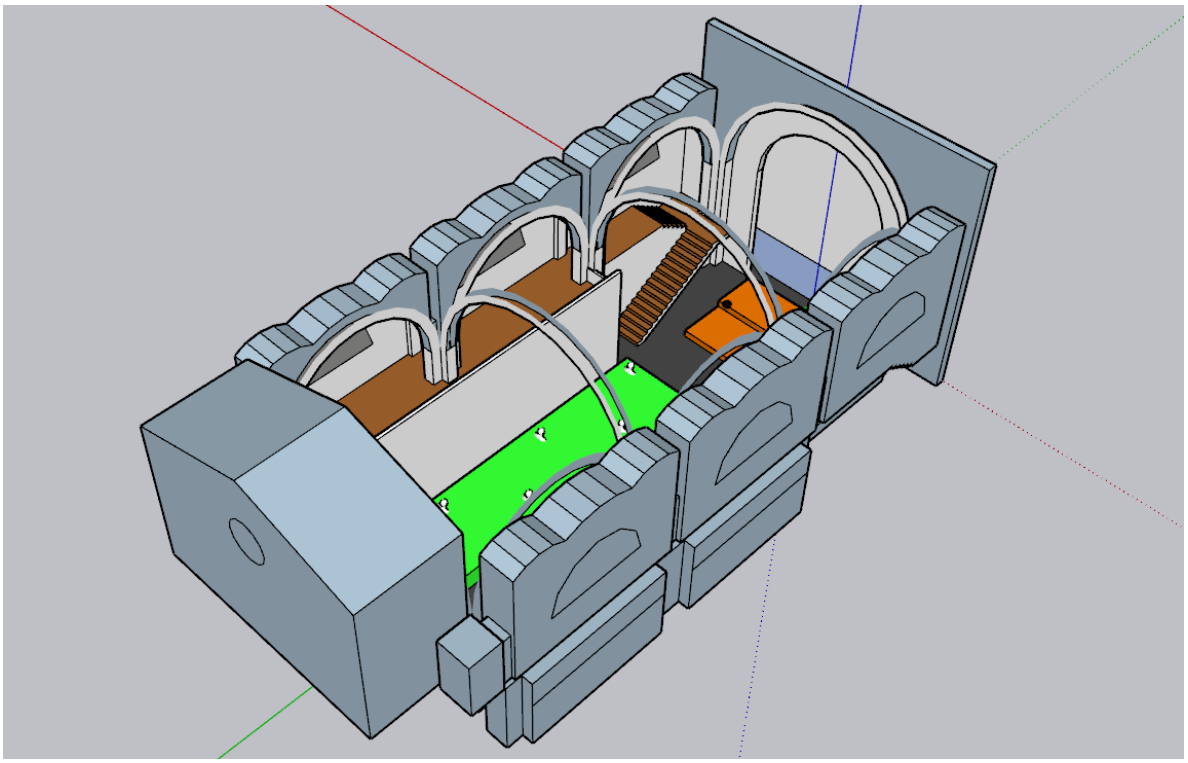

Figure 50. Internal view of the model, with assigned materials

Another crucial aspect involved the modelling of the audience area. Previous studies and simulation program manuals consistently advise simplifying the audience area by representing it as a box and subsequently introducing suitable absorption and scattering values in the simulation. This approach significantly expedites both the design and calculation processes of the numerical model.

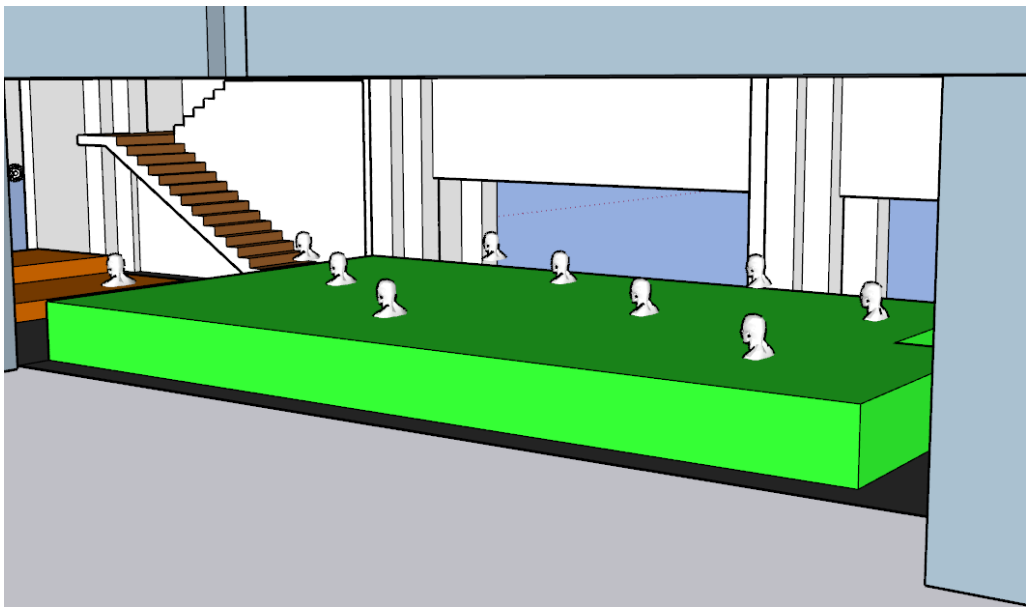

Figure 51. Audience area box, modelled within SketchUp program

4.2.2 Geometry exportation to simulation software

Subsequently, the geometric model was imported into the simulation software with the assistance of third-party plug-ins:

- **Sk2Geo (v1.4.9.7)** is a plug-in developed by the French company Euphonia, which facilitates the export of data from SketchUp to CATT-Acoustic. La Salle University of Barcelona, licensed for CATT-Acoustic, approved the acquisition of this tool to streamline the import of the model into the simulation software, as the demo version allowed exporting only up to 20 surfaces. Sk2Geo efficiently exports all vertices and planes of the model in a single .GEO file, along with a separate .GEO file for materials, considering the materials assigned to the surfaces in SketchUp. A notable advantage is the presence of source and receiver components that can be directly integrated into the SketchUp model (see Figure 51); the plug-in exports two files (.SRC and .REC) whose coordinates are automatically detected in the numerical model.
- **SU2ODEON (v1.09)** is a freely available plug-in developed by ODEON A/S, enabling the export of a unified .par file that seamlessly interfaces with the simulation software. It maintains the subdivision into layers to facilitate material assignment, and any changes made to the SketchUp model can be imported while preserving the previously established settings, such as absorption coefficients and positions of sources and receivers.

Regarding the correct reading of the model within the simulation software, CATT-Acoustic maintains its rigid approach and does not permit any open or overlapping surfaces, providing only a generic reading error without specifying the exact cause. On the other hand, ODEON exhibits greater tolerance, allowing up to 20% of rays to escape, and provides visualization tools like 3D Investigate Rays and 3D Billiard to identify the source of errors.

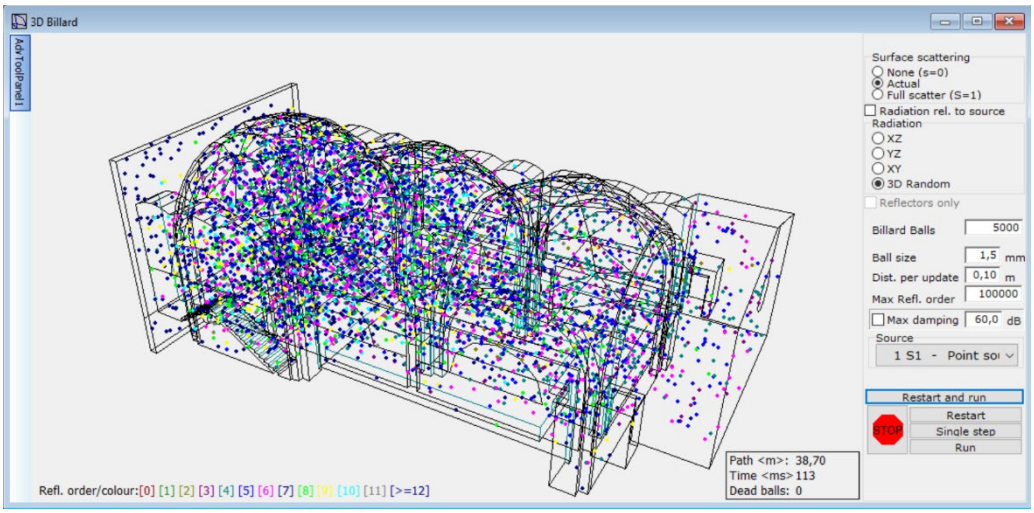

Figure 52. 3D Billiard view in ODEON

Once the model's accuracy and proper integration with the simulation software were verified, the calibration of the acoustic criteria could proceed.

4.2.3 CATT-Acoustic calibration

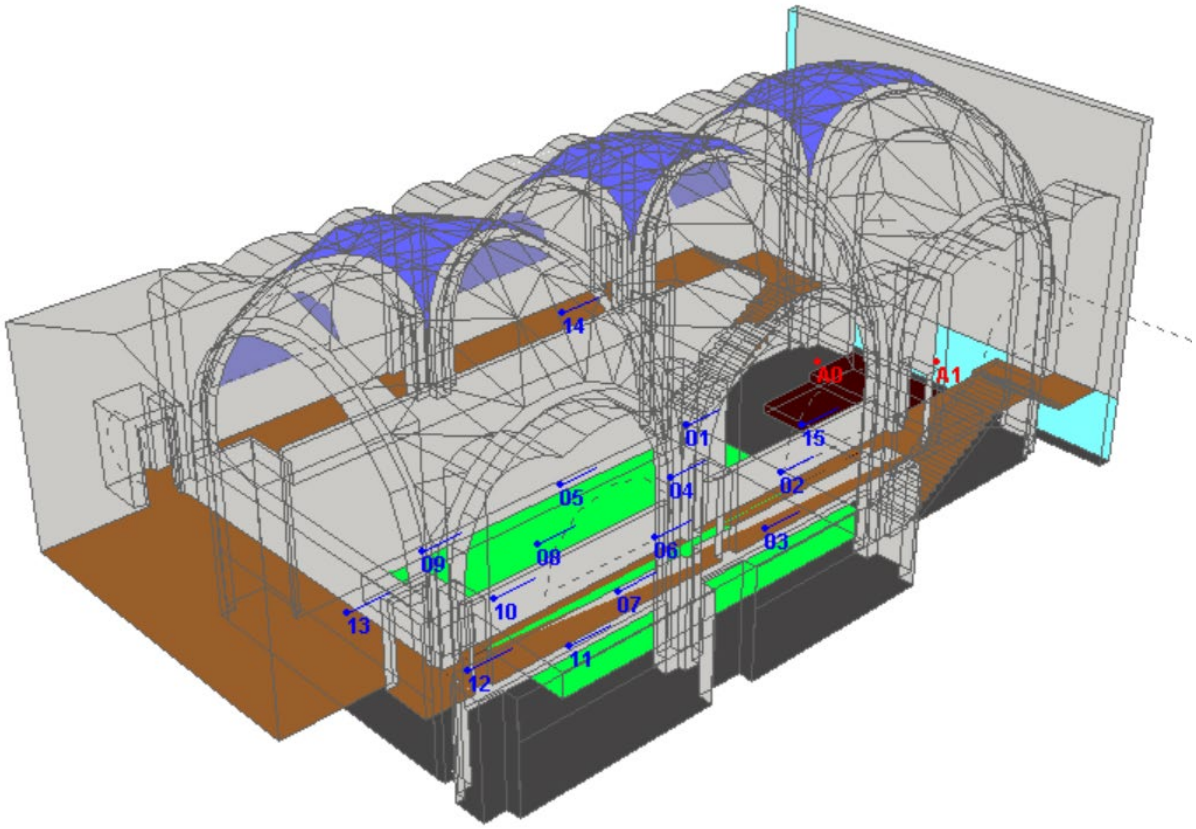

Figure 53. Calibration layout in CATT-Acoustic software simulation. View of sources and receivers inside the 3D model.

To import the model into CATT-Acoustic, a dedicated "sk2geo" folder was created, containing the files exported using the plug-in. In the Modeling panel, the General Settings item was accessed to designate the aforementioned folder as both the input and output location. The geometry view and check settings were left unchanged. Upon clicking Save and Run, the numerical model was loaded, leading to the opening of two windows: a 3D viewer displaying the room and another called PL9 viewer, enabling the visualization and selection of individual planes of the model, along with their respective acoustic properties. Furthermore, several 2D views and an isometric view of the room were made accessible.

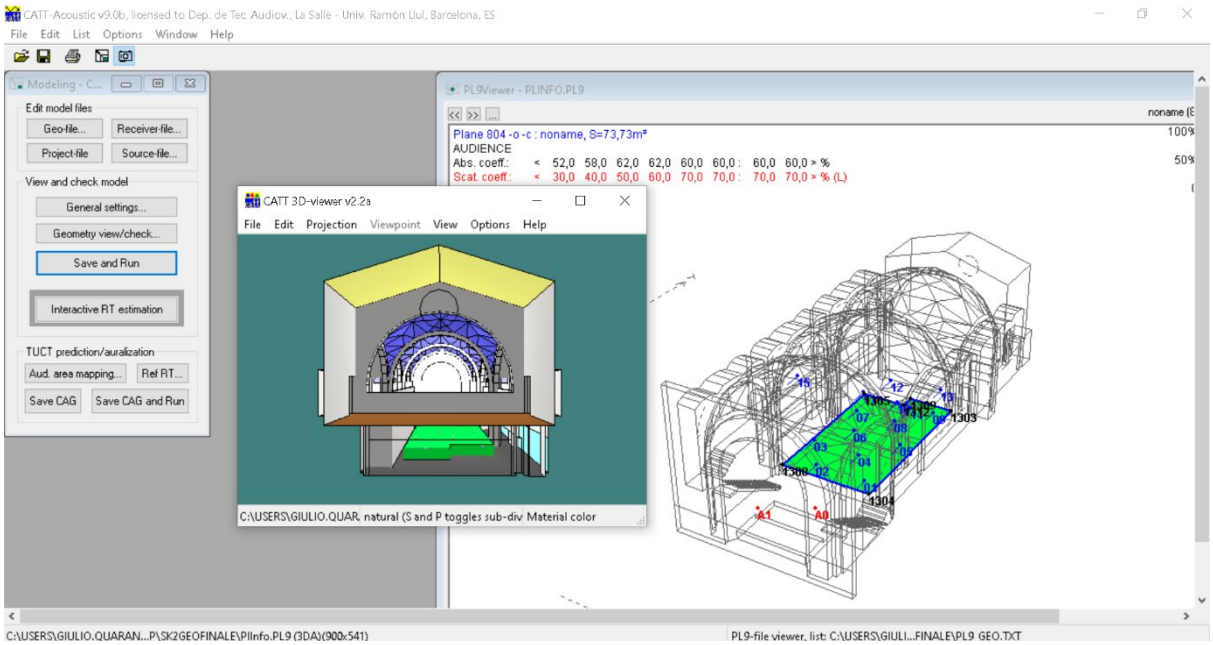

Figure 54. CATT-Acoustic opening view: modelling panel, 3D viewer and PLINFO

Several manual corrections were required within CATT-Acoustic to ensure the accurate representation of surfaces. For instance, the windows were configured as sub-divisions of the walls in which they are situated, enabling them to be recognized as surfaces with distinct acoustic properties. This step was essential to enhance the precision and reliability of the simulation results.

The following section outlines the primary steps undertaken for the calibration and extraction of the monaural acoustic criteria pertinent to the objectives of this thesis.

4.2.3.1 Sound sources and receivers

During the measurement campaign, precise measurements of the distances of sources and receivers from the walls were obtained, facilitating their incorporation into the numerical model.

As previously explained, in the case of CATT-Acoustic, all sources and receivers were first inserted into SketchUp using the components provided by the Sk2Geo plug-in, and then imported into the simulation software in .SRC and .REC format.

Omnidirectional sources were defined with a pink spectrum emission and a sound power of 90 dB at 1000 Hz.

Within the General Settings panel, all receivers were activated, while only one source was activated at a time. This approach allowed for the calculation of all relevant monaural descriptors, including G. The receivers were oriented towards the stage; however, given that these are omnidirectional sources and random incidence microphones, the orientation of the devices did not significantly impact the results.

4.2.3.2 Materials

The materials found within the room were categorized based on qualitative assessments, as a catalogue or technical data sheets with exact acoustic properties were not available for reference. The measured results indicated a slightly higher absorption at low frequencies (as discussed in section 3.3). Consequently, certain materials with specific elastic properties, which likely function as resonators and absorb low frequencies, were identified. For instance, the vaulted ceiling is suspected to be constructed of thin brick panels, typical of Catalan vaults in the region, with air cavities behind them that may act as resonators. Similarly, the stage appears to be made of wood panels with an air gap underneath, which could enhance its low-frequency absorption characteristics. These observations were made for various other materials within the room as well.

All the data collected in this work is sourced from previous studies. Both the CATT-Acoustic and Odeon software platforms offer an extensive repository of data derived from authoritative sources, encompassing a wide array of expert contributions in acoustics, including luminaries such as Beranek, Dalenbäck, Christensen, and others. An Excel spreadsheet, generously shared by the la Salle research group, consolidates these references, facilitating a convenient cross-reference of the chosen materials.

It is essential to acknowledge that uncertainty may exist when extracting absorption coefficients for various materials. Therefore, considering a certain tolerance range in assigning values is advisable, while ensuring that the physical properties of the materials are respected. Consequently, the absorption coefficients were slightly modified where necessary.

Table 10 presents the list of materials utilized in the study. Notably, the absorption values used are identical for both CATT-Acoustic and ODEON, as they serve as valid results for calibration in both software. Consequently, the same table will be applied in the subsequent section dedicated to ODEON.

Regarding the scattering values provided, the first value of 0.05 pertains to the default value assigned in ODEON, whereas the second value 0.1 represents the default value in CATT-Acoustic, which remains consistent across all octave bands. An additional discussion is warranted for the audience area. For the sake of simplicity, a scattering value of 0.7 has been specified, referring to the average mid-frequency of 707 Hz, according to the ODEON algorithm. However, it is crucial to acknowledge that in CATT-Acoustic, the scattering values are manually assigned for each octave band. Specifically, from 125Hz to 4000Hz, the scattering values are 0.3, 0.4, 0.5, 0.6, 0.7, and 0.7, respectively.

Material	Scattering	Absorption					
		125 Hz	250 Hz	500 Hz	1000 Hz	2000 Hz	4000 Hz
Granite floor	0.05/0.1	0.01	0.01	0.01	0.01	0.02	0.03
Plaster	0.05/0.1	0.01	0.01	0.01	0.02	0.03	0.04
Vaults	0.05/0.1	0.10	0.08	0.04	0.01	0.01	0.01
Wood floor	0.05/0.1	0.15	0.11	0.08	0.06	0.08	0.10
Wooden door	0.05/0.1	0.20	0.16	0.08	0.06	0.10	0.10
Ordinary window	0.05/0.1	0.40	0.26	0.11	0.06	0.05	0.03
Stained-glass window	0.05/0.1	0.25	0.13	0.03	0.02	0.02	0.02
Stage	0.05/0.1	0.32	0.24	0.11	0.06	0.08	0.20
Unoccupied seats	0.70	0.52	0.58	0.62	0.62	0.60	0.60

Table 10. Scattering and absorption coefficient of pre-existing materials.

After assigning all the materials to their respective surfaces, a preliminary estimation of the reverberation time (RT) can be obtained to assess its correlation with the measured values. The Interactive RT estimation panel displays a graph containing Sabine's and Eyring's RT curves. By clicking on the "Start trace" button, an approximate calculation of the T-30 is performed. This step provides a rough indication of the RT based on the material assignments in the model.

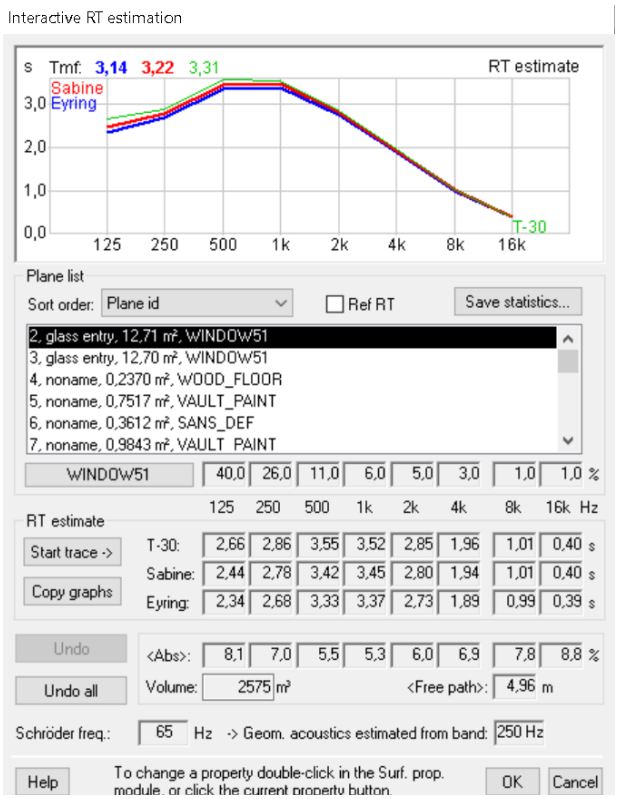

Figure 55. Interactive RT estimation performed in CATT-Acoustic before the calibration

4.2.3.3 Model calibration

By clicking on the *Aud. Area mapping* button, the setup window is opened to select the horizontal surface of the audience that will be considered for the calculation of the acoustic criteria. The audience area box has been assigned a height of 0.8 m, therefore a mapping height of 0.4 m above the audience plane is chosen. Consequently, the acoustic criteria value grid is calculated at a height of 1.2 m, in accordance with the measurement procedure where microphones were placed at the same height.

Within CATT-Acoustic, the calibration process is facilitated through the use of an external tool called The Universal Cone-Tracer (TUCT). To initiate the calibration, one must access TUCT by clicking on *Save CAG and Run*. Subsequently, a new window will appear, where the computational calculation can be initiated by selecting the *Map measures* button. For the calculation setup, an automatic number of rays was set at 24780. To determine the length of the echogram, it is recommended to use a minimum value of 2/3 of the highest measured RT value. In this case, to be sure, a value of 4000 ms was set for the impulse response calculation. Finally, air absorption was activated. With this configuration, the calibration process is now ready to be computed.

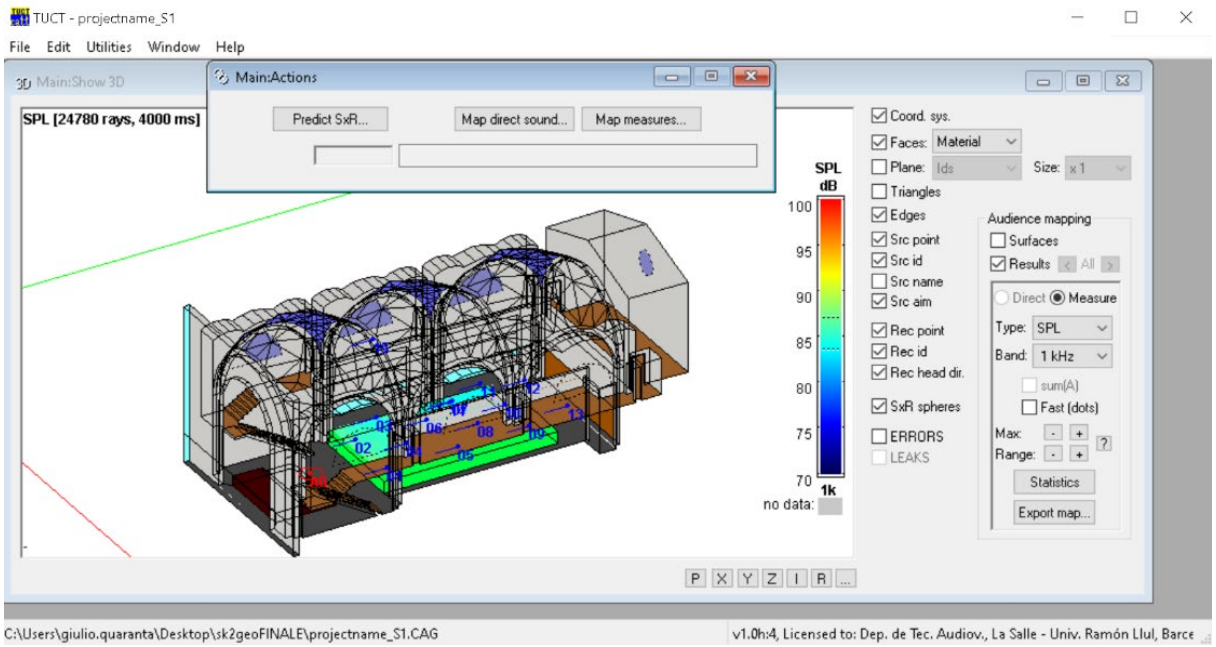

Figure 56. TUCT external tool

Upon completion of the calculation, a grid of values corresponding to the audience plan is presented. The software offers various views and provides the option to select the desired descriptor for analysis from the drop-down menu.

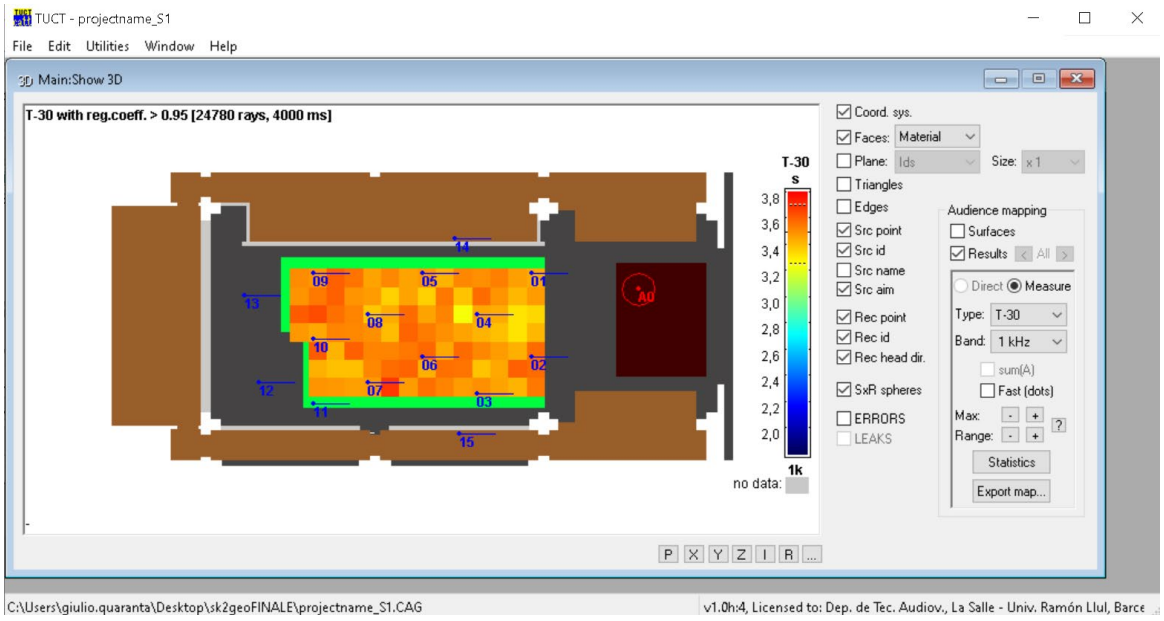

Figure 57. Example of T30 CATT-Acoustic grid plan, at 1000 Hz

Table 11 presents a comprehensive summary of all the acoustic criteria simulated in CATT-Acoustic, which were subsequently compared with the measurement values within the JND (Just Noticeable Difference) range established by the ISO 3382-1 standard (see par. 1.2.2). The Just Noticeable Difference (JND) is the minimum perceptible variation that the human ear can

detect. In other words, it is the smallest change in a specific acoustic criteria that the human auditory system is capable of perceiving. This sensitivity threshold plays a crucial role in evaluating the accuracy and reliability of acoustic measurements and simulations.

	Measured		Simulated (CATT-Acoustic)		Variations	
	S1	S2	S1	S2	S1	S2
$T_{30,M}$ (s)	3.63	3.63	3.57	3.54	0.02	0.02
EDT_M (s)	3.65	3.67	3.6	3.6	0.02	0.03
$C_{80,3}$ (dB)	-4.3	-4.2	-4.0	-4.1	0.3	0.2
$D_{50,3}$ (%)	0.16	0.18	0.18	0.18	0.01	0.01
$T_{S,3}$ (s)	253	253	245	244	8	10
STI_{male}	0.40	0.40	0.39	0.39	0.01	0.0 1

Table 11. CATT-Acoustic model calibration: all the differences between measured and simulated values are within the JND provided by ISO 3382 (T_{30} and EDT = 5 %, C_{80} = ±1 dB, D_{50} = 0.05, T_S = 10 ms, STI = 0.03) (ISO 3382-1, 2009). All the values are considered in unoccupied state. "M" and "3" subscripts identify those values averaged over the central octave bands, respectively 500÷1000 Hz and 500÷2000 Hz.

4.2.4 ODEON calibration

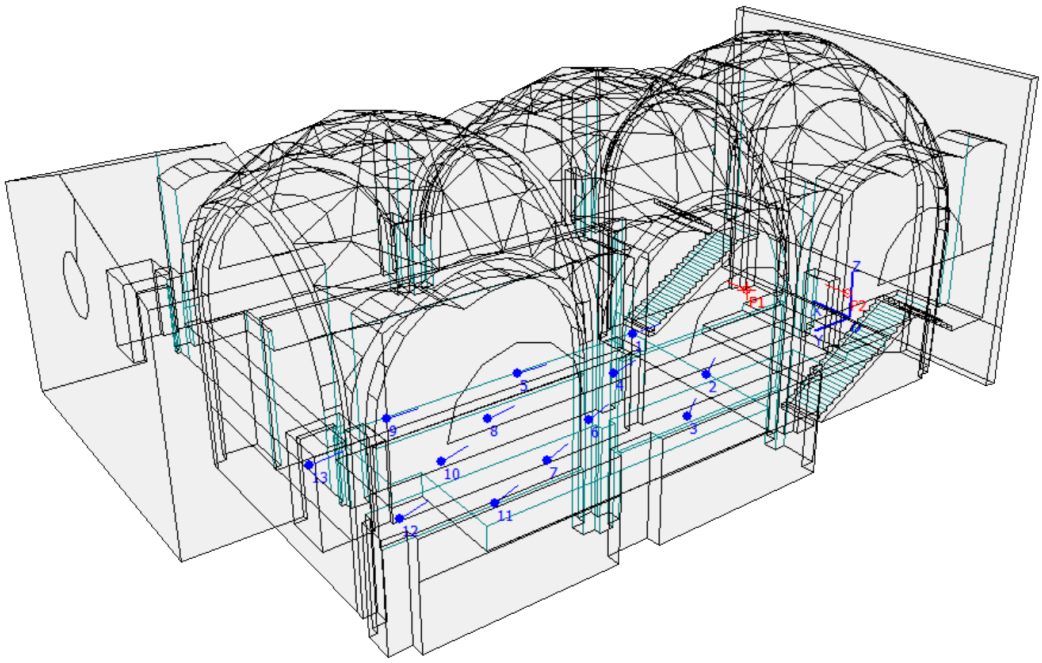

Figure 58. Calibration layout in ODEON software simulation. View of sources and receivers inside the 3D model.

The process of importing the numerical model into ODEON is notably faster and more intuitive. It involves selecting the single .par file exported from SketchUp by clicking on the "File" menu and choosing *Open Room*. Subsequently, the model is displayed, as shown in Figure 58. ODEON provides a 3D visualization tool of the model called 3D OpenGL, which is color-coded based on the absorption levels of the materials. The colour green and light blue represent greater absorption at low frequencies, while the colour red indicates greater absorption at high frequencies.

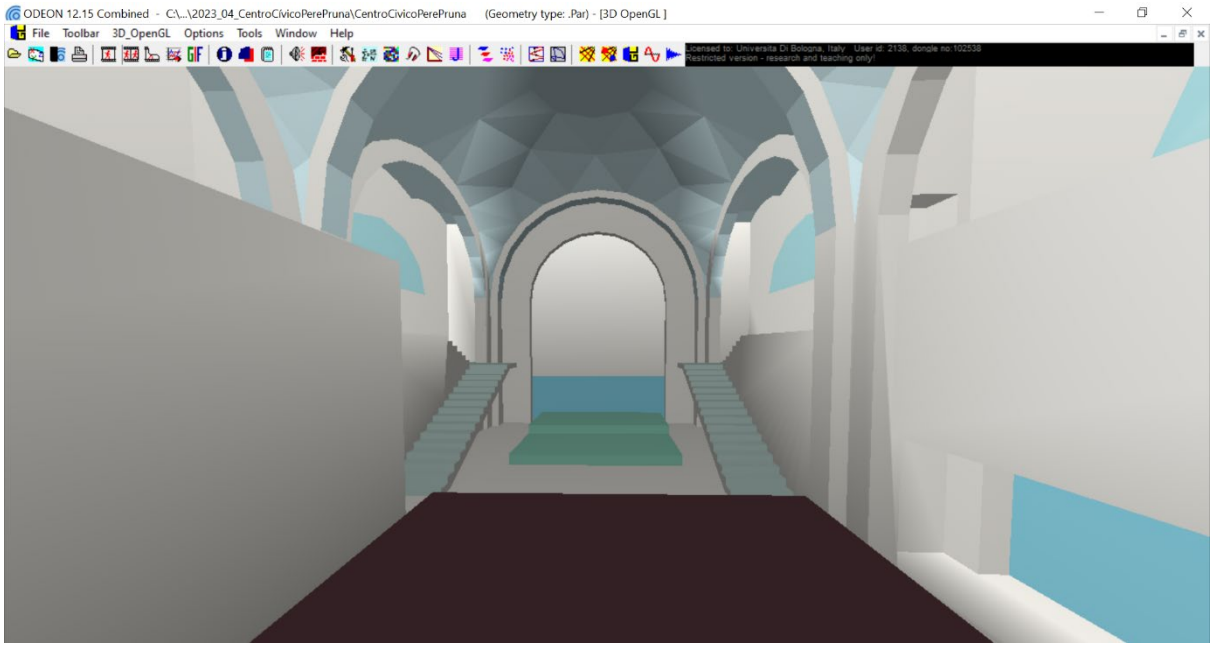

Figure 59. 3D OpenGL model visualization

In contrast to CATT-Acoustic, ODEON has the capability to automatically detect and separate overlapping planes, such as windows, from other surfaces within the model. Consequently, no manual modifications were necessary in this regard.

4.2.4.1 Sound sources and receivers

The placement of sources and receivers was meticulously performed through manual procedures. Each position's distance from the Cartesian axes was accurately measured and subsequently recorded as coordinates within the *Source Receiver List* section in ODEON. The sound sources were designated as point sources, characterized by their omnidirectional emission, while an overall gain of 31 dB was set for the computation of the sound strength descriptor, G (as explained in section 4.1.2.3). To ensure precise calculations of the acoustic criteria, particularly the G value, it is imperative to activate only one source at a time during the assessment.

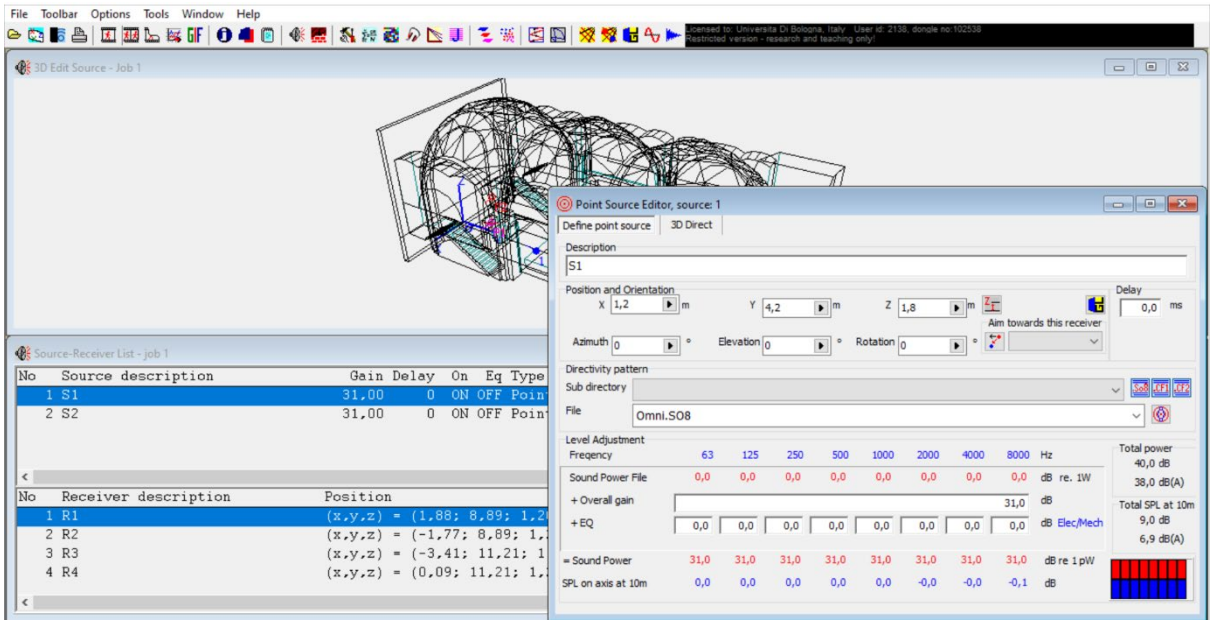

Figure 60. Source Receiver List displayed in ODEON

4.2.4.2 Materials

The absorption coefficient values utilized for the materials in Odeon were the same as those used in CATT-Acoustic (as described in par. 4.2.3.2). However, in Odeon, these coefficients were manually created and assigned in the "Material List" section. The assignment of materials to surfaces was based on the corresponding layer names established in SketchUp; for instance, the "vaults" material was created and assigned to the layer with a similar name.

As previously elucidated, the scattering coefficient value is entered as a singular value at the average mid-frequency of 707 Hz. This value, in turn, determines the scattering curve across all octave bands.

In Odeon, the Wall Type can be adjusted to control the behaviour of sound rays upon hitting a surface. The options include Normal, Exterior, and Fractional types, which affect how Reflection Based Scattering is calculated for sound reflecting from surfaces:

- *Normal* is the default setting.
- *Exterior* designates a surface as an exterior surface, even if it was not initially detected as such by Odeon. This results in less diffraction being applied at the lowest frequencies.
- *Fractional* is suitable for surfaces that form a part of a larger whole, such as surfaces forming a curved wall or a dome. These individual surfaces should not introduce significant edge diffraction due to their individual areas.

The Fractional wall type was selected for the curved surfaces of the vaults in order to disregard the diffraction caused by the geometric approximation of the model's edges.

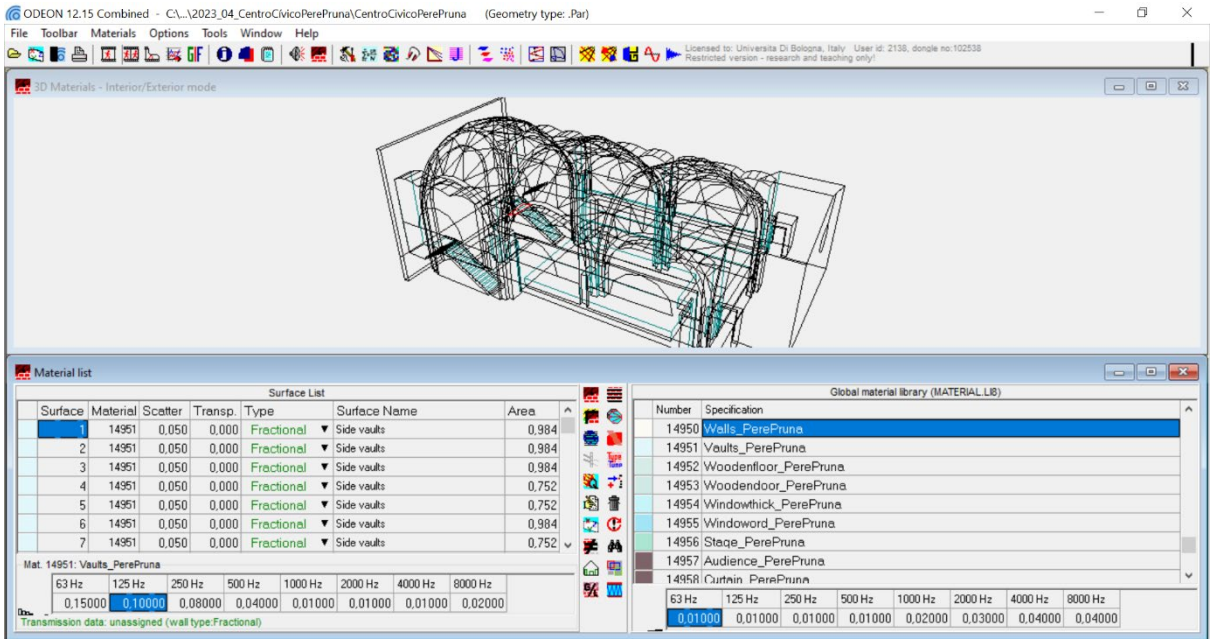

Figure 61. ODEON Material List

ODEON is equipped with two global reverberation time calculation tools that are independent of the positions of the receivers.

The first analysis is facilitated through the *Quick Estimate* tool, which relies on analytical formulas such as Sabine's and Eyring's. These formulas consider the absorption quantity and volume of the room, but do not take into account the actual geometry and position of materials. The tool provides reverberation times of Sabine, Eyring, and Arau-Puchades, and offers insights into various aspects, including the distribution of equivalent absorption area (in m^2 Sabine) across materials and octave bands, as well as an estimate of the room's volume and total surfaces. Moreover, the tool aids in determining the suggested total absorption area to add in order to achieve the desired reverberation time.

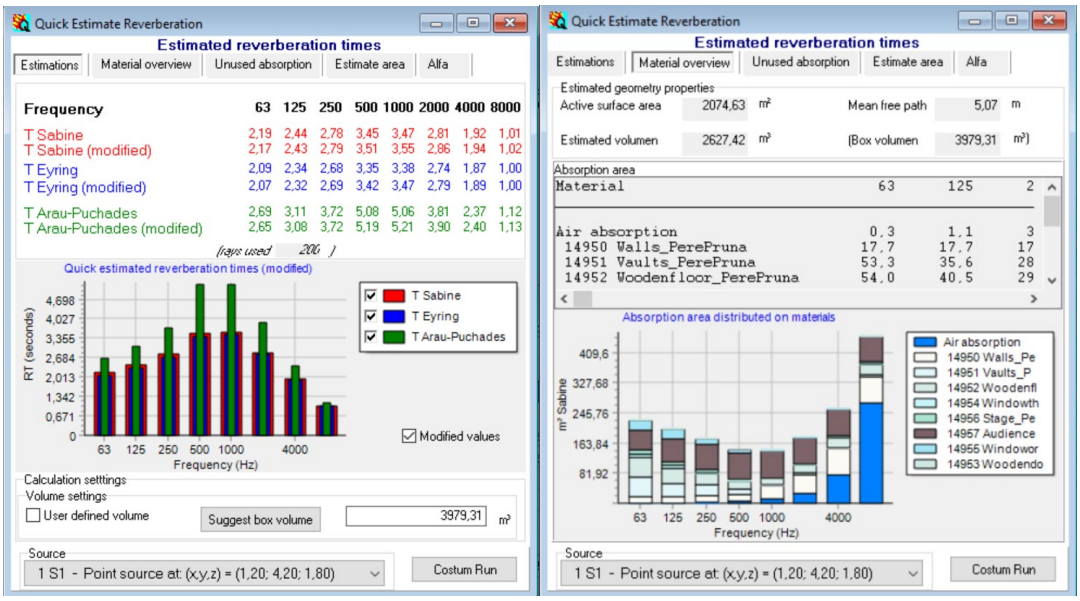

Figure 62. Quick Estimate Reverberation tool

The second estimation tool available in ODEON is the *Global Estimate*, which utilizes ray tracing to compute the overall/global reverberation time in the room. Compared to the Quick Estimate tool, the Global Estimate offers higher accuracy in its calculations. The estimation is dependent on the selected source from the bottom drop-down menu. However, it is essential to note that the calculation is receiver-independent, providing an average result for the entire room. In reality, specific locations within the room may have significantly lower or higher reverberation time values.

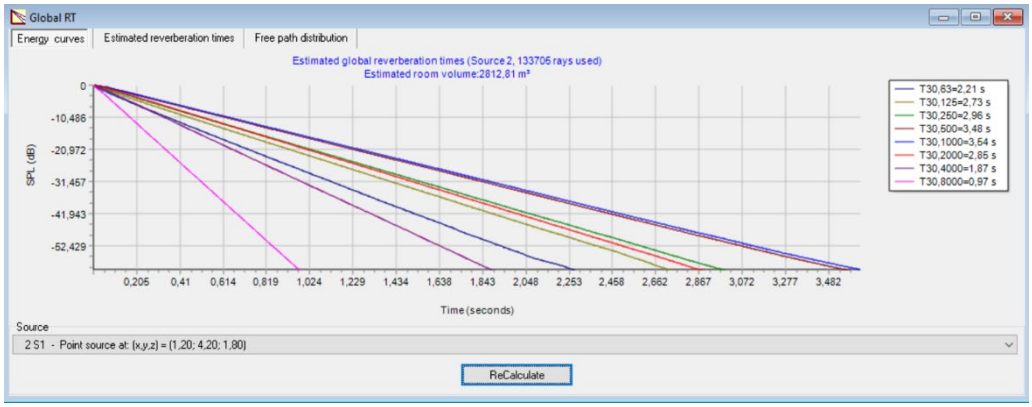

Figure 63. Global RT estimate tool

Both tools offer the capability of promptly verifying the accurate correspondence of the reverberation time values within the respective octave bands concerning the measurements. This verification can be performed before conducting the actual calculation, facilitating an early assessment of the results.

4.2.4.3 Room setup and grid definition

Another crucial step prior to calculating the criteria involves the configuration of the rays' number and the echogram length, which is accomplished through a tool named "Room Setup" within ODEON. This tool offers three pre-set buttons – *Survey*, *Engineering*, and *Precision* – that suggest the ideal number of rays for calculating the impulse responses based on the project's requirements. In this case, the *Engineering* button was chosen as it provided a suitable balance between accuracy and computational efficiency. The length of the echogram is set to 4000 ms, consistent with the configuration used in CATT-Acoustic. The recommended number of late rays is set to 1424, while the number of early rays is set to 2848.

ODEON distinguishes between early rays and late rays when selecting the number of rays. As mentioned earlier (see par. 4.1.1), the transition order for reflections is set to 2. Consequently, ODEON employs different algorithms depending on the order of reflection. The early reflections method comprises a combination of the Image Source method (ISM) and the Early Scattering method (ESM), where the decay curve's contribution arises from image sources and secondary sources. On the other hand, the late reflections method is based on the Ray Radiosity method (RRM), with contributions exclusively from secondary sources.

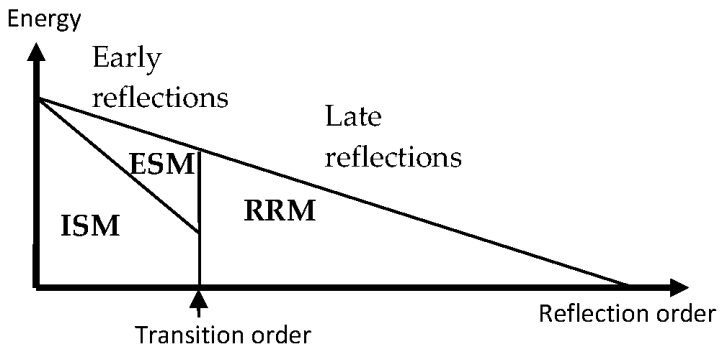

Figure 64. Early and late reflections method computed in ODEON

Ultimately, the selection of the plane for criteria calculation is required. This entails utilizing the *Define Grid* function to choose the horizontal plane of the audience where the acoustic criteria will be computed, and the corresponding grid of values will be presented. Similar to the procedure in CATT-Acoustic, the acoustic criteria value grid is computed at a standardized height of 1.2 meters by setting a height of 0.4 meters above the audience box, ensuring a consistent and uniform approach in both software applications.

4.2.4.4 Model calibration

Subsequently, the local calculation of acoustic criteria is conducted, differentiated for each individual point of sources and receivers. This phase constitutes the actual simulation, as the resulting descriptors are receiver-dependent and directly comparable to the impulse response measurements obtained in the physical room.

The calibration process is accomplished through the *Job List* feature, offering the options to calculate single point responses, multi-point responses, and grid responses. For this particular study, two job calculations have been generated, with the first activating source S1, and the second activating source S2. Both simulations involve the computation of multi-point responses and grid responses.

By initiating the computational calculation with the *Run single job* command, the software executes the relevant processes. Subsequently, the *View Multi-Point Response* function facilitates access to numerous tables containing all the acoustic criteria of interest. These tables are initially organized by receiver, followed by individual values distributed across octave bands and averaged over all receivers.

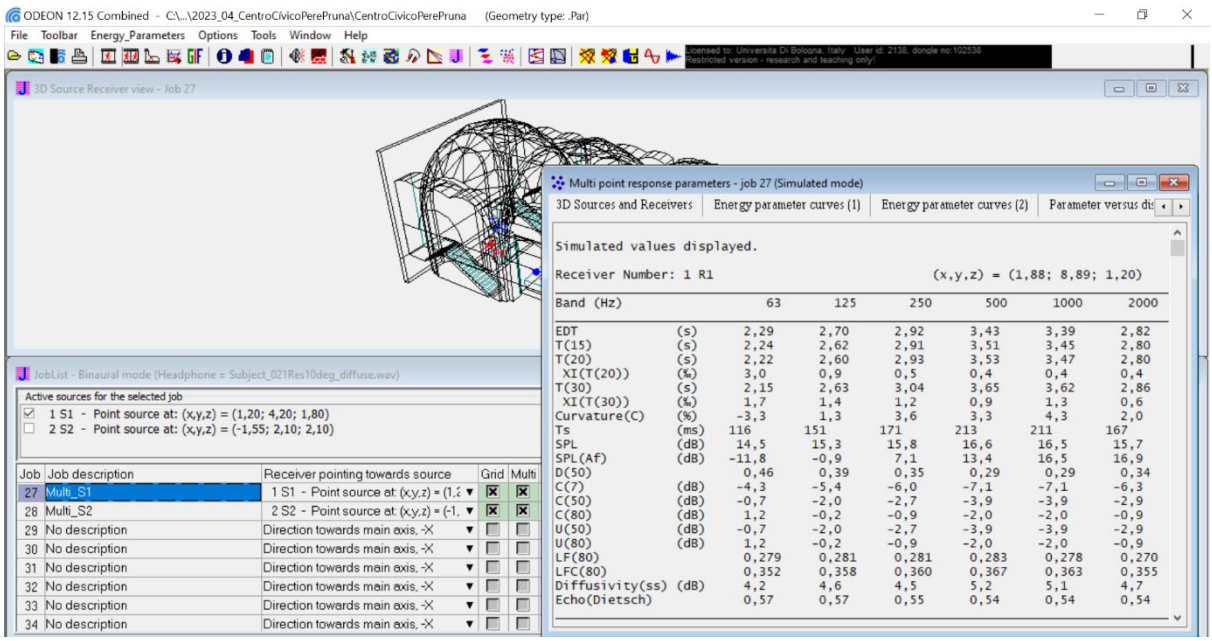

Figure 65. Multi-point response simulation computed in ODEON

Moreover, the *View Grid Response* option allows for the visual representation of the grid of values corresponding to each specific descriptor, facilitating a comprehensive analysis of the results.

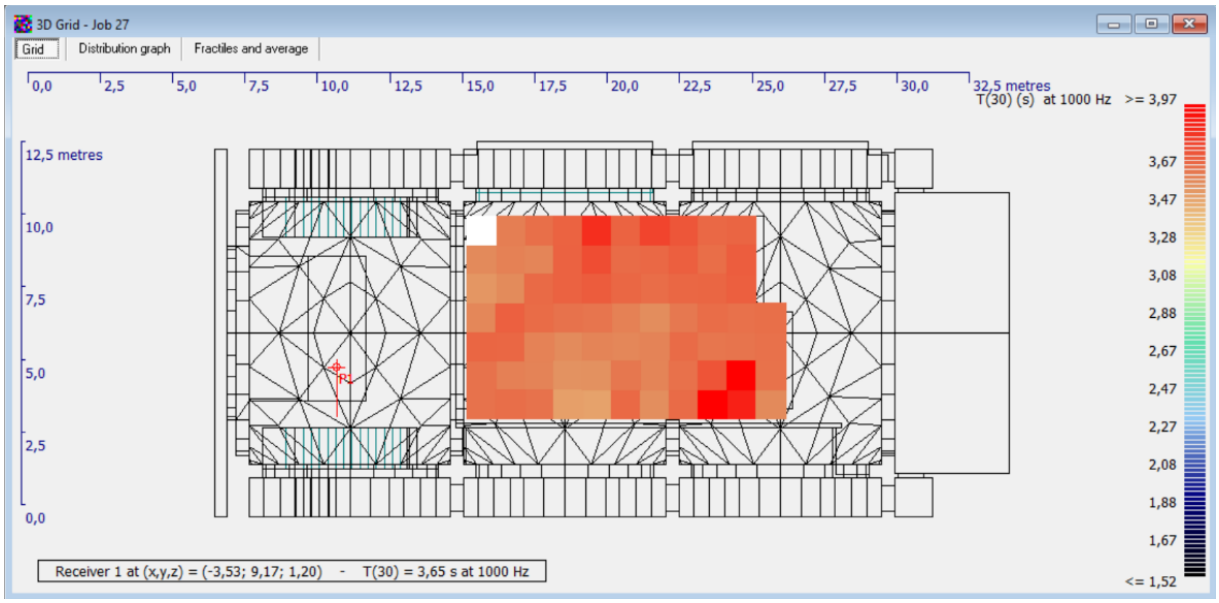

Figure 66. Example of T30 ODEON grid plan, at 1000 Hz

The acquired acoustic criteria are concisely summarized in Table 12, which presents a comparative analysis with the values obtained from the actual measurements. It is noteworthy that all the values lie within the range of the Just Noticeable Difference (JND) as stipulated by the ISO 3382-1 standard.

	Measured		Simulated (Odeon)		Variations	
	S1	S2	S1	S2	S1	S2
$T_{30,M}$ (s)	3.63	3.63	3.69	3.51	0.02	0.03
EDT_M (s)	3.65	3.67	3.6	3.7	0.02	0.01
$C_{80,3}$ (dB)	-4.3	-4.2	-4.5	-4.8	0.2	0.5
$D_{50,3}$ (%)	0.16	0.18	0.16	0.17	0.00	0.01
$T_{S,3}$ (ms)	253	253	250	256	3	3
STI_{male}	0.40	0.40	0.38	0.39	0.02	0.01

Table 12. ODEON model calibration: all the differences between measured and simulated values are within the JND provided by ISO 3382 (T_{30} and EDT = 5 %, C_{80} = ±1 dB, D_{50} = 0.05, T_S = 10 ms, STI = 0.03) (ISO 3382-1, 2009). All the values are considered in unoccupied state. "M" and "3" subscripts identify those values averaged over the central octave bands, respectively 500÷1000 Hz and 500÷2000 Hz.

The forthcoming chapter will entail a comprehensive examination, encompassing the acoustic measurements and the simulations executed using the software. This meticulous analysis will serve to validate the accuracy of the calibration of each descriptor with precision and detail.

4.3 Results analysis

4.3.1 Sound energy distribution

A distinct examination is warranted for the qualitative distribution of sound energy represented by the parameter G.

According to the semi-reverberant theory, in a room the sound field is a combination of a direct component and a reverberant one. Thus, the strength criteria G is expressed by the following formula:

$$G(r) = 10 \log\left(d + 31200\frac{T}{V}\right)\ dB$$

Where:

d is the sound energy of the direct sound and it corresponds to

$$d = \frac{100}{r^2}$$

r is the source-receiver distance, in meters;

T is the reverberation time, in seconds;

V is the volume of the room, in m^3.

However, it is noteworthy that Barron and Lee's extensive studies on concert halls have revealed deviations from the classical principles, particularly in the context of the total reflected sound level, which is shown to vary with source-receiver distance instead of remaining constant. Their *revised theory* proposes a model where the total sound comprises a direct sound component and a linearly decaying reflected component that commences upon the arrival of the direct sound. The observed weakening of early energy as one moves away from the source accounts for the primary disparity between Barron and Lee's findings and the values estimated using the semi-reverberant method. Barron and Lee's model incorporates three energy components: the direct field (d), early reflections energy (e_r), and late reflections energy (l), considering a threshold of 80 ms as the demarcation between early and late reflections. The expression for the total sound pressure level (G_{BL}) according to Barron and Lee's *revised theory* is as follows:

$$G_{BL}(r) = 10\ log(d + e_r + l)\ dB$$

Where:

$$d = \frac{100}{r^2}$$

$$e_r = \left(31200\frac{T}{V}\right)e^{-\frac{0.04r}{T}}(1 - e^{-\frac{1.11}{T}})$$

$$l = \left(31200\frac{T}{V}\right)e^{-\frac{0.04r}{T}}e^{-\frac{1.11}{T}}$$

The equation of the Revised Theory proposed by Barron and Lee can be expressed as follows:

$$G_{BL}(r) = 10\,log\left(\frac{100}{r^2} + 31200\frac{T}{V}e^{-0.04r/T}\right)\,dB$$

This equation incorporates an additional component that depends on the reverberation time (T) and the source-receiver distance (r). This component accounts for the decay of sound energy in the reverberant field (Barron & Lee, 1988).

The architectural characteristics of a church often lead to a more pronounced decay of the first reflections than anticipated by the *revised theory* proposed by Barron and Lee. Elements such as vaults, chapels, and columns in the church structure contribute to a significant attenuation of the early reflected sound energy as the distance between the sound source and the receiver increases. This phenomenon has been substantiated by numerous studies conducted on various churches (Cirillo & Martellotta, 2005).

The outcomes of both the simulations and acoustic measurements pertaining to the sound energy distribution are presented in two graphs, juxtaposed with the curve derived from the *revised theory* as shown in Figure 67. The plotted parameter is defined as a generic ΔL, as the values have been shifted relative to the actual value of G, in order to analyse the decay of sound energy in the space as the sound-receiver distance increases, which proves to be the most significant aspect.

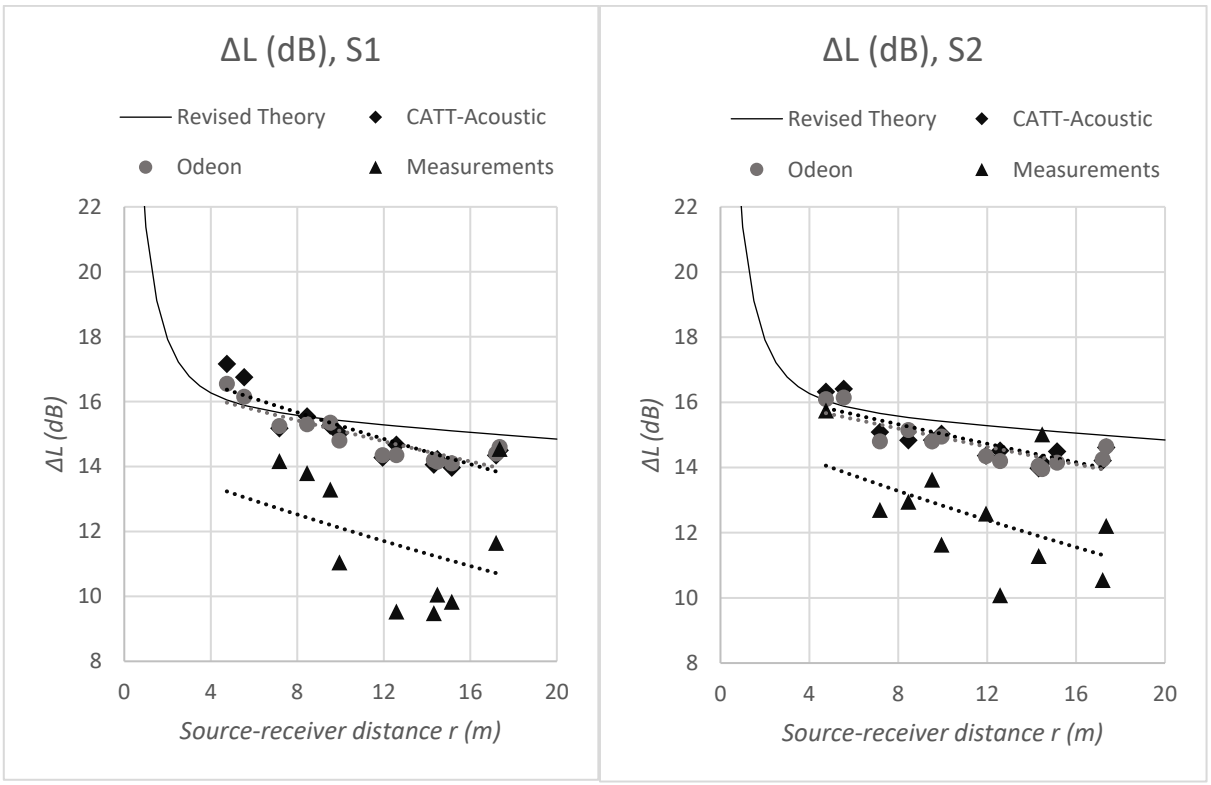

Figure 67. Sound energy distribution comparison between Barron and Lee's Revised Theory, measured and simulated values.

Upon thorough analysis of the graphs, it is evident that the ΔL values exhibit a slightly more pronounced slope in comparison to the prediction of the *revised theory*. This statement holds true for both the simulation values – which closely align with the *revised theory* curve – and the measurement values. This behaviour, as observed, is typical of churches. It is important to highlight that Barron and Lee's theory primarily concentrates on the study of chamber music halls, whereas churches demonstrate different behaviour due to the attenuation of the early reflections.

Furthermore, it can be observed that the trends in the acoustic simulations fall in an intermediate position between the *revised theory* curve and the actual decay of sound energy obtained from measurements. The measurements exhibit more variable values; however, the slope of the curve confirms the sound energy behaviour typical of a church inside the Pere Pruna Hall.

The subject at hand would merit further investigation, but for the scope of this thesis, we confine our analysis to a qualitative examination of the results.

4.3.2 Calibration comparison between measurement and GA software

Following, a series of paired graphs is provided, which individually analyse the monaural criteria under examination, allowing for a comprehensive comparison between the acoustic measurements and simulations conducted.

All graphs are categorized according to the sound source and octave band division. The resulting curves offer a clear depiction of the achieved level of calibration accuracy for the descriptors. Error bars have been included, corresponding to the aforementioned JND values, thus allowing to quantify this accuracy. In fact, with few exceptions, a rather high precision has been attained.

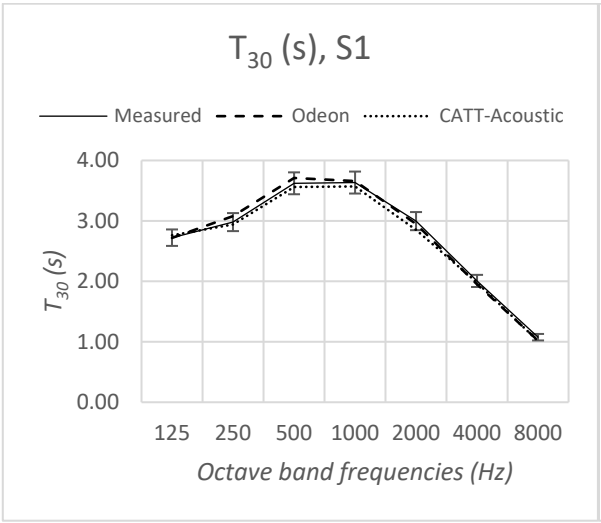

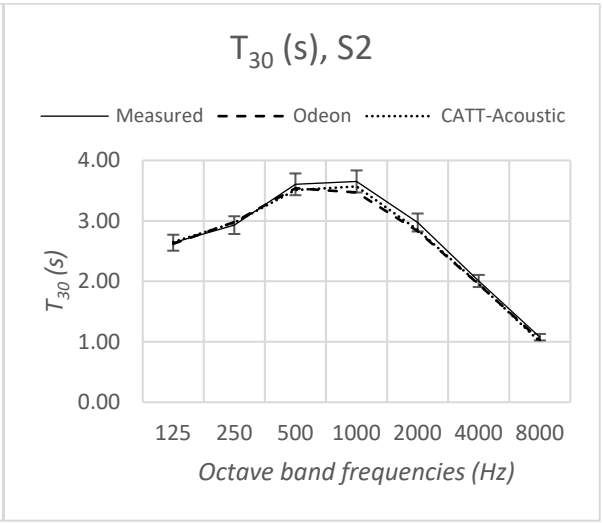

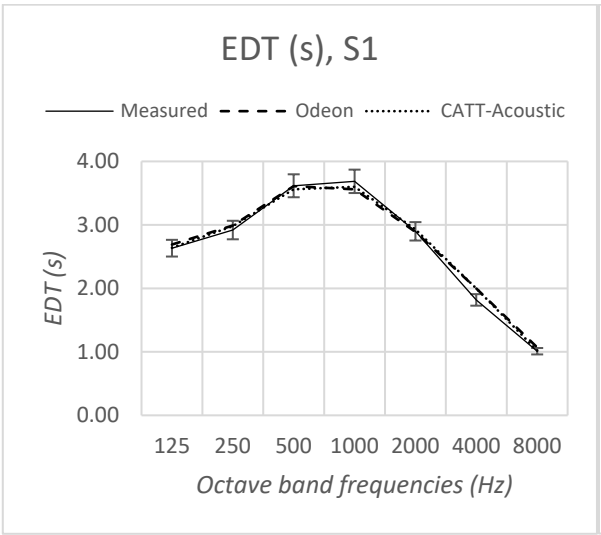

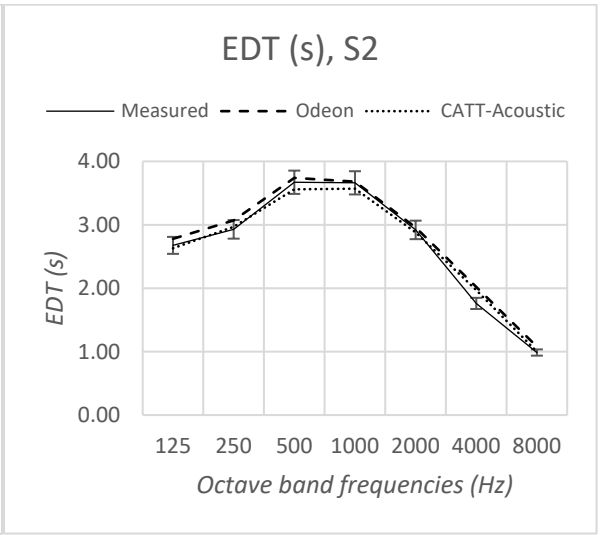

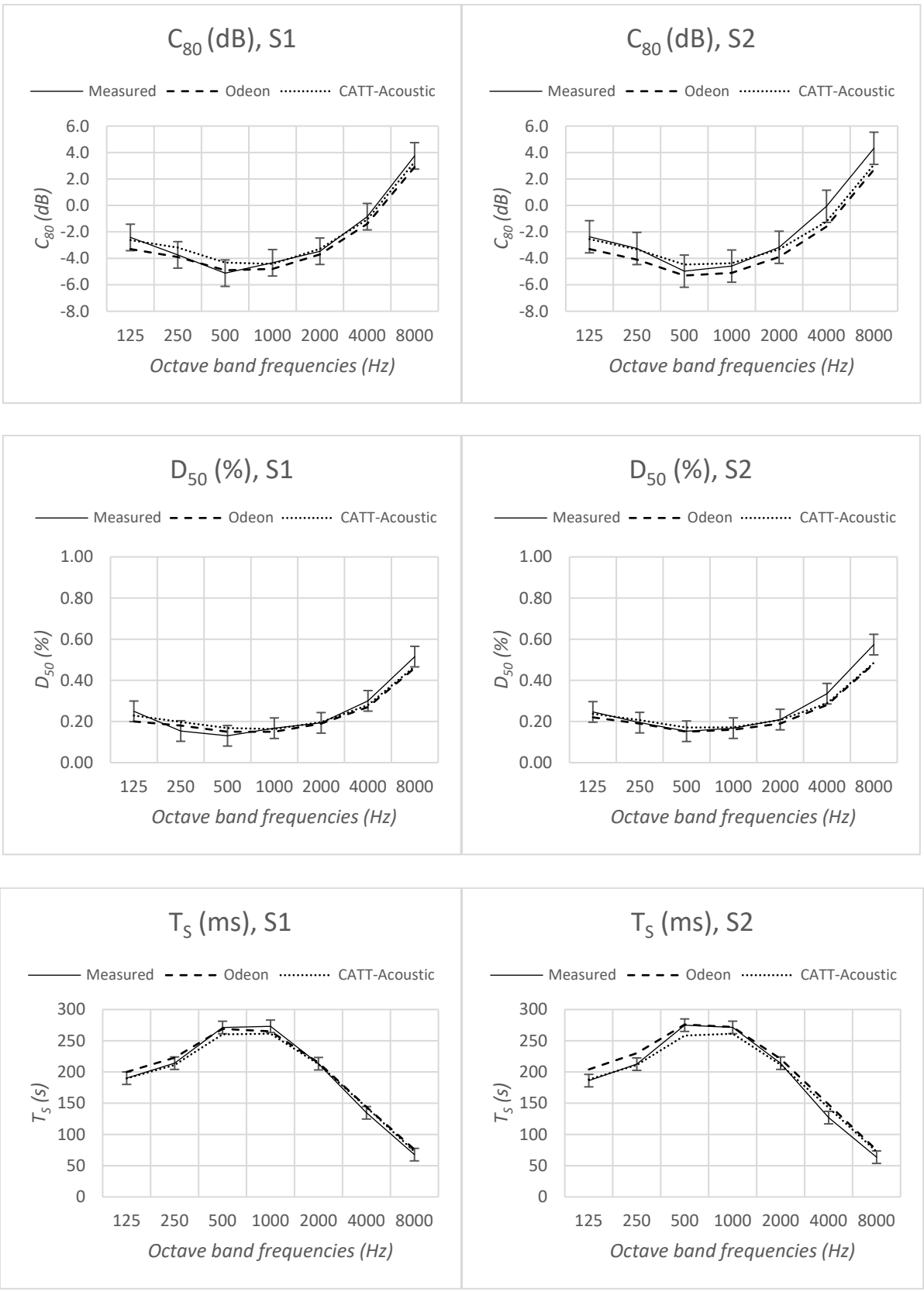

Figure 68. Comprehensive list of acoustic criteria comparison graphs. Curves show differences between measured and simulated acoustic room criteria.

In general, among all the analysed curves, a common trend can be observed. The curves derived from the ODEON simulation tend to exhibit slightly more pessimistic outcomes compared to those obtained from the CATT-Acoustic simulation. Notably, the reverberation criteria, including EDT, T_{30}, and T_S, demonstrate slightly elevated values in the curves associated with the ODEON simulation. Additionally, the clarity criteria C_{80} and D_{50} derived from ODEON indicate slightly lower values. Nevertheless, these differences are of minimal significance and largely imperceptible, as they fall well within the JND range.

One of the primary objectives to be pursued is the reduction of the reverberation criteria – thereby enhancing clarity – particularly in the critical mid-frequency range (500 and 1000 Hz). These frequencies are extremely relevant for both musical and speech acoustics.

5 Proposals for acoustic treatment

5.1 General overview of the intervention

The acoustic treatment intervention in the Pere Pruna Hall presents significant complexity due to its historical and artistic heritage. Preserving elements like frescoes, vaults, stained glass windows, columns, and arches is imperative, making it crucial to avoid any invasive alterations for an acoustic improvement project. Consequently, the surfaces available for intervention are limited, necessitating careful selection and evaluation.

After extensive discussions involving the research groups and the management of the Pere Pruna cultural association, it was determined that the most suitable option is to focus on the recent installations, specifically the thin white brick walls added during the 1990s renovation. These portions of the walls, located in the lower part of the hall, do not possess any artistic significance. As shown in the Figure 69, these horizontal bands offer an excellent opportunity for the implementation of the acoustic correction project through the placement of absorbent panels.

In addition to this approach, complementary measures, such as the use of curtains and upholstered chairs, will contribute to further attenuating the reverberation present in the room. Finally, the vertical columns positioned between the aforementioned bands can accommodate additional absorbing elements, such as bass traps and similar corner components.

This comprehensive strategy aims to achieve an optimal balance between preserving the hall's architectural integrity and enhancing its acoustic qualities.

Considering the versatile nature of the room, which serves as a venue for chamber orchestra, choral music performances and conferences, we will explore the potential of introducing movable elements, which can be selectively introduced or removed as needed, allowing for flexible adjustments in the room's acoustic characteristics based on the specific requirements of each event. This approach aims to provide variable acoustics, catering to temporary needs and ensuring an optimal acoustic environment for different types of gatherings and activities.

Figure 69. Acoustic correction area: the available horizontal bands of the light brick walls are marked in red.

The fundamental objective of the acoustic intervention will encompass three key aspects: firstly, to enhance the level of absorption of the hall; secondly, to attain a notable reduction of the reverberation – and consequent increase of sound clarity – especially at mid-frequencies; and lastly, to ensure a uniform perception of all criteria in every point of the audience area.

5.2 Acoustic design

5.2.1 Target room criteria

It is essential to emphasize that there are no universally definitive acoustic criteria values. This is particularly true for versatile spaces such as the one in focus, where ideal acoustic properties vary significantly and are contingent on the specific activities taking place. Nonetheless, a multitude of research studies have enabled the identification of a favorable range of target values, both for chamber music halls and churches. Table 13 compiles these optimal values, both for chamber music halls (Hidaka & Nishihara, 2004) and for churches (Berardi, 2012).

$T_{30,M,occ}$ (s)	$EDT_{M,occ}$ (s)	$C_{80,3}$ (dB)	$D_{50,3}$ (%)	$T_{S,3}$ (ms)	Ref.
1.2 ÷ 1.8	1.5 ÷ 1.7	0 ÷ 2	–	< 120	Hidaka
–	2.1 ÷ 4.2	–	> 0.20	< 300	Berardi[1]
–	0.8 ÷ 1.0	–	> 0.50	< 150	Berardi[2]

[1]Music, [2]Speech

Table 13. Target values taken as reference point for the acoustic design. The first line provides the optimal values for chamber music halls parameters according to studies by Hidaka and Nishihara. The second and the third lines respectively provide the optimal values for music and speech indices inside a worship space when used as multi–purpose hall according to studies by Berardi. "M" and "3" subscripts identify those values averaged over the central octave bands, respectively 500÷1000 Hz and 500÷2000 Hz.

The Pere Pruna Hall, as previously discussed, exhibits a hybrid acoustic-architectural configuration, situated midway between that of a church and a chamber music hall. Additionally, acknowledging the occasional utilization of the hall for choral performances, which necessitate greater reverberation, it is pertinent to regard RT values of approximately 2 seconds as acceptable. Hence, the primary objective of this investigation is to adjust the existing room criteria to align them as closely as feasible with the specified target values.

5.2.2 Proposed materials

The aim of the treatment is to increase absorption, especially at mid-frequencies, which are crucial for both speech and music, and in our case, particularly challenging. Given the variable acoustic nature we intend to impart to the hall, it has been determined that the most advantageous approach involves employing absorbent materials of diverse characteristics, each with distinct capabilities across various frequency ranges. This strategy aims to achieve an enhancement in acoustic quality spanning the entire audible frequency spectrum, with a specific emphasis on the mid-frequency range.

The first product selected for this project is the ABSORBER CS, manufactured by the German company Gerriets. ABSORBER CS is highly versatile and is well-suited for auditoriums with variable acoustic requirements. Its exceptional density, weighing approximately 560 g/m² or, has earned ABSORBER CS an acoustic absorption rating from class A to class C, indicating its high sound-absorbing properties.

Figure 70. Acoustic fabric ABSORBER CS, example of application

The composition of the polyester fibre fabric Trevira CS gives the product excellent performance in the mid to high frequencies, thanks to its capacity for *absorption by porosity*. Sound waves, in fact, become trapped between the fibres of the fabric and are absorbed due to friction with the air, which dissipates the mechanical energy of the wave, transforming it into heat.

Among the various available options, we have chosen the "Application 3", which possesses the following features:

- Evenly hung panel with 100 % fullness.
- Mode of installation: G-100 according to DIN EN ISO 354.
- Distance from wall: 100 mm.
- Acoustic absorption value: $\alpha_w = 0.8$

- Acoustic absorption class: B

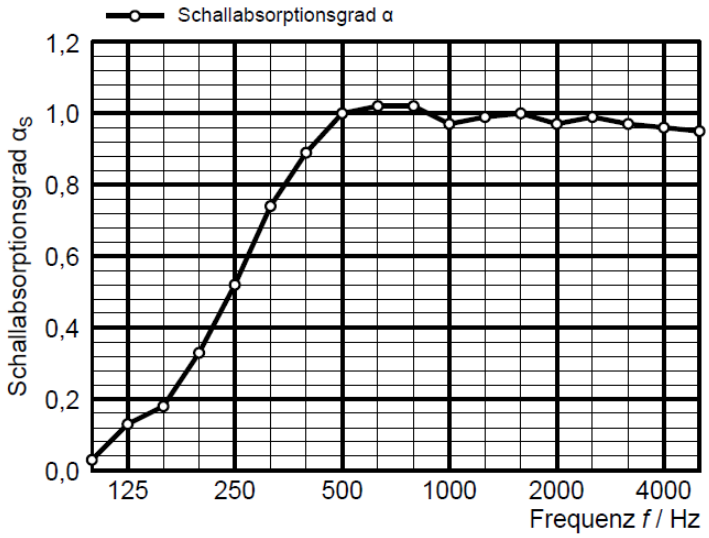

Figure 71. ABSORBER CS sound absorption coefficient graph as a function of frequency in octave band

The second product selected for the intervention is the perforated panel PAP018, manufactured by the Spanish company Decustik, based in Barcelona. It consists of Medium Density Fiberboard (MDF) panels with a thickness ranging from 12 to 16 mm, featuring aligned holes of the same diameter. These panels are installed with a rear air plenum, partially filled with porous material such as mineral wool. The surface finishes can be rough, melamine-coated, wood veneered, painted, or lacquered. In our case, the chosen panel has the following specifications:

- Hole diameter: 8 mm
- Hole spacing: 16x16 mm aligned
- Perforated area: 17%
- Thickness: 16 mm
- Size: 2400x1600 mm
- Air plenum: 200 mm
- Mounting: slotted

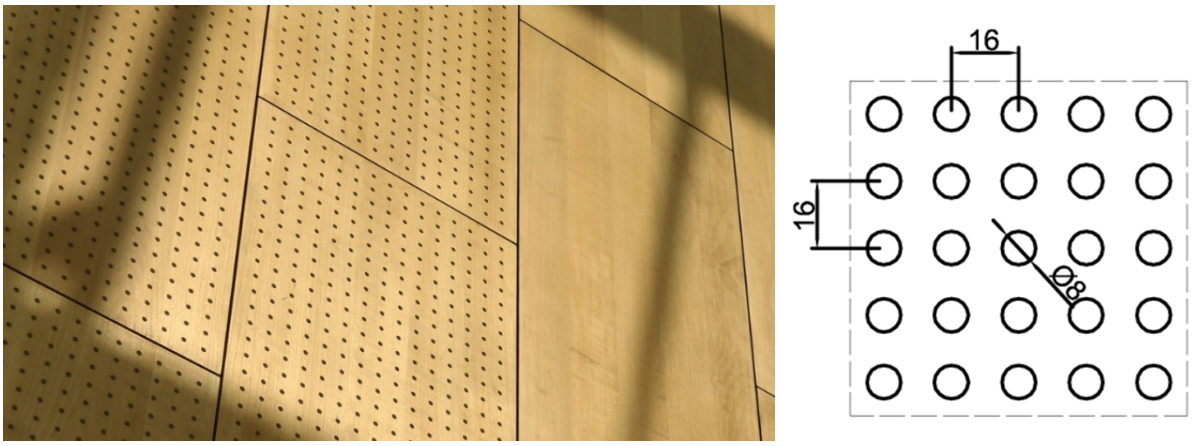

Figure 72. Perforated panel PAP018. On the right, some geometrical features

Perforated panels are particularly suitable for achieving a high level of wide-range acoustic absorption. The absorption system is, in fact, hybrid: the wooden panels absorb through *membrane resonance*, meaning they rely on the principle of oscillation of a vibrating membrane coupled with an elastic material such as air or a porous material, which dampens and dissipates the vibration within the panel. Additionally, the holes function as multiple *Helmholtz resonators*, akin to numerous bottleneck openings that trap sound. Depending on the diameter and length of the hole (hence, the thickness of the panel), as well as the volume of the cavity behind it, the dissipation of sound energy will occur at a specific resonant frequency rather than another, typically within the low-frequency range.

The combination of these absorption systems generates an element capable of absorbing sound across the entire audible frequency spectrum, as illustrated in Figure 73.

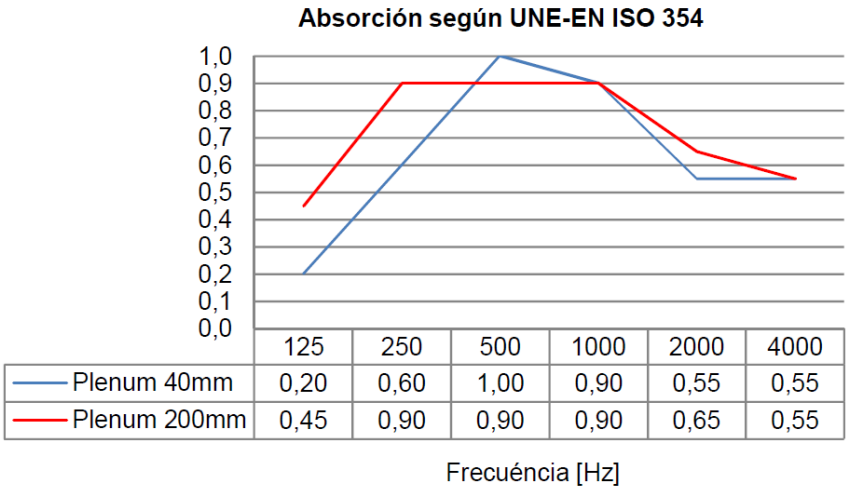

Figure 73. PAP018 sound absorption coefficient graph as a function of frequency. The air plenum 200 mm, corresponding to the red line, is selected for the treatment project

Lastly, the third product that may occasionally be used is the Tri-Trap Corner Bass Trap, provided by the company GIK Acoustics, based in London. This is a freestanding triangular prism made of wood, constructed with a solid core capable of supporting 22.5 kg of weight. It is available in 9 standard GIK fabric colors, all of which are 100% polyester. Additionally, caps are available in black, white, or blonde wood veneer. Customization is also possible according to specific requirements.

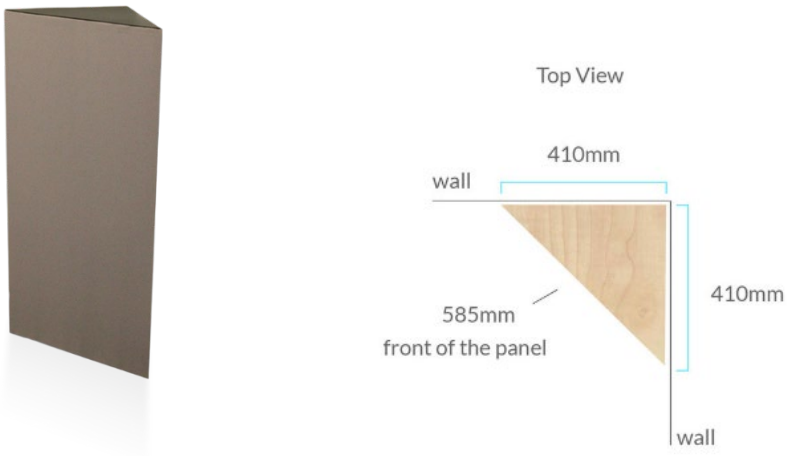

Figure 74. Tri-Trap model. On the right, top view with some geometrical features

This product is particularly suitable as an integration element to enhance absorption at low frequencies, where needed. The absorption system, in this case as well, relies on membrane resonance. The company offers the option to add band limiters to narrow the absorption range to low frequencies, thereby enhancing its efficiency.

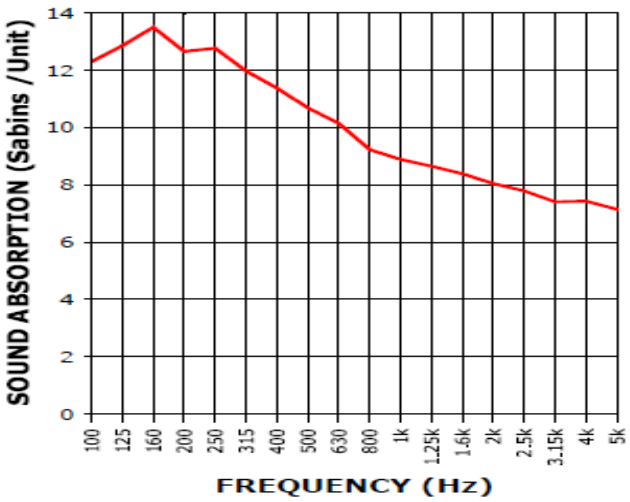

Figure 75. Tri-Trap Sound absorption graph in Sabins/unit, as a function of frequency

In addition to these considerations, the acoustic simulation will account for fully occupied seats, consisting in an increased absorption. Furthermore, the audience area has been expanded to encompass the entire available space, resulting in a total $S_A = 84\ m^2$ (see Figure 76). This yields a ratio $V/S_A = 31$ (m), a value that aligns closely with those obtained in the studies by Hidaka and Nishihara and is more suitable for chamber music halls (Hidaka & Nishihara, 2004).

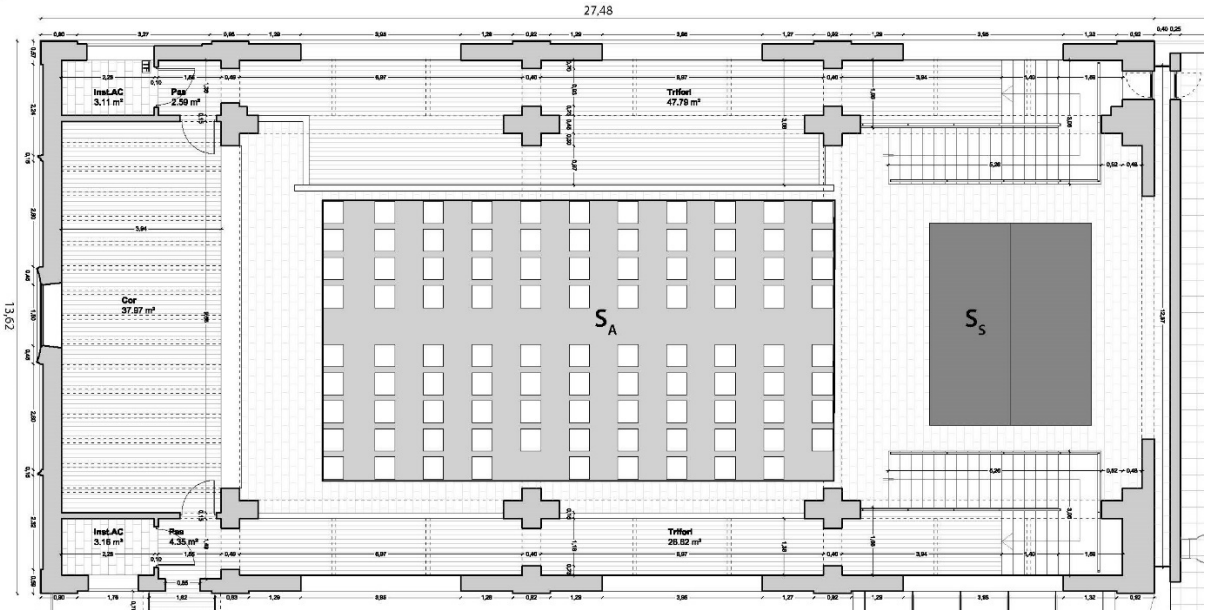

Figure 76. Plan of the hall with increased audience area S_A

Table 14 compiles the absorption coefficients of all the aforementioned elements, by octave band, along with the corresponding scattering coefficients at a frequency of 707 Hz. The value of 0.05 is the default value used in Odeon, whereas 0.1 is the default value in CATT-Acoustic.

Material	Scattering	Absorption					
		125 Hz	250 Hz	500 Hz	1000 Hz	2000 Hz	4000 Hz
Occupied seats	0.7	0.62	0.72	0.8	0.83	0.84	0.85
ABSORBER CS	0.55	0.09	0.50	0.86	0.90	0.90	0.86
PAP018	0.05/0.1	0.41	0.81	0.81	0.81	0.59	0.50
Tri-Trap Corner	0.05/0.1	0.96	0.95	0.79	0.66	0.60	0.55

Table 14. Scattering and absorption coefficient of proposed materials.

A 10% reduction has been applied for safety on all absorption coefficients. This is because companies that provide this data often tend to overestimate the results obtained in the laboratory and keep them high for sales purposes. A different approach was taken for the Tri-Trap Bass Trap: the provided data is in Sabins, a measure corresponding to the equivalent absorption area, expressed by the following equation:

$$A = \alpha S_0$$

Where

α is the absorption coefficient,

S_0 is a reference area equal to 1 ft^2 = 0.093 m^2

Therefore, the value in Sabins was converted to obtain the absorption coefficient, and then it was reduced by 20% due to very high and unrealistic values.

In the following section, the results of the simulations carried out with both Catt-Acoustic and Odeon software will be presented and analysed. The effectiveness of the implemented interventions will be discussed.

5.3 Acoustic simulation and final results

For the sake of thoroughness in presenting results and to afford the client the opportunity to choose the most suitable solution, it has been determined to propose two distinct configurations:

Configuration 1: Sole utilization of draped curtains along all accessible white brick wall surfaces. The inclusion of perforated panels is excluded in this configuration, with a preference for augmenting the number of bass traps to offset low-frequency absorption.

The primary aim of this solution is the absorption of mid-high frequencies, leading to a reduction in reverberation time and late reflections, particularly within these frequency bands. This approach is more suited to mixed activities involving both music and speech, as it tends to slightly enhance speech intelligibility.

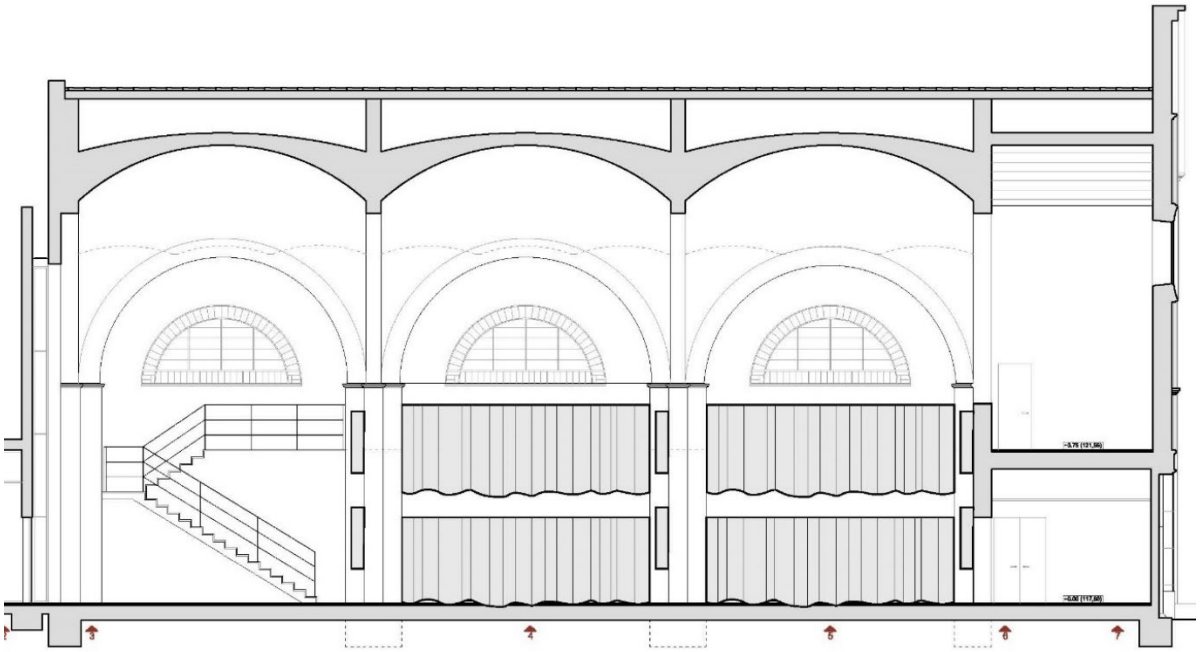

Figure 77. Configuration 1, proposal layout: longitudinal section

As shown in Figure 77, the first configuration comprises:

1. Draped curtains installed on two levels along all available horizontal surfaces of the white walls. The ability to extend and retract the curtains allows them to be brought above the ventilation ducts and used only during events, thereby increasing the equivalent absorption area.
2. Double rows of corner bass traps on the vertical columns to compensate for the lack of low-frequency absorption. Eight bass traps in total are positioned on the columns,

Configuration 2: Mixed utilization of draped curtains and perforated panels. Consequently, a reduced number of bass traps will be incorporated since there is already some low-frequency absorption in place.

This second solution entails a broader-spectrum absorption, covering the entire range of audible frequencies. It is better suited for orchestral or choral activities where emitted frequencies span from low to high indiscriminately.

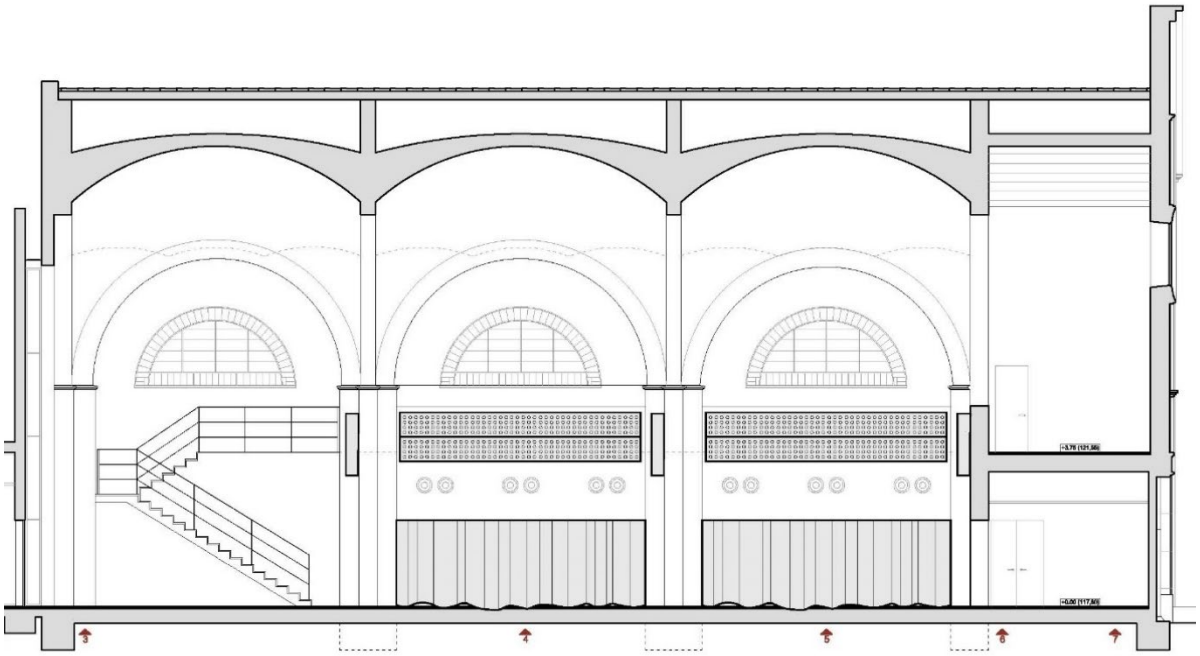

Figure 78. Configuration 2, proposal layout: longitudinal section

Therefore, the second configuration consists of:

1. Draped curtains installed in the lower section of the horizontal surfaces.
2. Perforated panels in the upper section, above the ventilation ducts. The equivalent absorption area is smaller, but the solution is fixed and provides a consistent reduction in reverberation in the room, as needed.
3. A single row of corner bass traps in the upper part, as low-frequency absorption is already partly provided by the perforated panels. Therefore, four bass traps are used.

For the two configurations, two distinct models were created in SketchUp, then imported into the acoustic simulation software, CATT-Acoustic and Odeon, and studied separately. This approach provided the opportunity to make specific adjustments to each case and analyse the differences in results between the two solutions.

5.3.1 Configuration 1: exclusive use of curtains

Simulated post-operam results for the first configuration are presented in Table 15. The same absorption coefficients for the proposed materials were used for both simulation software.

	Ante-operam (measured)		Post-operam			
			CATT-Acoustic		Odeon	
	S1	S2	S1	S2	S1	S2
$T_{30,M}$ (s)	3.63	3.63	1.97	1.96	2.09	2.05
EDT_M (s)	3.65	3.67	2.23	2.25	2.08	2.09
$C_{80,3}$ (dB)	-4.3	-4.2	-1.5	-1.4	-1.2	-0.8
$D_{50,3}$ (%)	0.16	0.18	0.29	0.29	0.31	0.34
$T_{S,3}$ (s)	253	253	153	152	141	136
STI_{male}	0.40	0.40	0.46	0.47	0.46	0.48

Table 15. Configuration 1: comparison between ante–operam measured values and post–operam simulated values for acoustic criteria. Results are shown for both source positions, averaged over all the receivers positions. "M" and "3" subscripts identify those values averaged over the central octave bands, respectively 500 - 1000 Hz and 500 - 1000 - 2000 Hz.

Next, a comprehensive list of paired graphs is provided, where all the individual monoaural acoustic parameters under examination are analysed separately. These graphs present a comparison between the pre-intervention values measured in the hall and the post-intervention values obtained from the simulations following the acoustic treatment modifications.

All the graphs are categorized for each individual source position and in octave bands.

A consistent trend is evident in the curves generated from the values extracted from both CATT-Acoustic and Odeon. This observation underscores the effectiveness of the simulations and the reliability of the results.

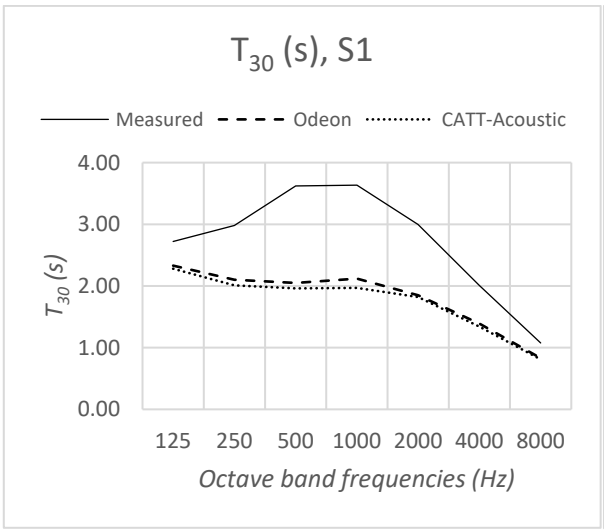
T30 (s), S1
Measured
Odeon
CATT-Acoustic
4.00
3.00
2.00
1.00
0.00
T30 (s)
125 250 500 1000 2000 4000 8000
Octave band frequencies (Hz)

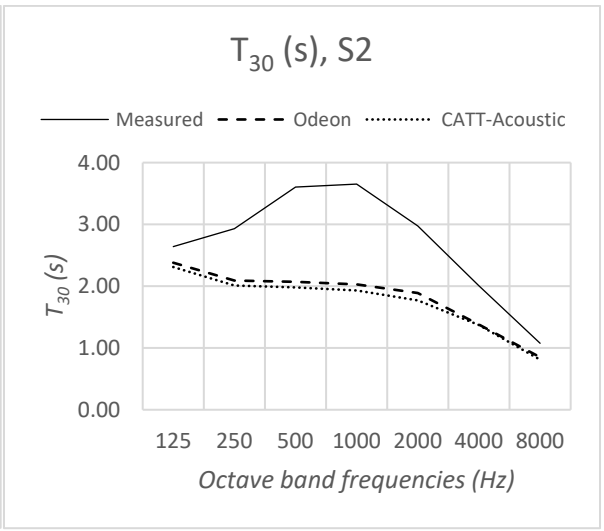
T30 (s), S2
Measured
Odeon
CATT-Acoustic
4.00
3.00
2.00
1.00
0.00
T30 (s)
125 250 500 1000 2000 4000 8000
Octave band frequencies (Hz)

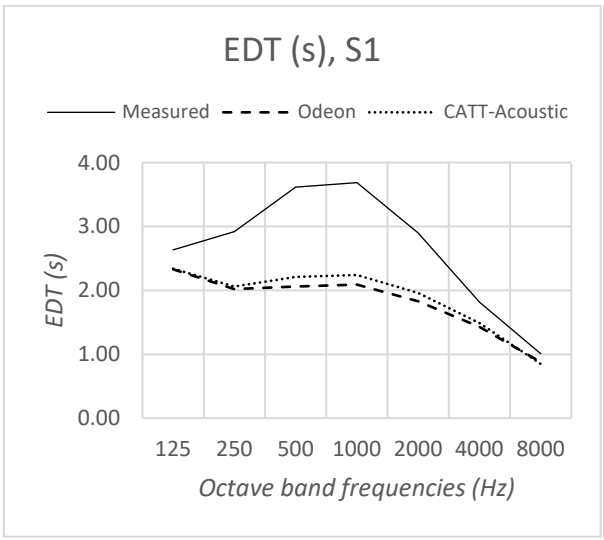
EDT (s), S1
Measured
Odeon
CATT-Acoustic
4.00
3.00
2.00
1.00
0.00
EDT (s)
125 250 500 1000 2000 4000 8000
Octave band frequencies (Hz)

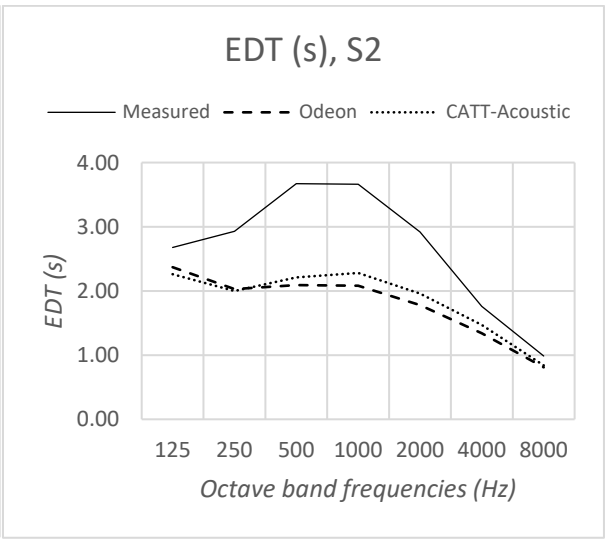
EDT (s), S2
Measured
Odeon
CATT-Acoustic
4.00
3.00
2.00
1.00
0.00
EDT (s)
125 250 500 1000 2000 4000 8000
Octave band frequencies (Hz)

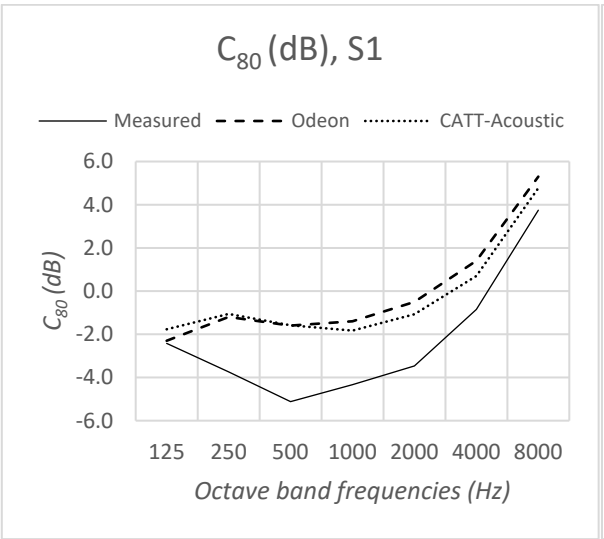
C80 (dB), S1
Measured
Odeon
CATT-Acoustic
6.0
4.0
2.0
0.0
-2.0
-4.0
-6.0
C80 (dB)
125 250 500 1000 2000 4000 8000
Octave band frequencies (Hz)

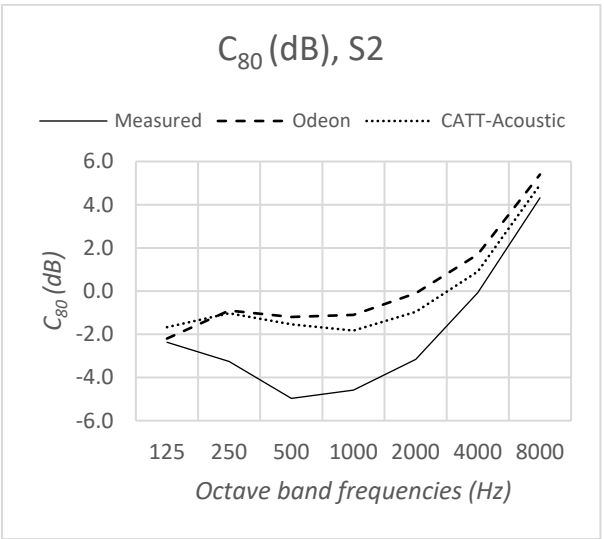
C80 (dB), S2
Measured
Odeon
CATT-Acoustic
6.0
4.0
2.0
0.0
-2.0
-4.0
-6.0
C80 (dB)
125 250 500 1000 2000 4000 8000
Octave band frequencies (Hz)

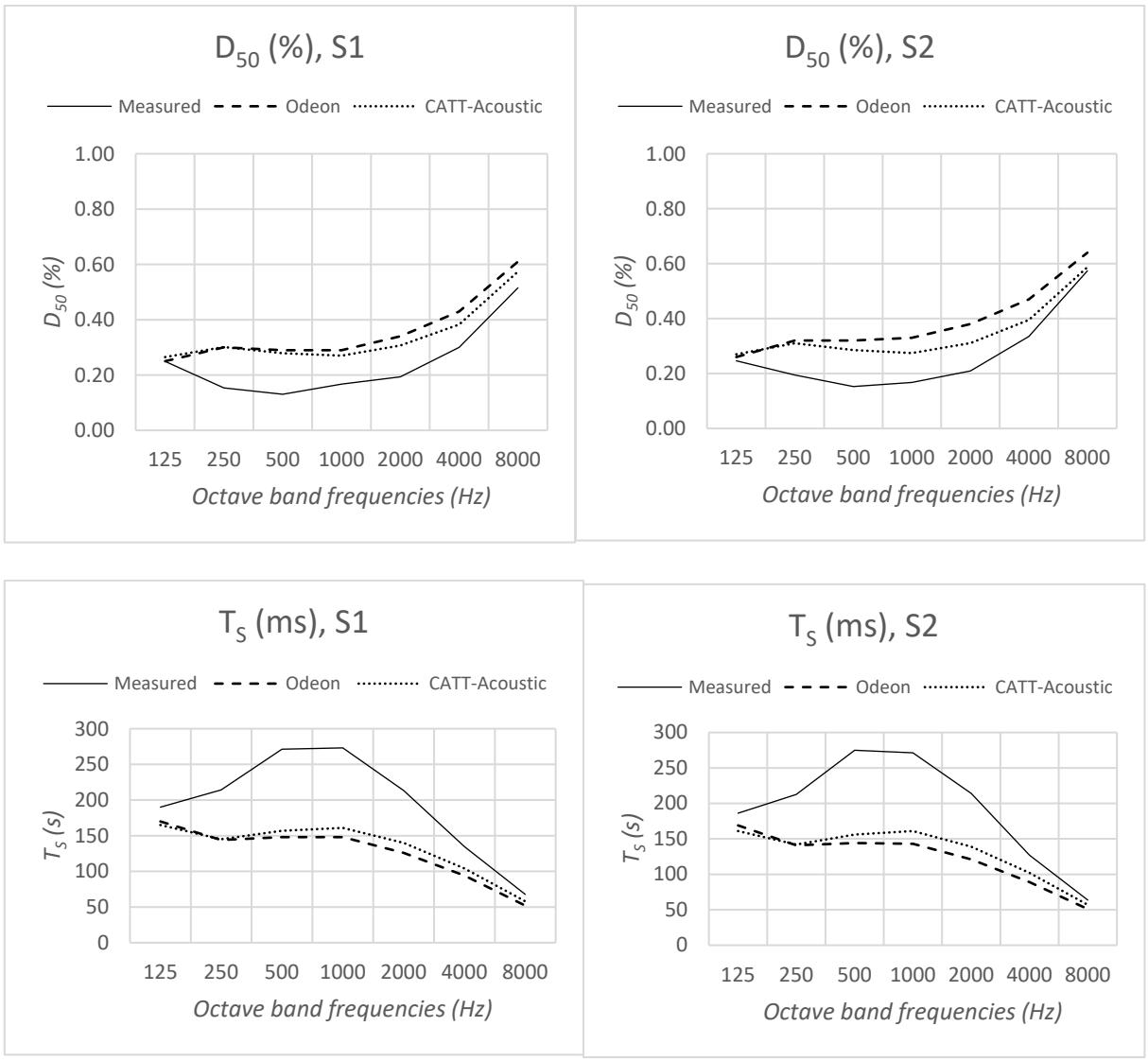

Figure 79. Configuration 1: acoustic criteria comparison graphs. Curves show differences between ante-operam measured and post-operam simulated acoustic room criteria.

It is possible to observe a significant improvement in the acoustic conditions of the hall. The obtained values closely approach the target room criteria shown earlier. As expected, the treatment is less effective at lower frequencies, where the values remain slightly higher. Regarding the reverberation values, the curves show a decreasing trend from low to high frequencies, with a reduction of almost 2 seconds at 500 and 1000 Hz. Furthermore, the speech intelligibility values related to the STI, as presented in the table, also demonstrate an increase in quality in the assessment considered by the standard (refer to section 1.2.3).

However, due to the absence of absorption in the upper vaulted portion, the clarity levels remain somewhat low, slightly below the range of optimal values required. Nevertheless, the results achieved are more than satisfactory.

Figure 80 presents photorealistic images of the intervention. It is possible to observe the installation of the curtains and corner bass traps.

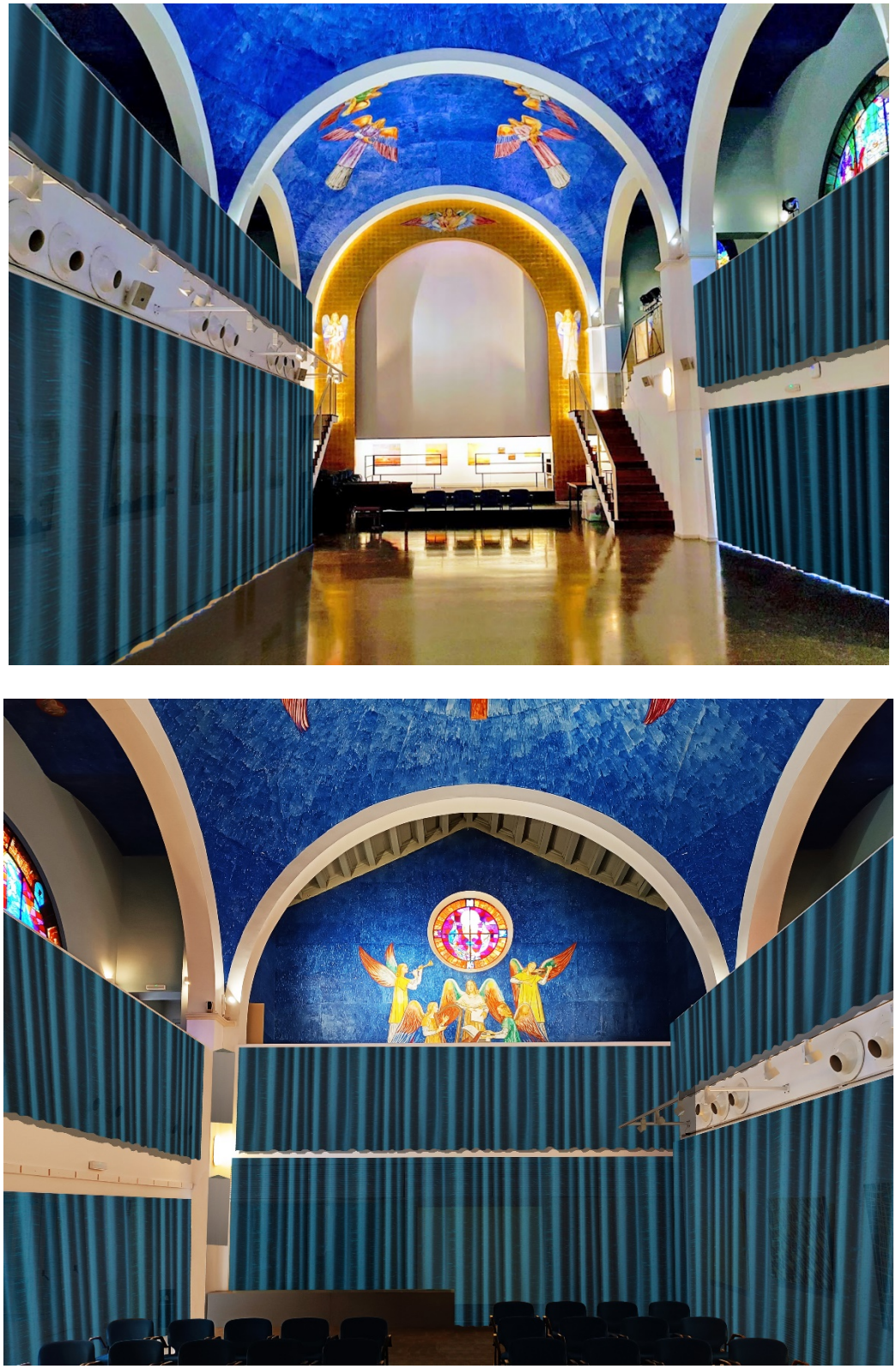

Figure 80. Configuration 1: final result of the acoustic treatment project.

5.3.2 Configuration 2: mixed use of curtains and perforated panels

Simulated post-operam results for the second configuration are presented in Table 16. Also in this case, the absorption coefficients are the same for both simulation software.

	Ante-operam (measured)		Post-operam			
			CATT-Acoustic		Odeon	
	S1	S2	S1	S2	S1	S2
$T_{30,M}$ (s)	3.63	3.63	2.06	2.00	2.29	2.17
EDT_M (s)	3.65	3.67	2.29	2.30	2.28	2.23
$C_{80,3}$ (dB)	-4.3	-4.2	-1.8	-1.7	-1.5	-1.3
$D_{50,3}$ (%)	0.16	0.18	0.26	0.28	0.28	0.30
$T_{S,3}$ (s)	253	253	160	158	151	150
STI_{male}	0.40	0.40	0.45	0.46	0.46	0.47

Table 16. Configuration 2: comparison between ante–operam measured values and post–operam simulated values for acoustic criteria. Results are shown for both source positions, averaged over all the receivers positions. "M" and "3" subscripts identify those values averaged over the central octave bands, respectively 500 - 1000 Hz and 500 - 1000 - 2000 Hz.

Similarly for this configuration, a comprehensive list of all the examined parameters is provided, distinguishing between the two source positions and across all primary octave bands. This approach enables a graphical representation of the differences in results compared to the first treatment type.

In this case as well, apart from some anomalies – particularly in the case of reverberation time – it is possible to discern a common trend among the outcomes obtained using the two simulation software, confirming a reliable behaviour of the two simulation software. However, it should be noted that the curve patterns differ significantly from those of the first configuration.

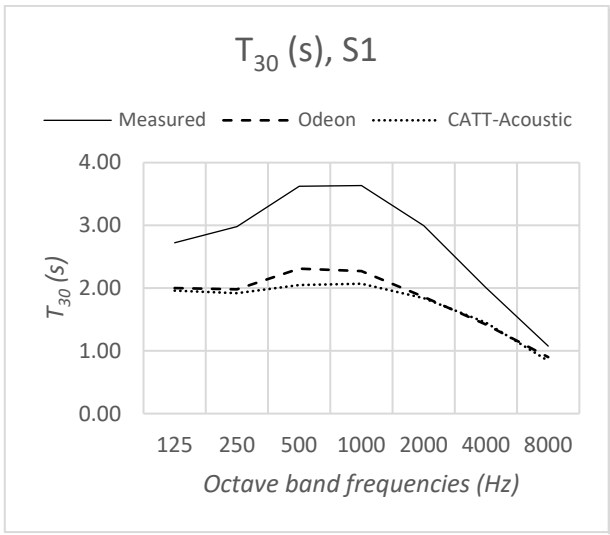
T30 (s), S1
Measured
Odeon
CATT-Acoustic
4.00
3.00
2.00
1.00
0.00
T30 (s)
125 250 500 1000 2000 4000 8000
Octave band frequencies (Hz)

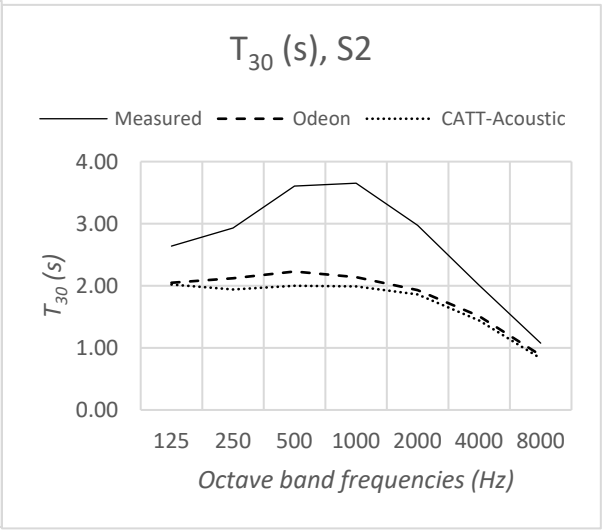
T30 (s), S2
Measured
Odeon
CATT-Acoustic
4.00
3.00
2.00
1.00
0.00
T30 (s)
125 250 500 1000 2000 4000 8000
Octave band frequencies (Hz)

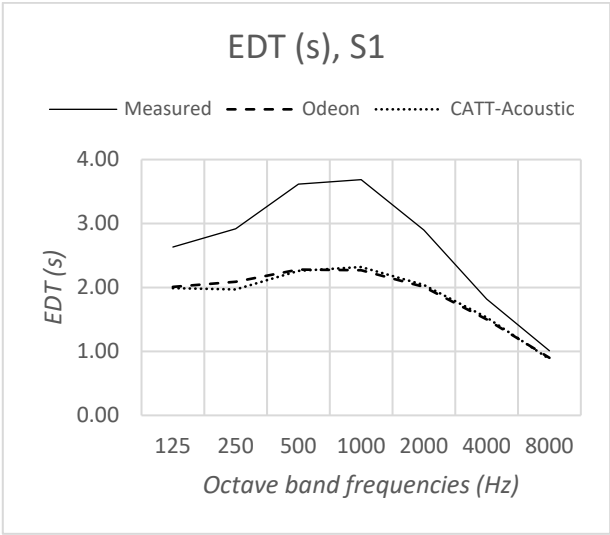
EDT (s), S1
Measured
Odeon
CATT-Acoustic
4.00
3.00
2.00
1.00
0.00
EDT (s)
125 250 500 1000 2000 4000 8000
Octave band frequencies (Hz)

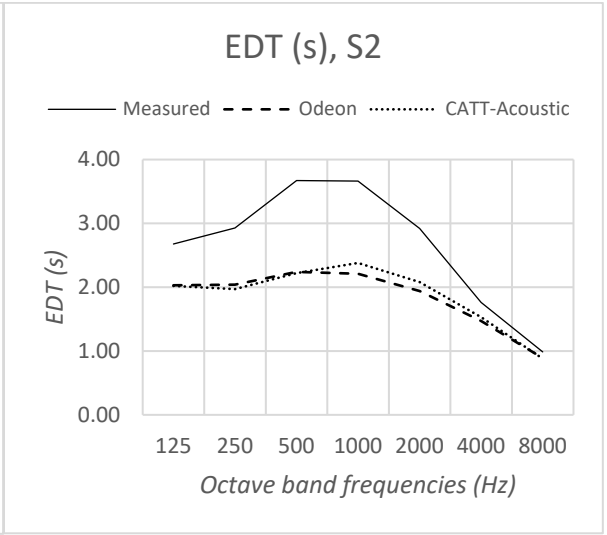
EDT (s), S2
Measured
Odeon
CATT-Acoustic
4.00
3.00
2.00
1.00
0.00
EDT (s)
125 250 500 1000 2000 4000 8000
Octave band frequencies (Hz)

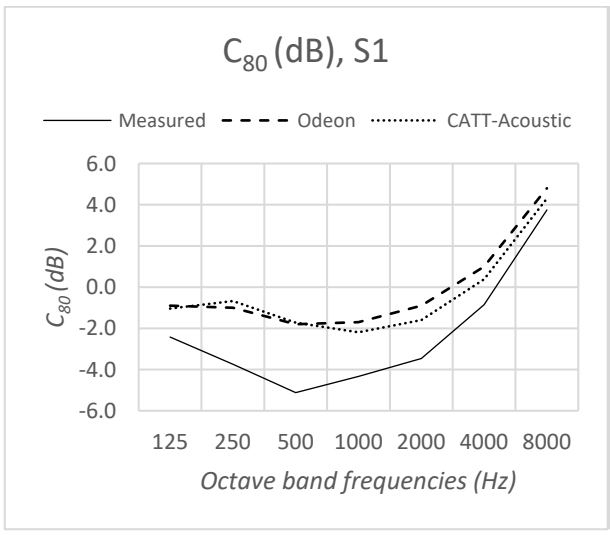
C80 (dB), S1
Measured
Odeon
CATT-Acoustic
6.0
4.0
2.0
0.0
-2.0
-4.0
-6.0
C80 (dB)
125 250 500 1000 2000 4000 8000
Octave band frequencies (Hz)

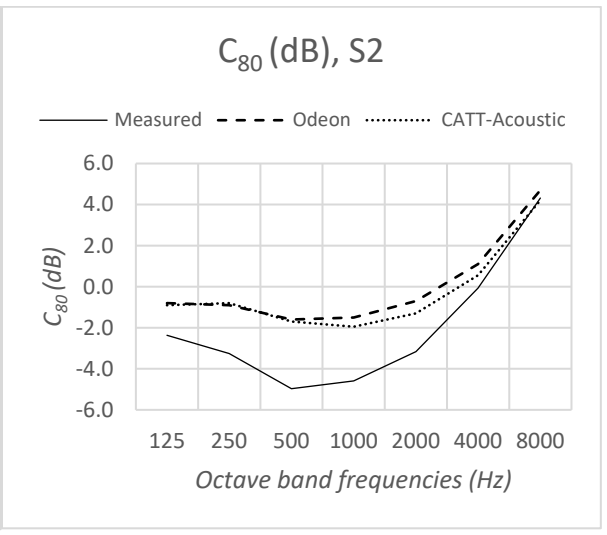
C80 (dB), S2
Measured
Odeon
CATT-Acoustic
6.0
4.0
2.0
0.0
-2.0
-4.0
-6.0
C80 (dB)
125 250 500 1000 2000 4000 8000
Octave band frequencies (Hz)

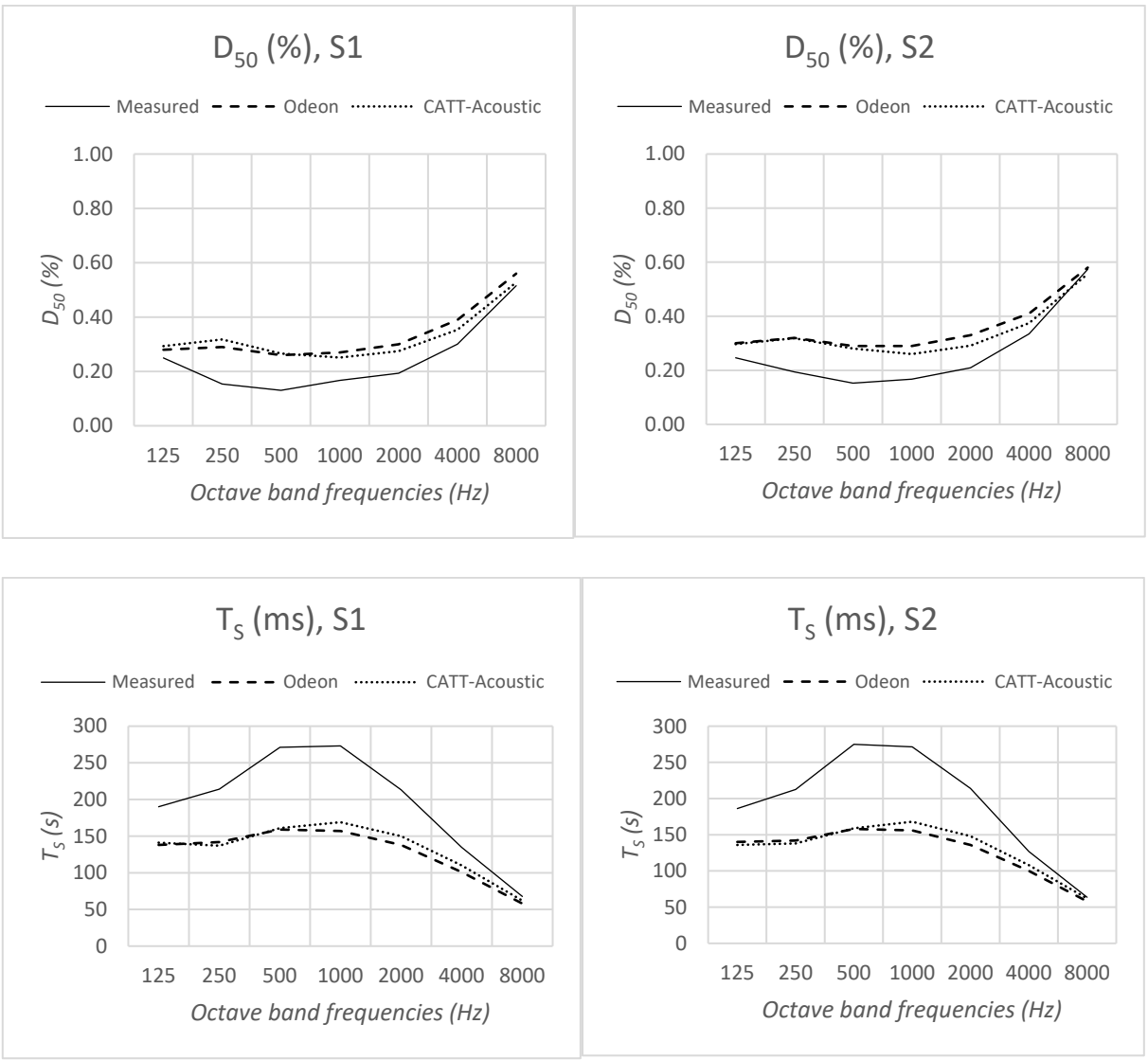

Figure 81. Configuration 2: acoustic criteria comparison graphs. Curves show differences between ante-operam measured and post-operam simulated acoustic room criteria.

In this second configuration, notably improved results are observed at lower frequencies, with lower reverberation times and slightly higher clarity values. However, CATT-Acoustic appears to be generally more pessimistic at higher frequencies, tending to provide less favourable values compared to Odeon, except for the T30.

In both simulations, it is evident that the curve patterns differ from the first configuration, with an upward trend towards the mid-high frequencies indicating a lower degree of absorption and, consequently, slightly lower speech intelligibility. Indeed, the STI results return values slightly lower than the first configuration but still fall within the range of values considered acceptable by standards. Overall, this second solution significantly enhances the acoustic conditions of the room.

Figure 82 presents the final result of the second proposed solution.

Figure 82. Configuration 2: final result of the acoustic treatment project.

Conclusions

Throughout this comprehensive study, an in-depth acoustical analysis of Pere Pruna Hall, a former church in Barcelona, has been conducted. The investigation encompassed a comparative assessment of two prominent acoustic simulation software platforms, namely CATT-Acoustic and Odeon. The complexity of the research arises from the transformation of this space, originally designed for ecclesiastical purposes, into a versatile multi-purpose hall suitable for chamber music and conferences.

First, an extensive theoretical introduction has been presented to provide a contextual framework for the research and establish a foundational understanding of the field of Room Acoustic within which the project operates. Following this comprehensive overview, it was possible to scrutinize the case study with a more discerning eye. The Pere Pruna Hall, characterized by a hybrid configuration bridging the realms of a church and an exhibition/concert space, is placed into a contextual perspective.

In adherence to established protocols and standards, meticulous acoustic measurements were carried out, following the guidelines outlined in ISO 3382-1. Subsequent post-processing procedures facilitated the extraction of monoaural acoustic criteria, including T_{30}, EDT, D_{50}, C_{80}, T_S, G, and STI. These parameters served as invaluable metrics for assessing the perceived acoustic quality from the perspective of the listeners in various positions within the hall. By quantifying these criteria, the research transcended subjective impressions and unveiled the concrete challenges inherent in the space. Specifically, it was identified that excessively prolonged reverberation times stemmed from late reflections interfering with the direct sound, resulting in diminished clarity and intelligibility – a clear impediment to optimal acoustic conditions.

Several factors contributed to the adverse acoustic conditions within the former church, including its lofty vaulted ceilings, the employment of acoustically rigid construction materials, and its voluminous dimensions. These elements collectively engendered an acoustic environment that necessitated careful remediation.

In pursuit of reliable insights closely mirroring real-world conditions, a numerical model was meticulously crafted in the SketchUp modelling software, replicating the architectural geometry and acoustical attributes of the physical space. Subsequently, this numerical model served as the foundation for acoustic simulations conducted using both CATT-Acoustic and Odeon, two

prominent Geometrical Acoustic simulation software applications. It is essential to note that these software tools exhibit both approximations and computational limitations. Odeon distinguished itself through its expedient and user-friendly interface, rendering it particularly accessible for users. Furthermore, Odeon displayed a higher tolerance for potential geometric modelling errors, enhancing its reliability in accommodating real-world architectural variations.

In light of the acoustic deficiencies identified within the former church, a comprehensive treatment project has been formulated. The objective is to adjust the acoustic environment to accommodate the diverse array of events and activities that the hall now hosts, encompassing chamber music, choral performances, and conferences. To achieve this, distinct optimal target acoustic criteria were established for each activity, guiding the research toward tailored solutions.

Two distinct configurations emerged from these endeavours. The first configuration comprises an exclusive use of draped fabric curtains and is well-suited for mixed events that encompass both music and speech, carefully balancing the acoustic requirements of each. The second configuration prioritizes uniform absorption across the audible frequency spectrum by mixing different absorbent materials such as curtains, perforated panels and corner bass traps, catering to a range of events with distinct acoustic demands.

Both proposed solutions have demonstrated significant acoustic enhancements, notably reducing reverberation criteria while enhancing clarity and speech intelligibility. Specifically, both the reverberation time (T_{30}) and the Early Decay Time (EDT) exhibited a reduction of more than 1.5 seconds in the mid to high frequencies, which is a significant achievement. The baricentric time (T_S) also decreased by approximately 100 ms, approaching the recommended target values from Hidaka and Berardi's studies. Regarding clarity parameters, the C_{80} improved by more than 3 dB, and the D_{50} increased by over 10 percentage points. Lastly, the speech intelligibility parameter STI showed a substantial improvement, reaching a level that can be considered sufficiently good for speech comprehension.

The results achieved can be deemed more than satisfactory in line with the objectives of the research project.

However, there are certain logistical aspects that were not addressed in the current study due to practical reasons, but they are worthy of mention and could be interesting for future implementation in the acoustic treatment project.

Currently, the Pere Pruna Hall is equipped with an amplification system consisting of 6 JBL Control 25 speakers positioned along the white side walls, approximately at the height of the ventilation systems. These speakers are typically used to amplify voice during presentation or conference events.

If we were to consider this amplification system in the acoustic calibration process, it is likely that the contribution of direct sound would be slightly higher in the audience area. This could result in a slightly higher level of clarity and speech intelligibility. However, after listening to the opinions of the cultural centre's management and examining the technical specifications of these speakers, it is evident that their performance is insufficient to significantly improve the situation. This is due to their unsuitable directivity for the intended purpose and limited sound emission power relative to the surrounding space.

Therefore, another interesting proposal for the future could involve replacing the amplification system with more capable loudspeakers. This would lead to a substantial increase in the contribution of direct sound and early reflections, consequently improving speech intelligibility and clarity levels.

Another aspect worth considering is the incorporation of absorbing elements in the horizontal plane, perpendicular to the walls where the acoustic treatment project has been implemented. This approach allows for a more comprehensive influence on sound wave absorption in all directions, thus avoiding the formation of normal modes and achieving even more uniform absorption.

However, the matter is rather complex since it is not feasible, for preservation of the artistic elements discussed earlier, to attach absorbing panels, such as acoustic baffles, to the ceiling or along the archways, as we have addressed on multiple occasions. Consequently, an alternative method should be contemplated, such as the installation of a removable system of curtains suspended along the upper-level balconies, which can be opened and closed as needed. This approach would significantly reduce the path length of sound waves, thereby decreasing the quantity of reflections in the audience area.

In conclusion, this research underscores the transformative potential of acoustical treatment in converting a former church into a versatile multi-purpose hall. While the results are commendable, they also shed light on the complex nature of architectural acoustics – a field characterized by its intricacies and uncertainties. As we navigate this ever-evolving discipline,

the need for continued exploration and adaptation to harness the full potential of acoustic design is evident. Consequently, the application of the proposed solutions is highly recommended, as they hold the promise of greatly enhancing the Pere Pruna Hall's acoustical quality, thus enriching the auditory experiences of its patrons for various events and activities.

Bibliography

Ando, Y. (1983). Calculation of subjective preference at each seat in a concert hall. *The Journal of the Acoustical Society of America*, *74*(3), 873–887. https://doi.org/10.1121/1.389874

Ando, Y. (1985). *Concert Hall Acoustics*. Springer-Verlag, Heidelberg.

Ando, Y., & Nishio, K. (1996). On the relationship between the autocorrelation function of continuous brain waves and the subjective preference of the sound field in change of the IACC. *The Journal of the Acoustical Society of America*, *100*(4), 2787–2787. https://doi.org/10.1121/1.416473

Ando, Y. (1998). *Architectural Acoustics: Blending Sound Sources, Sound Fields, and Listeners*. AIP Press / Springer-Verlag.

Arnela, M., et al. (2018). Construction of an Omnidirectional Parametric Loudspeaker Consisting in a Spherical Distribution of Ultrasound Transducers. *Sensors*, *18*(12), Article 12. https://doi.org/10.3390/s18124317

Arnela, M., Martínez-Suquía, C., & Guasch, O. (2021). Characterization of an omnidirectional parametric loudspeaker with exponential sine sweeps. *Applied Acoustics*, *182*, 108268. https://doi.org/10.1016/j.apacoust.2021.108268

Arnela, M., Martínez-Suquía, C., & Guasch, O. (2022). Measurement of the reverberation time in room acoustics using an omnidirectional parametric loudspeaker and exponential sine sweeps. *Proc. of the 28th International Congress on Sound and Vibration (ICSV28)*, 5.

Barron, M., & Lee, L. (1988). Energy relations in concert auditoriums. I. *The Journal of the Acoustical Society of America*, *84*(2), 618–628. https://doi.org/10.1121/1.396840

Barron, M. (1993). *Auditorium Acoustics and Architectural Design*. Taylor & Francis.

Barron, M. (2013). Objective assessment of concert hall acoustics using Temporal Energy Analysis. *Applied Acoustics*, *74*(7), 936–944. https://doi.org/10.1016/j.apacoust.2013.01.006

Beranek, L. L. (1996). *Concert and Opera Halls: How They Sound*. Published for the Acoustical Society of America through the American Institute of Physics.

Beranek, L. L. (2004). *Concert halls and opera houses: Music, acoustics, and architecture* (2nd ed., Vol. 41). Springer-Verlag New York, Inc., 175 Fifth Avenue, New York, NY 10010, USA.

Berardi, U. (2012). A Double Synthetic Index to Evaluate the Acoustics of Churches. *Archives of Acoustics*, *37*(4), 521.

Bork, I. (2005). Report on the 3rd Round Robin on Room Acoustical Computer Simulation — Part I-II. Acta Acustica United with Acustica, 91, 740–763.

C.L. Christensen (2020). *ODEON room acoustics software v15 User's Manual*, ODEON A/S, DTU Science Park, Diplomvej, building 381, DK-2800 Kgs. Lyngby, Denmark.

Cirillo, E., & Martellotta, F. (2005). Sound propagation and energy relations in churches. *The Journal of the Acoustical Society of America*, *118*, 232–248. https://doi.org/10.1121/1.1929231

Dalenbäck B.I.(2011). *CATT-Acoustic v9.0 User's Manual*, CATT, Mariagatan 16°, SE-41471 Gothenburg, Sweden.

D'Orazio, D., Fratoni, G., & Garai, M. (2017). *Acoustics of a chamber music hall inside a former church by means of sound energy distribution. 45*(4), 16.

Dietrich, P., Guski, M., Pollow, M., Muller-Trapet, M., Masiero, B., Scharrer, R., & Vorlander, M. (2012). *ITA-Toolbox—An Open Source MATLAB Toolbox for Acousticians*.

Dirac, P. A. M. (1930). *The Principles of Quantum Mechanics*. Clarendon Press, Oxford.

Fausti, P., & Farina, A. (2000). Acoustics measurements in Opera Houses: Comparison between different techniques and equipment. *Journal of Sound and Vibration*, *232*(1), 213–229. https://doi.org/10.1006/jsvi.1999.2694

Fratoni, G., Hamilton, B., & D'Orazio, D. (2022). Feasibility of a finite-difference time-domain model in large-scale acoustic simulations. *The Journal of the Acoustical Society of America*, *152*(1), 330–341. https://doi.org/10.1121/10.0012218

Hidaka, T., & Nishihara, N. (2004). Objective evaluation of chamber-music halls in Europe and Japan. *The Journal of the Acoustical Society of America*, *116*, 357–372. https://doi.org/10.1121/1.1760112

IEC 60268-16:2020. (2020). *Sound system equipment - Part 16: Objective rating of speech intelligibility by speech transmission index.* International Electrotechnical Commission, Geneva, Switzerland.

Isbert, A. C. (1998). *Diseño acústico de espacios arquitectónicos*. Edicions UPC, Universitat Politécnica de Catalunya, Jordi Girona Salgado 31, 08034 Barcelona.

ISO 3382-1:2009. (2009). *Acoustics—Measurement of room acoustic parameters—Part 1: Performance spaces.* International Organization of Standardization, Geneva, Switzerland.

James, A. (2016). Common pitfalls in computer modelling of room acoustics. *Acoustic Ltd*, *38*(1), 9.

Kuttruff, H. (2016). *Room Acoustics* (6th ed.). CRC Press. https://doi.org/10.1201/9781315372150

Long, M. (2014). *Architectural Acoustics*. Academic Press.

Pätynen, J., Katz, B. F. G., & Lokki, T. (2011). Investigations on the balloon as an impulse source. *The Journal of the Acoustical Society of America*, *129*(1), EL27–EL33. https://doi.org/10.1121/1.3518780

Sabine, W. C. (1922). *Collected papers on acoustics*. Cambridge, Harvard University Press; [etc., etc.]. http://archive.org/details/cu31924015414331

Sayin, U., Artís, P., & Guasch, O. (2013). Realization of an omnidirectional source of sound using parametric loudspeakers. *The Journal of the Acoustical Society of America*, *134*(3), 1899–1907. https://doi.org/10.1121/1.4817905

Schroeder, M. R. (1965). New Method of Measuring Reverberation Time. *The Journal of the Acoustical Society of America*, *37*(6), 1187–1188. https://doi.org/10.1121/1.1939454

Schroeder, M. (1987). Statistical parameters of the frequency response curves of large rooms. *Journal of The Audio Engineering Society*. https://www.semanticscholar.org/paper/Statistical-parameters-of-the-frequency-response-of-Schroeder/46dca8013ca05df84390b7b8f5217613aca6dc6e

Thompson, E. (2004). *The Soundscape of Modernity: Architectural Acoustics and the Culture of Listening in America, 1900-1933*. MIT Press.

Westervelt, P. J. (1963). Parametric Acoustic Array. *The Journal of the Acoustical Society of America*, *35*(4), 535–537. https://doi.org/10.1121/1.1918525

Appendix A. Sound sources comparison for acoustics measurements

In the field of acoustics, conducting various types of tests and measurements typically requires the use of omnidirectional sound sources. Two types of such sound sources have been employed within this work: the dodecahedral loudspeaker, which is widely utilized for room acoustics testing worldwide, and the Omnidirectional Parametric Loudspeaker (OPL), which is presently in the testing phase and was developed by the Human-Environment Research (HER) Group of La Salle Ramon Llull University of Barcelona. Recent research has proposed the latest OPL prototype as a possible alternative to the conventional polyhedron loudspeakers that are currently available on the market (Arnela et al., 2018).

In the event that the measurements obtained using the omnidirectional speakers prove to be invalid, alternative approaches, such as the use of an impulsive source like a balloon burst, may be employed (see par. 6.3).

Dodecahedral sound source

The dodecahedron loudspeaker is typically constructed with twelve speakers mounted on a twelve-sided symmetric frame. Originally developed as a tool for acoustic measurements in concert halls, it has since become a widely used device for various acoustic tests, including sound insulation and open field propagation.

Figure 83. Example of dodecahedral sound source model, developed by CESVA

The dodecahedral loudspeaker is considered to be highly effective in terms of diffuse sound propagation and is relatively close to being omnidirectional. Additionally, the quantity and dimensions of the loudspeakers enable a high sound pressure level to be achieved, resulting in a favourable signal-to-noise ratio in compliance with international technical standards to ensure the validity of measurements and prevent contamination from background noise.

However, at high frequencies, the dodecahedron's omnidirectionality diminishes due to the directionality of sound waves, which could compromise the accuracy of measurement results. Moreover, the device is bulky and cumbersome to transport.

OPL sound source

An omnidirectional parametric loudspeaker (OPL) is a device consisting of hundreds of ultrasound transducers set on a spherical surface. Each transducer emits an ultrasonic collimated beam that contains an audible signal modulated in amplitude. The sound waves demodulate in the air via the Parametric Acoustic Array (PAA) phenomenon, and become audible (Westervelt, 1963). This results in the production of hundreds of sound beams in all directions, giving to the loudspeaker a highly omnidirectional character.

Recent research has demonstrated that the Exponential Sine Sweeps (ESS) can significantly increase the OPL's sound power level by enabling it to concentrate all the emitted power in a single frequency, compared to broadband excitation signals such as white or pink noise (Arnela et al., 2021).

These improvements have made it possible to use the OPL for room acoustic measurements, with the latest prototype producing promising results in Reverberation Time measurements, as per ISO 3382-2 for ordinary rooms (Arnela et al., 2022). The HER group has conducted these measurements in a reverberation chamber and compared them to those obtained using a commercial dodecahedron loudspeaker.

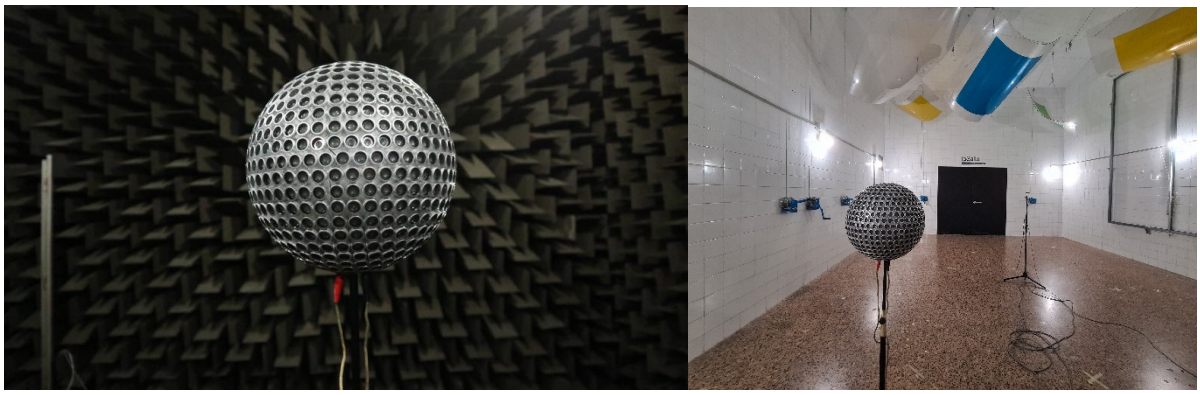

Figure 84. OPL prototype. On the right: experimental setup in the reverberation chamber of La Salle - URL.

The next step for this research is to conduct acoustic measurements in concert and/or multifunctional halls to validate the OPL's performance and the accuracy of the measurements obtained.

As previously elucidated, utilizing the Exponential Sine Sweeps (ESS) technique permits the acquisition of higher ultrasonic power levels and, in turn, higher audible sound pressure levels, consequently augmenting the signal-to-noise ratio. However, the results obtained from the Reverberation Time (RT) measurements reveal that the lower the frequency, the lower the signal-to-noise ratio of the decay curve. This behaviour is attributed to the Preferential Audibility Area (PAA) phenomenon, which favours the emission of higher frequencies compared to the lower frequencies. As a result, the OPL may encounter power level difficulties at very low frequencies (63 or 125 Hz).

Aside from this inconvenience, the OPL noticeably enhances the directivity of dodecahedral sources, particularly in the high frequency range, while also being significantly smaller in size and weight.

Impulsive sources

Section 7.3 of ISO 3382-1 acknowledges the use of true-impulse sources, including but not limited to pistol shot, spark gap impulses, balloon burst, and wooden clapper, for acoustic measurements. These sources exhibit specific spectral characteristics, directionality, and varying power response. For example, the characteristics of balloon burst depend on the size, inflation level, and popping mechanism (Pätynen et al., 2011).

The main disadvantage of these methods is their lack of repeatability, which necessitates taking multiple measurements for each position. Moreover, good omnidirectionality is not always guaranteed.

However, these sources typically exhibit good frequency response and signal-to-noise ratio. Additionally, they are portable and inexpensive, making them practical when transport limitations or budgetary constraints are present.

A final comment: pros and cons of each sound source

In conclusion, there are several factors that can influence the quality and reliability of measurement methods, including power level, directionality, repeatability, weight and transport limits, costs, hardware and computational requirements, and measurement positions. All of these factors can potentially compromise the measurement results (Fausti & Farina, 2000).

Impulsive sources, while highly portable and cost-effective, suffer from a lack of repeatability and non-optimal directionality. On the other hand, dodecahedral sources offer good

omnidirectionality, albeit not at high frequencies, and a good signal-to-noise ratio, but they are difficult to transport due to their weight.

The new OPL attempts to overcome these issues, improving omnidirectionality, weight, and transportability, although it still underperforms compared to the dodecahedron at low frequencies under current conditions.

Overall, the choice of measurement method should be carefully evaluated based on the specific requirements and constraints of the given application.

Appendix B. Technical data sheets of proposed materials

Schallabsorptionsgrad nach ISO 354

Messung der Schallabsorption in Hallräumen

Auftraggeber: Gerriets GmbH, Im Kirchenhürstle 5-7, 79224 Umkirchen
Prüfgegenstand: Vorhanggewebe Absorber CS
Aufbau 3: 100 % Faltenzugabe, Montageart G-100 gemäß DIN EN ISO 354

Aufbau:
Absorber CS
100 % Trevira CS, Schwer entflammbar nach DIN 4102 B1

Zustand:
100 % Faltenzugabe, Wandabstand 100 mm
Die Montageart entspricht dem Typ G-100 gemäß DIN EN ISO 354

Flächengewicht ca. 560 g/m²
Spezischer Strömungswiderstand gemäß DIN EN 29053: R_s = ca. 1.300 Pa s/m

Abmessungen des Vorhangs ohne Befestigungskonstruktion: Breite 3,50 m x Höhe 3,00 m
An der Hallraumdecke ist ein Stahlwinkel mit einer Schenkellänge von 6 cm befestigt. Die Abhängung des Materials erfolgte an dem Stahlwinkel mittels Gummischlaufen. Zwischen Stahlwinkel und Vorhangoberkante bestand eine Überlappung von 2 cm.

Raum: Hallraum
Volumen: 199,60 m³
Prüffläche: 10,50 m²
Prüfdatum: 20.07.2009

	θ [°C]	r. h. [%]	B [kPa]
Ohne Probe	23,4	51	95,7
Mit Probe	23,5	52	95,7

Akkreditiertes Prüflaboratorium nach ISO/IEC 17025
DAP-PL-2485.10

Frequenz [Hz]	α_s Terz	α_p Oktave
100	* 0,03	
125	0,13	0,10
160	0,18	
200	0,33	
250	0,52	0,55
315	0,74	
400	0,89	
500	1,00	0,95
630	1,02	
800	1,02	
1000	0,97	1,00
1250	0,99	
1600	1,00	
2000	0,97	1,00
2500	0,99	
3150	0,97	
4000	0,96	0,95
5000	0,95	

* Absorptionsfläche kleiner als 1,0 m²
α_s Schallabsorptionsgrad nach ISO 354
α_p Praktischer Schallabsorptionsgrad nach ISO 11654

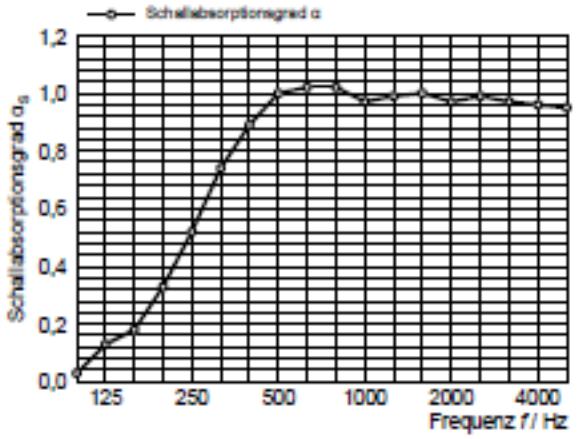

Bewertung nach ISO 11654:
Bewerteter Schallabsorptionsgrad α_w = 0,85
Schallabsorberklasse: B

MÜLLER-BBM Planegg, 29.07.2009
Prüfbericht Nr. M71 419/6
Anhang A
Seite 3

FICHA TÉCNICA DE PRODUCTO
PANELES ACÚSTICOS

decustik

REFERENCIA **PAP018**

DESCRIPCIÓN Panel acústico perforado con agujeros alineados

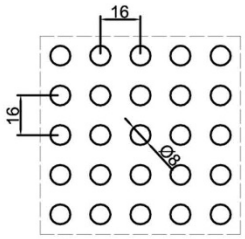

CARACTERÍSTICAS TÉCNICAS

Paso entre agujeros (mm)		16x16 Alineado
Diámetro agujero (mm)		Ø 8
Prof. agujero (mm)		Pasante
Superficie perforada (%)		19,6
Absorción acústica		
Plenum 40mm	α_w	0,65
	NRC	0,75
Plenum 200mm	α_w	0,70
	NRC	0,85
Clase de absorción		C
Lana Mineral		40mm 30kg/m^3

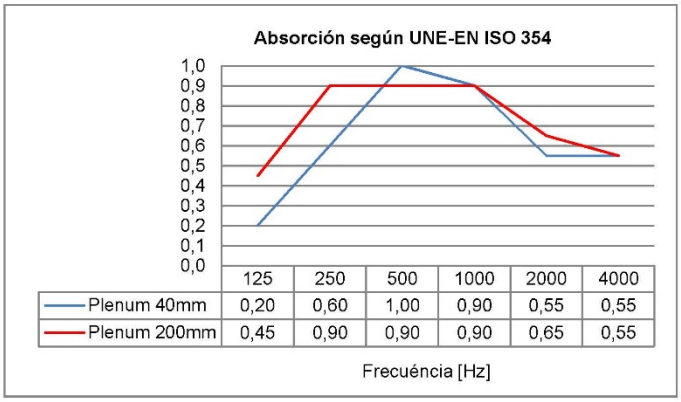

	125	250	500	1000	2000	4000
Plenum 40mm	0,20	0,60	1,00	0,90	0,55	0,55
Plenum 200mm	0,45	0,90	0,90	0,90	0,65	0,55

CARACTERÍSTICAS GENERALES

Materiales de base
MDF Estándar D-s2,d0
MDF Ignifugo B-s2,d0 (núcleo rojo o natural)
MDF Coloreado en masa D-s2,d0
MDF Coloreado en masa B-s2,d0

Espesor (mm)
16mm y 12mm (MDF)
Para otros materiales y espesores, consultar

Peso medio aprox. (kg/m²)
7,5 (MDF Estándar 12mm) 9,5 (MDF Ignífugo 12mm)
10,0 (MDF Estándar 16mm) 12,5 (MDF Ignífugo 16mm)

Formatos (mm)
MDF 12mm : 600x600 / 1200x600
MDF 16mm : 2400x600 / 1200x600
Para otras dimensiones, consultar

Acabado final
Sin acabado Rechapado de madera natural barnizada
Lacado a color RAL Laminado alta presión (HPL) Melamina
Para otros acabados, consultar

APLICACIONES

Revestimiento muros (MDF 16mm)	Falso techo (MDF 12mm)
Sin mecanización	Sin mecanización
Ranura	Semi oculto
	Oculto registrable v6

DECUSTIK®
www.decustik.com
C/ Llevant, 2 - P.I. Mas Les Vinyes
08570 Torelló (BARCELONA)
T. +34 8590838 / F. +34 938596394
comercial@decustik.com

GIK Acoustics
Solutions. Innovations. Quality.

Product Datasheet

3731 Northcrest Rd, Ste 29
Atlanta, GA 30340
770-986-2789

Tri-Trap Corner Bass Trap©

DESCRIPTION

Constructed with a solid core, the Tri-Trap© is a 47" tall, freestanding triangular prism able to hold up to 50 pounds in weight. The Tri-Trap©'s clean, professional design means it does not have to be mounted to the wall or corners and is stackable for floor-to-ceiling coverage. Customizable options include Full Range/broadband or Range Limiter membrane system. Available in 9 standard , 100% polyester GIK fabric colors. Caps available in black, white or blonde wood veneer.

Standard Size	Weight per unit	Quantity per Box
23.5" front face 16.5" x 16.5" sides 47" tall	15 lbs	2 bass traps

GIK Acoustics Greensafe

- **Class A Fire Rated**
- Constructed with Knauf Insulation with **ECOSE** technology
- Manufactured with **PureBond,** LEED certified Columbia Forest Products' (made in the USA) formaldehyde-free technology

ECOSE TECHNOLOGY

PureBond. FORMALDEHYDE-FREE TECHNOLOGY

CLASS A FIRE RESISTANCE

Children & Schools GREENGUARD Indoor Air Quality Certified

AVAILABLE ADD-ON OPTIONS

- Proprietary **Range Limiter** membrane system to retain more high end
- **GIK Scatter Plate** for built-in diffusion
- **Guildford of Maine** fabric upgrades available

MOUNTING / INSTALLATION

The GIK Acoustics Tri-Trap Corner Bass Trap© is intended to be freestanding or stacked floor-to-ceiling. However, if you wish to mount a Tri-Trap in a wall-to-wall corner, we recommend using L brackets on the side walls so the Tri-Trap sits like a shelf.

TEST RESULTS

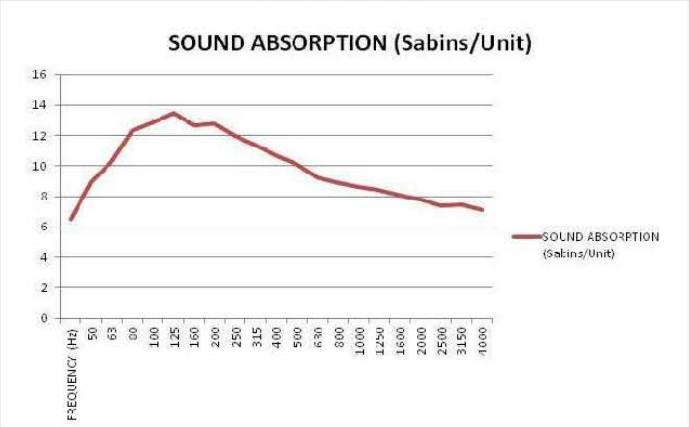

The Tri-Trap© was lab tested at the prestigious Riverbank Acoustical Laboratory and showed to have true effects at 50Hz and below. The Tri-Trap© has been effectively designed to absorb more low end, but also does an excellent job of absorbing the high end, creating smooth sound absorption from 50 Hz to 5000 Hz.